
Review of Key-and-Bladder structures

P. Ferracin

EuroCirCol WP5 Special Meeting
CERN
20 January, 2016

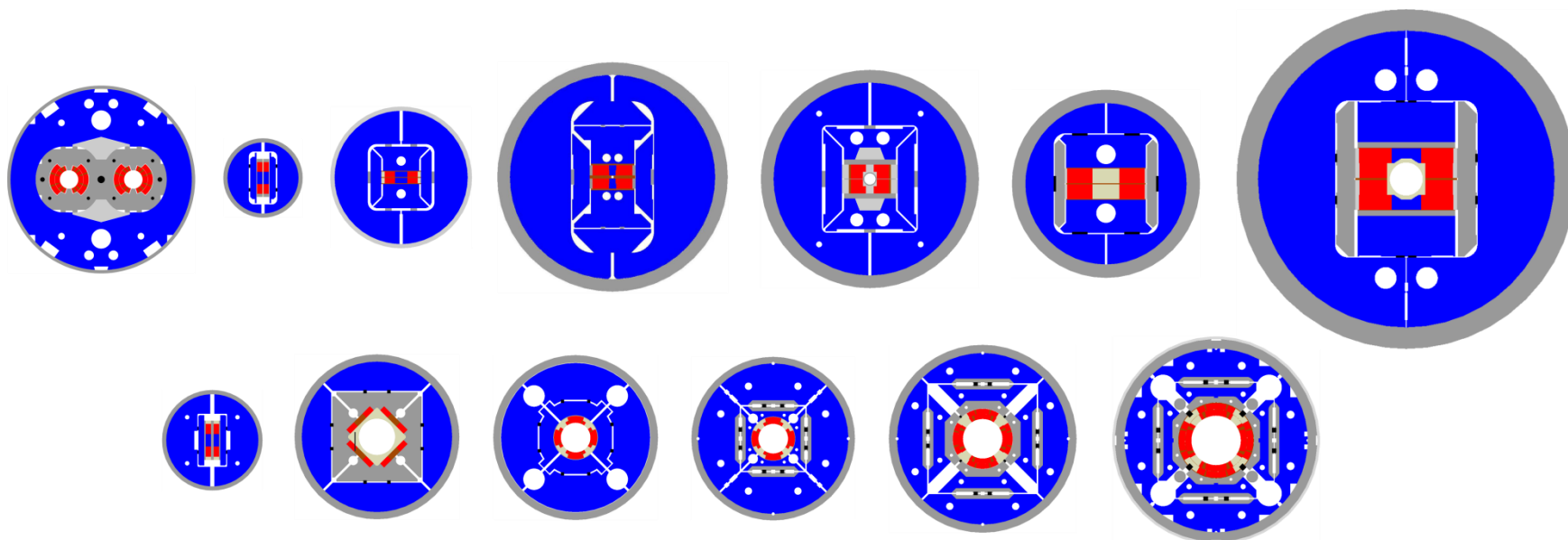


Outline

- Overview
- General concept
- Loading steps
- Design criteria
- Assembly steps
- Axial loading
- Additional topics
 - Alignment
 - Aluminum shell segmentation
 - Lhe containment

Overview

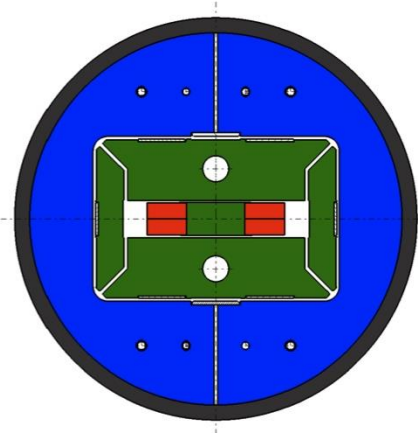
- Shell-based support structures
 - With LHC dipole, and RD3 and SMC missing



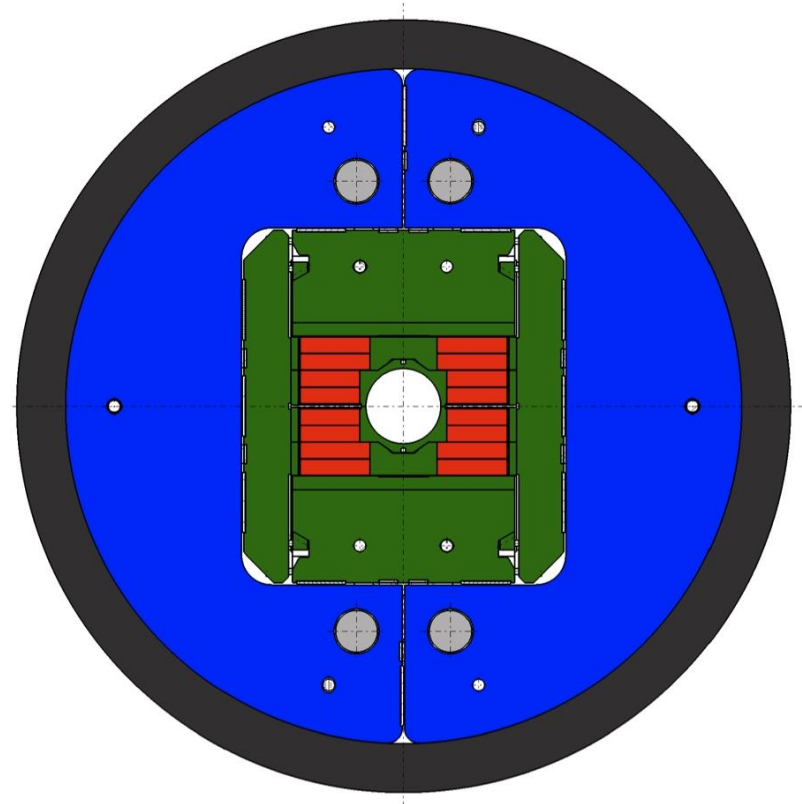
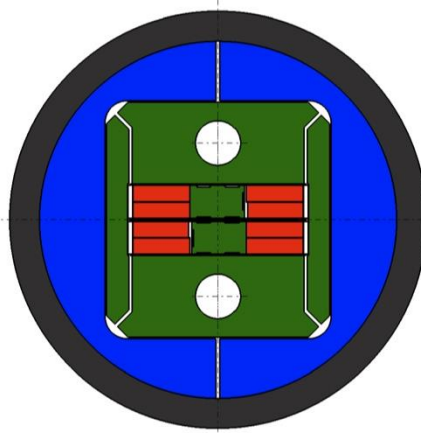
Overview

FRESCA2

SMC

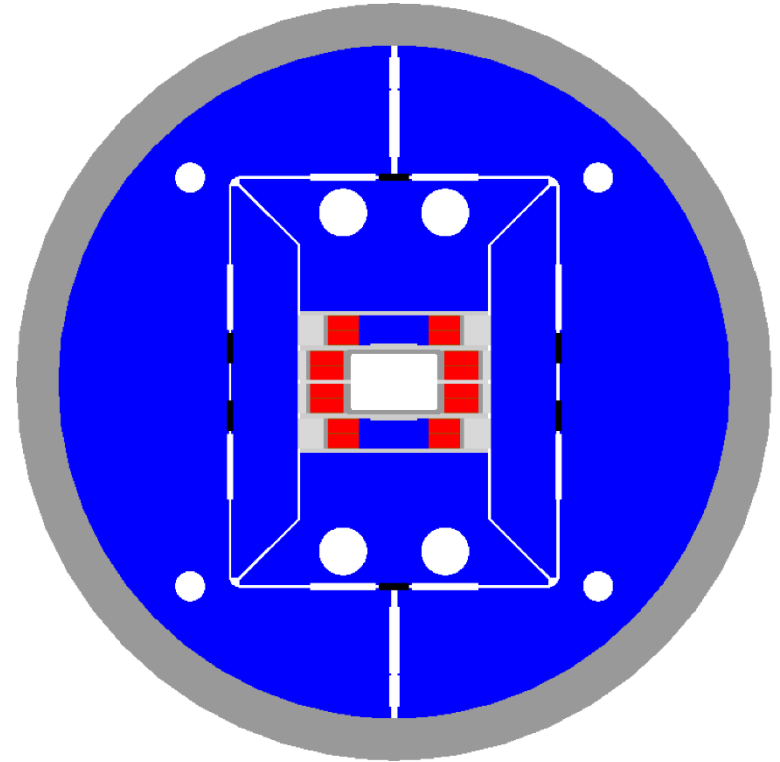
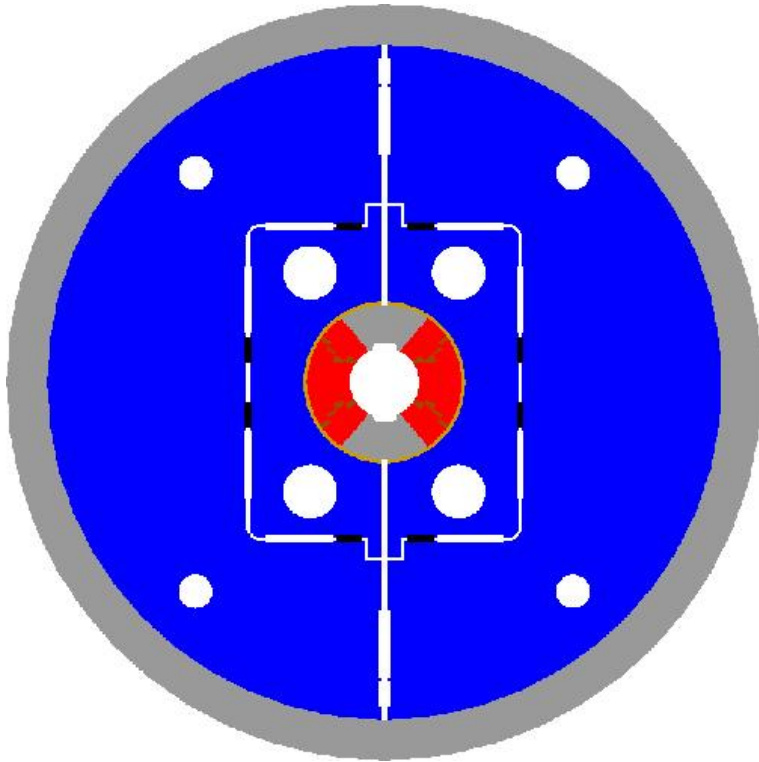


RMC



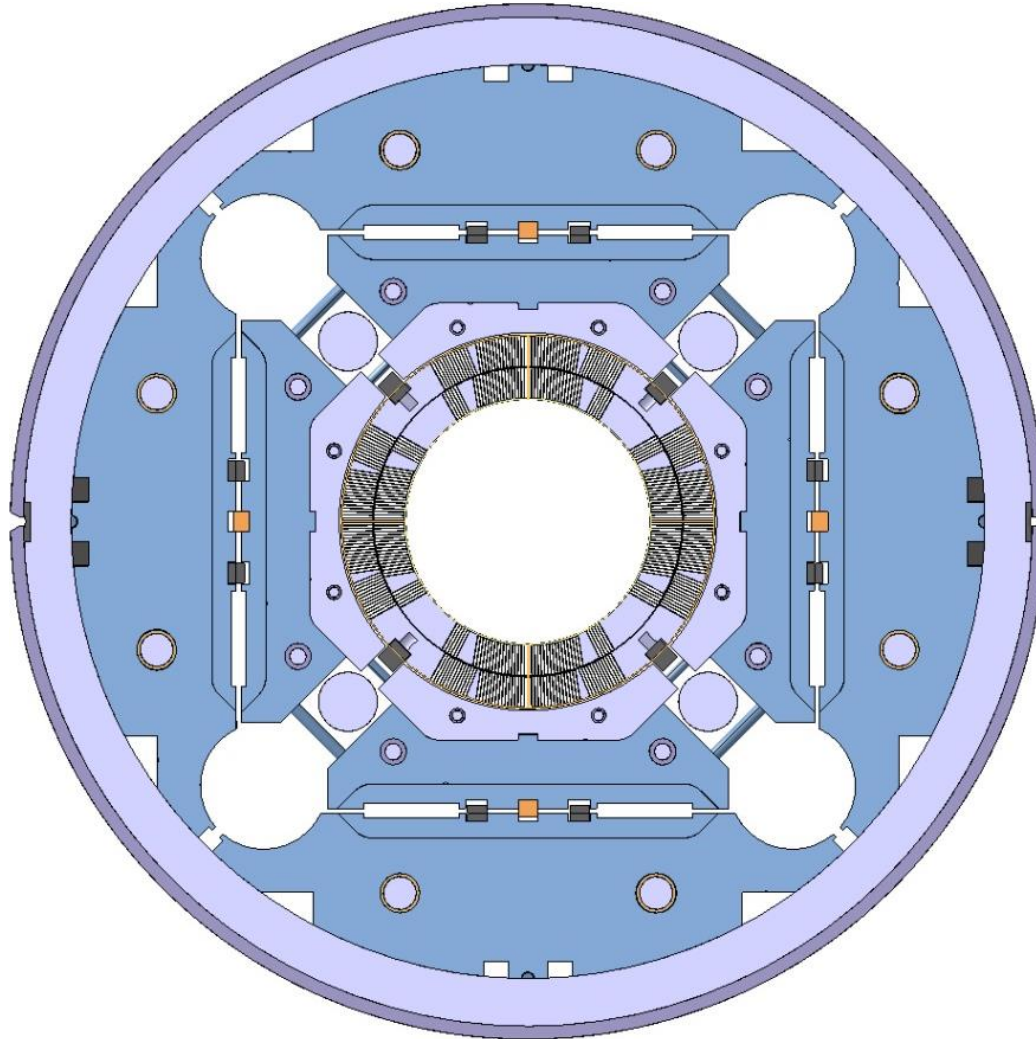
Overview

The LD1 design study



Overview: MQXF

First “attempt” of accelerator quality magnet



The Use of Pressurized Bladders for Stress Control of Superconducting Magnets

Shlomo Caspi, Steve Gourlay, Ray Hafalia, Alan Lietzke, Jim O'Neill, Clyde Taylor, and Alan Jackson

Abstract—LBNL is using pressurized bladders in its high field superconducting magnet program. Magnet RD3; a 14 T race track dipole; has been assembled and pre-stressed using such a system. The bladder, placed between the coil pack and the iron yoke, can provide 70 MPa of pressure while compressing the coil pack and tensioning a 40 mm thick structural Aluminum shell. Interference keys replace the bladder's functionality as they are deflated and removed leaving the shell in 140 MPa of tension. During cool down, stress in the shell increases to 250 MPa as a result of the difference in thermal expansion between the Aluminum shell and the inner iron yoke. A number of strain gauges mounted onto the shell were used to monitor its strain during assembly, cool-down and testing. This technique ensures that the final and maximum stress in the shell is reached before the magnet is ever energized.

The use of a structural shell and pressurized bladders has simplified magnet assembly considerably. In this paper we describe the bladder system and its use in the assembly of a 14T Nb3Sn magnet.

Index Terms—bladder, pressurize, stress, superconducting.

I. INTRODUCTION

Lorentz forces generated by high field dipole magnets are too large to be handled by self-supporting collars. Experience with Nb3Sn magnets has shown that replacing the collars with a thin spacer and using structural rings or wire wrap over the yoke improves the magnet structure. In the past, two different techniques have been tried. Magnet D20 [1]; a 13 T dipole; was assembled by wrapping a high-tension stainless steel wire over the yoke. In contrast, a shrink fit structural Aluminum tube was used in the assembly of Twente University 12 T dipole magnet [2]. In both cases the final pre-stress results were less than desirable even though attempts were made to assure high tolerances.

A. PRESSURIZED BLADDER SYSTEM (PBS)

It became apparent that if we want high pre-stress, good control during assembly and a cost effective magnet, a change of course would be required. We need to identify ways to generate measurably large forces in combination with relaxed coil tolerances.

Using a hydraulic bladder system meets these three goals. An inflated bladder is a "smart shim" that compensates for

low tolerances and can deliver large forces. Consequently there is no need for intermediate collars and pre-stress is delivered directly from the bladders and keys to the structural shell. Determining the stress of the shell can easily be done by measuring its strain. Bladders can be pressurized with melted liquid metal, as was done in the assembly of an ECR sextupole [3], or; as it was accomplished here; with the use of high water pressure and interference keys.



Figure 1. A bladder made from welded stainless steel sheets. The inlet tube is seen at the lower right corner.

Bladder technology was tested with a series of small bladders (25mm wide by 150mm long), made from two 0.254mm (0.010") thick stainless steel sheets, with a 1/8" stainless tube (0.2" wall) as a supply line.

Initially, bladders were welded by hand, but as progress was made an outside shop was used to laser weld them. The final main bladders used in RD3 were 190 mm wide and 890 mm long. Its internal pressure and the compliance of the coils and structure control the overall bladder gap-size.

B. BLADDER TEST

The range of a reliable gap-size as a function pressure was determined experimentally. The maximum pressure a bladder can sustain before it bursts is a function of its stroke (the gap between the two sheets). To determine the bladder characteristic curve (for 0.010" thick stainless steel sheet) bladders were placed within a known gap between two stainless steel beams. The beams were bolted and held in a press. Using a hand pump the water pressure was raised to 70-85 MPa (10-12 Kpsi). Several times during the test the bladder was deflated and the gap size increased. The pressurization process was repeated until a burst occurred. Results are plotted in Fig. 2. Test bladders could be pressurized to 70 MPa at 3 mm without failure. Some bladders survived at 6 mm gap and 70 MPa (over 800 MPa of tensile stress on the stainless steel sheets). Bladders that could sustain high pressure and large gap size usually failed somewhere along the weld; poor performing bladders tended to fail near the supply line. No special provisions were made to round the bladder's corners and we have not experienced

any difficulties at those locations.

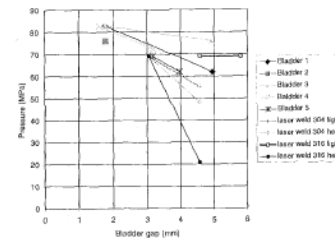


Figure 2. Pressure sustained by the bladder as a function of its gap.

C. Hydraulic System

Final magnet assembly used a commercial air driven pump system (Fig. 3), capable of delivering pressures up to 200 MPa.

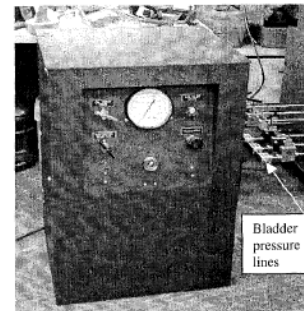


Figure 3. Bladder pressurizing unit.

II. RD3 ASSEMBLY

A. Dipole magnet RD3

Magnet RD3 [4] is a Nb3Sn common coil dipole expected to reach 14 Tesla in a 10 mm bore. At that field the average Lorentz side force is 15.4 MN/m (a total of 12.0 MN over the 780 mm coil length). A force of such magnitude can not be managed with a cantilever beam structure and tie-bolts as it was done in RT1 [5]. Further, a cantilever structure will not prevent the coils from separating over the gap. The

requirement for no coil separation, large forces, a fragile Nb3Sn coil and the need for reliable stress control made the use of bladders quite attractive.

The magnet is assembled from three sub-assemblies – a pre-assembled coil pack, a pre-assembled iron yoke and shell, and a set of keys and bladders (Fig. 6). The coil pack (Fig. 4) is an assembly of two inner coils, two outer coils (previously tested as RT1) and outer pads (iron). The coil-pack was pre-assembled and compressed with threaded pad-to-pad tie-rods. The iron yoke and shell were also pre-assembled in the vertical position and locked with temporary keys. The final magnet assembly of the coil pack and shell took place horizontally. Finally, bladders were inserted between yokes and pads with shims and special removable slip planes (to help during bladder extraction). As a precautionary measure auxiliary bladders were also used in the regions shown in Fig. 4. Bladders were inflated incrementally and temporary keys inserted every 15-20 MPa. After a final pressurization; corresponding to 85 MPa, final keys (1.5 mm thick) were inserted and the bladders deflated and removed with the aid of slip planes. The strain of the retaining Aluminum shell was measured continuously.

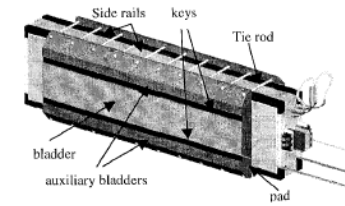


Figure 4. The coil pack is an assembly of coil modules between iron pads. On the pads facing away from the coils are key slots. Bladders are placed between keys

B. Concept of Operation

The balance of forces between the shell and coils takes place in several steps. Initially the shell pre-stress value is set at 150 MPa by the bladders and keys. During cool-down the stress increases to its final value of 250 MPa and remains unchanged during operation. The reason for that can be explained as follows (Fig. 5). Forces on the shell at point A are balanced by reactive forces between the two symmetrical halves of the magnet (point B). At point B reactive forces are carried by the coil and iron post. As the magnet is energized the increase in Lorentz force is balanced by an identical decrease in reactive forces in the post and side rails (Fig. 4), leaving the stress in the shell unchanged and minimum coil motion. The magnet was designed with enough pre-stress to keep a finite reactive force up to 16 T. In addition, during operation the combination of keys and pads protect the coils from bending. The pad's thickness was chosen in such a way

Manuscript received September 16, 2000.
Mail stop 46-16, LBNL, Berkeley CA 94720 USA
This work was supported in part by the Director, Office of Science, Office of High Energy and Nuclear Physics and Director, Office of Basic Energy Sciences under U.S. Department of Energy Contract No. DE-AC03-76SF0098.

Overview

2274

that while the side facing the yoke deforms, the side facing the coil remains flat.

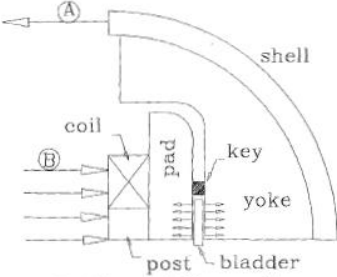


Figure 5. Fixtures related to RD3 magnet assembly

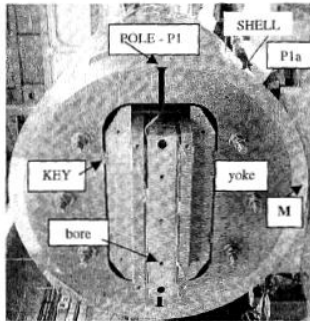


Figure 6. End view of RD3 showing the Aluminum shell, iron pads and yokes, 3 coil modules and keys between yokes and pads.

III. STRUCTURAL SHELL

A. Mechanical Model

In order to test the bladder in a geometry that is similar to RD3 we built a 1/3 scale mechanical model. We used a 6061 T6 aluminum tube (240 mm OD, 12.6 mm wall, 305 mm long) and standard off-the-shelf iron (equivalent to 1018). The yoke and pads were cut from 2" thick iron plates using an Electrical Discharge Machine (EDM). A simulated coil pack was made from aluminum blocks and an iron post clamped inside iron pads and tie rods (similar to Fig. 4). The shell was put into tension using two bladders and a hand pump. Water

pressure in the bladders was raised to 80 MPa before iron keys were inserted. After cool down to 4.2 K the shell reached a final pre-stress equivalent to a field of 15 T. We have concluded that the measured strain of the shell followed closely an ANSYS two-dimensional plane-stress model with friction. The strain-stress relations of the mechanical model and magnet RD3 are the same, but the size of the forces and displacements are different. The similarity between the two cases and the fact that, with proper key size, Lorentz forces should not contribute to an increase in the shell stress after the magnet is energized, makes the test results of a mechanical model identical to those obtained during the final magnet assembly. Pressurizing the bladders strain the outer aluminum shell. Strain gauges installed around the shell can be calibrated directly against the bladder pressure and compared with those calculated with the program ANSYS (Fig. 7).

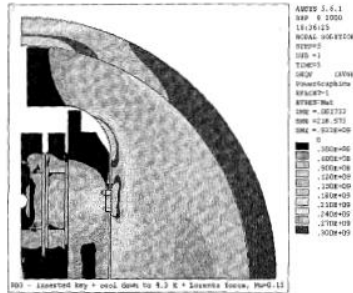


Figure 7. Van-Mises stress at 14 T

B. Magnet RD3

The RD3 shell was machined from a 2219-T852 Aluminum forging (740mm OD, 40mm wall and 890 mm long). The iron yoke laminations were cut from 2" plates using a water jet with a final machining. During assembly the shell strain was measured at all symmetrical points corresponding to M, P1a, and P1. Point P1a is a location that is both bending free and free from friction effects. Several gauges were instrumented to read strain in the axial direction. The measured strain at location M is plotted against the bladder pressure in Fig. 8. The horizontal data points correspond to the shell unloading and loading on temporary keys. Final size keys of 1.5 mm were used corresponding to a shell strain of 1830 microstrain. When the results are compared with ANSYS, the measured strain agrees well when a friction factor of 0.15 is applied between the yoke and the shell. That friction factor was down from a value of 0.25 observed in the mechanical model and in agreement with the improved surface quality used in the magnet parts. Location P1 at the pole area was instrumented

at both ID and OD locations. With the understanding that the shell will undergo bending at P1 we expected local yielding along the pole ID. The choice to allow local yielding was a way to avoid making the shell oval which would have resulted in a shell that is costly and more time consuming to make.

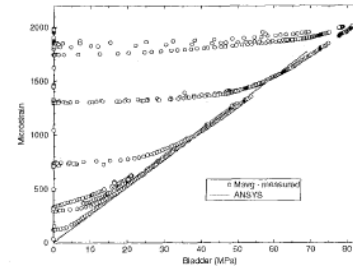


Figure 8. Strain of shell at point M during bladder operation.

Table I Shell stress-strain during assembly

LOCATION	RD3 MEASURED		ANSYS	
	STRAIN (MIC)	STRESS (MPa)	STRAIN (MIC)	STRESS (MPa)
MOD	1834	143	1770	138
P1a	2020	157	2134	166
POD	-657	-67	0	0.1
PIB	5120	400	4115	321

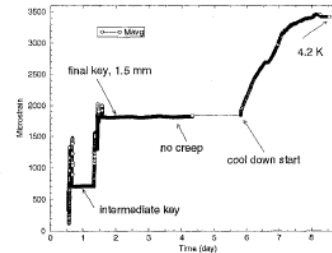


Figure 9. Strain as a function of time measured on the shell at point M.

Magnet assembly with bladders required no more than a couple of days. As shown in Fig. 9 only about 10% of strain loss occurs after the bladders are deflated. It is also apparent that there is no creep and the magnet structure maintained its

2275

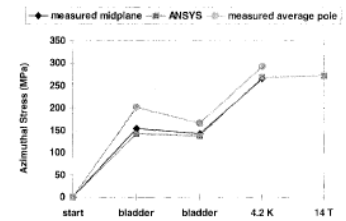


Figure 10. Stress of shell at various times.

strain many days following the assembly. During cool down we expected the strain in the shell to double. At 4.2K the strain increased to a measured value of 3420 microstrain compared with 3461 calculated by ANSYS (Fig. 10). That strain is equivalent to a stress of 267 MPa in the shell. As the magnet reaches its final field of 14 T we expect the shell to remain at that stress level and all inner coils to remain in contact (e.g. no coil separation as seen during the RT1 test [6]).

IV. CONCLUSION

We have demonstrated the use of high-pressure bladders in the assembly of high field superconducting magnets. Such a system can deliver a well-controlled pre-stress level to both coil and structure regardless of tolerances. This method also ensures a similar straightforward operation during magnet disassembly.

ACKNOWLEDGMENT

We are grateful to Roy Hannaford, Jim Swanson, Nate Liggins, Paul Bish, Hugh Higley, Evan Palmerston and Doyle Byford whose hard work and dedication keeps us all motivated.

REFERENCES

- [1] S. Caspi, K. Chow, D. Dieterich, A. Lietzke, A. McInturff and R. Scanlan "Development of high field dipole magnets for future accelerators," Proceedings of 15 International Conf. On Mag. Tech, Beijing China, pp 51-54, Oct. 1997.
- [2] A. den Ouden et al. "An experimental 11.4 T Nb3Sn LHC type of dipole magnet," IEEE Trans. Mag. Vol. 30, pp. 2520, 1995.
- [3] C. Taylor, S. Caspi, M. Leitner, S. Lundgren, C. Lyness, D. Wutte, S. T. Wang and J. Y. Chen "Magnet system for an ECR ion source," IEEE Trans on Applied Superconductivity, vol. 10, No. 1, pp. 224-227, March 2000
- [4] S. Caspi, M.Fong, S.Gourlay, R. Hafalia, A. Lietzke and J. Oneill, "RD3 Structure," SC-MAG 725, Lawrence Berkeley National Laboratory, June, 2000.
- [5] S. Caspi "RT1 structure," SC-MAG-707, Lawrence Berkeley National Laboratory, February, 2000.
- [6] S.Gourlay et al. "Fabrication and test of Nb3Sn racetrack coils at high field," this conference.

Outline

- Overview
- **General concept**
- Loading steps
- Design criteria
- Assembly steps
- Axial loading
- Additional topics
 - Alignment
 - Aluminum shell segmentation
 - Lhe containment

General concept

- Room temperature pre-load provided by bladders
 - About 30-50% of total pre-load
 - Large force, easily adjustable
- The rest from shell cool-down
 - Offset!
- In general, targeting 150-200 MPa on the coil at cold
 - 35 MPa in the LHC dipole
- Generally, less than 100 MPa coil stress at warm
- Peak stress reached from below
 - No “collaring peak”
- Yoke gap always open
 - Shell force directly to the coil
 - Still quite rigid

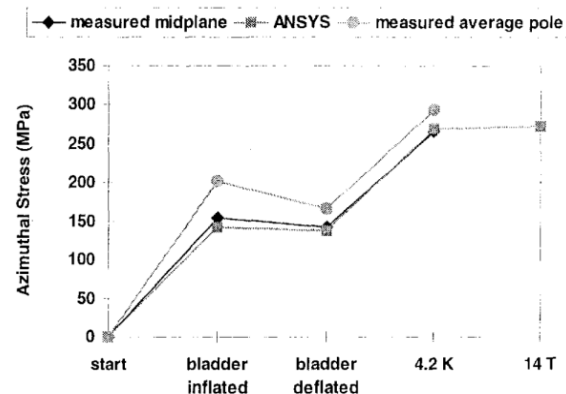
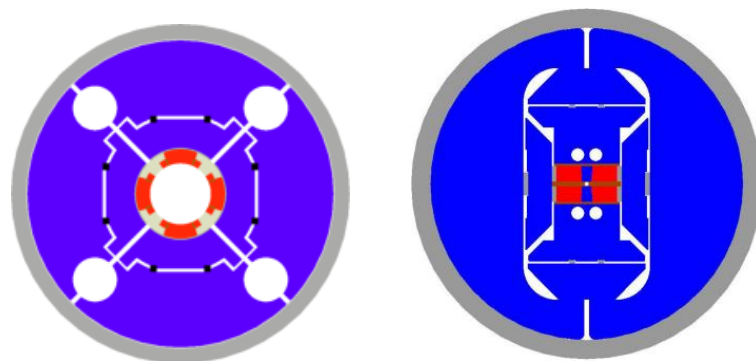


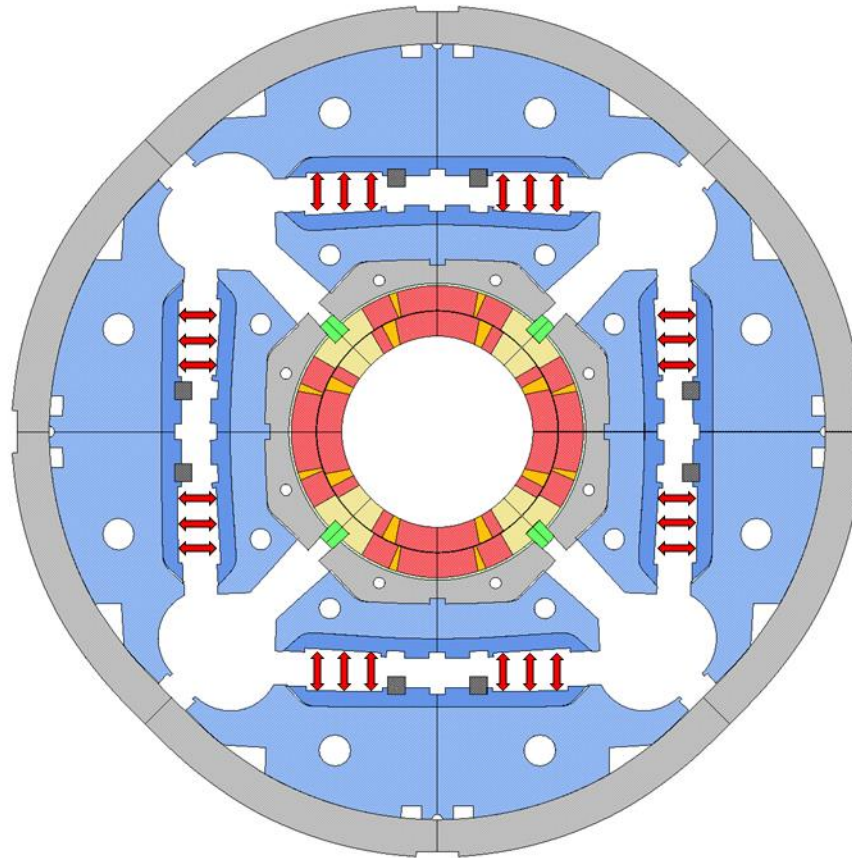
Figure 10. Stress of shell at various times.



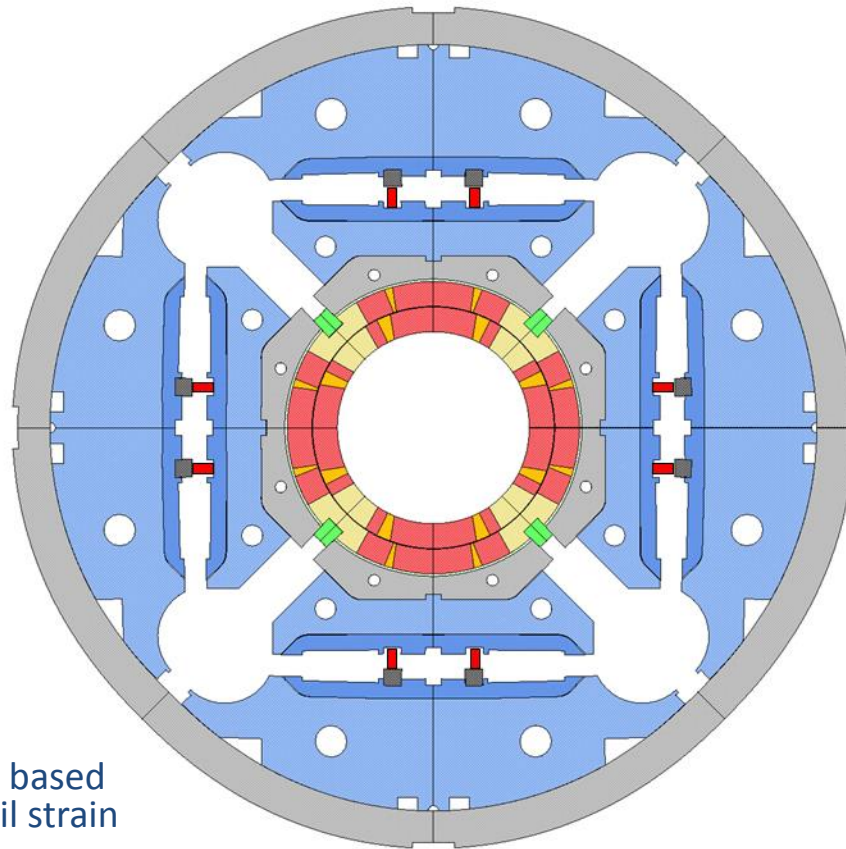
Outline

- Overview
- General concept
- Loading steps
- Design criteria
- Assembly steps
- Axial loading
- Additional topics
 - Alignment
 - Aluminum shell segmentation
 - Lhe containment

Bladders: 45 MPa (700 μm gap)

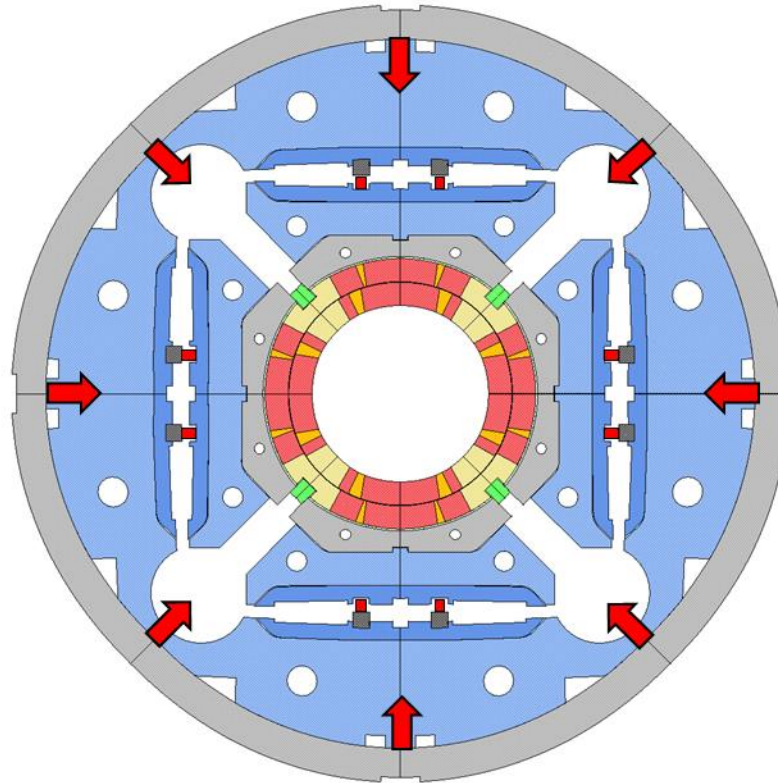


Key: 550 μm

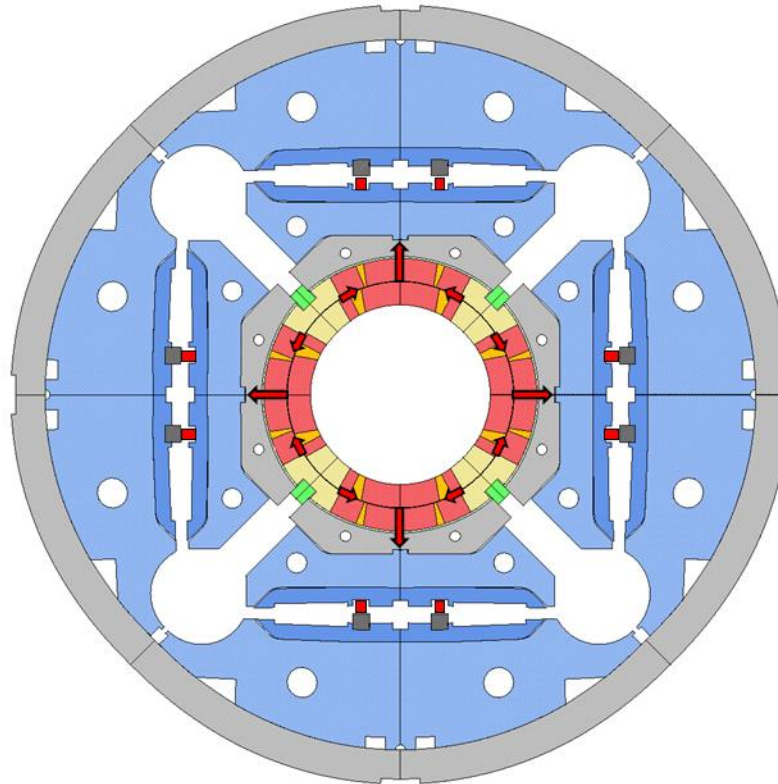


- We impose a coil stress based on shell stress, not a coil strain based on a cavity
 - Less sensitive to uncertainties on elastic modulus

Cool-down to 1.9 K



132.6 T/m

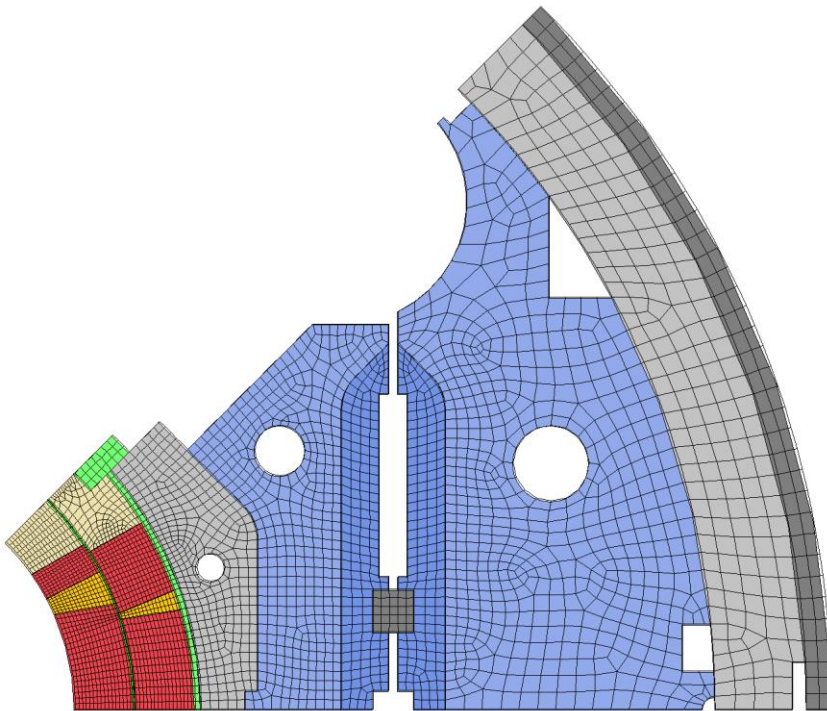


Outline

- Overview
- General concept
- Loading steps
- **Design criteria**
- Assembly steps
- Axial loading
- Additional topics
 - Alignment
 - Aluminum shell segmentation
 - Lhe containment

2D ANSYS model

- Potted Nb₃Sn coil „glued” with contact elements
- Contact elements between the structure parts model the friction
 - Friction coefficient $\mu=0.2$
- Continuous analysis of the magnet life-cycle
 - Bladders operation
 - Key insertion
 - LHe vessel installation
 - Cool-down
 - Magnetic forces
 - From ANSYS magnetic model
- “Plane stress”



Criteria (Frascati 2012)

- Pole-coil contact in pole-turns midpoint

$$p_{\text{cont}} \geq 2 \text{ MPa}$$

- Max bladder pressure

$$< 50 \text{ MPa}$$

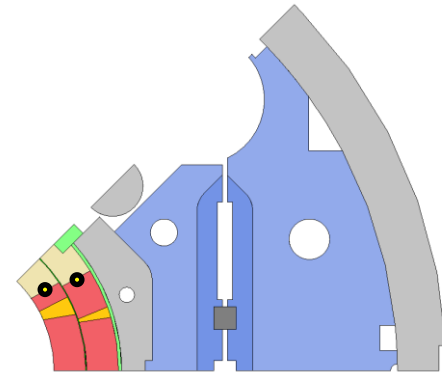
- Bladder should open the interf=interf_{nom} + 100μm

- $\sigma_{\text{eq coil max}} \leq 150\text{-}200 \text{ MPa}$ at
4.3K and 155 T/m
 $\leq 100 \text{ MPa}$ at 293K

- All components $\sigma \leq R_{p0.2}$

- For iron at 4.3K (brittle)

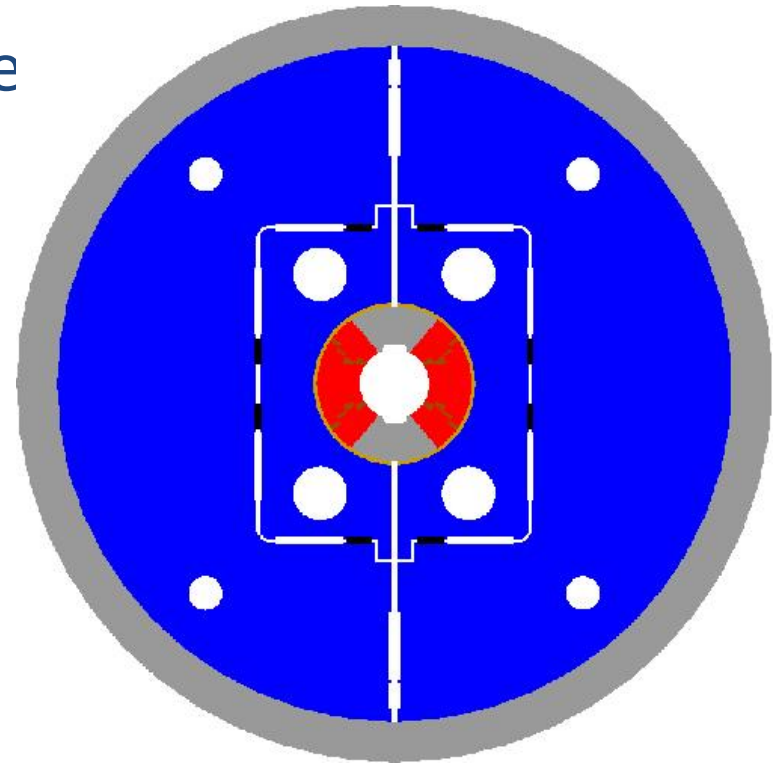
$$\sigma_l \leq \sim 200 \text{ MPa}$$



Material	$R_{p0.2}$ [MPa]	
	293 K	4.3 K
Al 7075	480	690
SS 316 LN	286	930
NITRONIC 40	353	1240
MAGNETIL	180	723
Ti 6Al 4V	827	1654

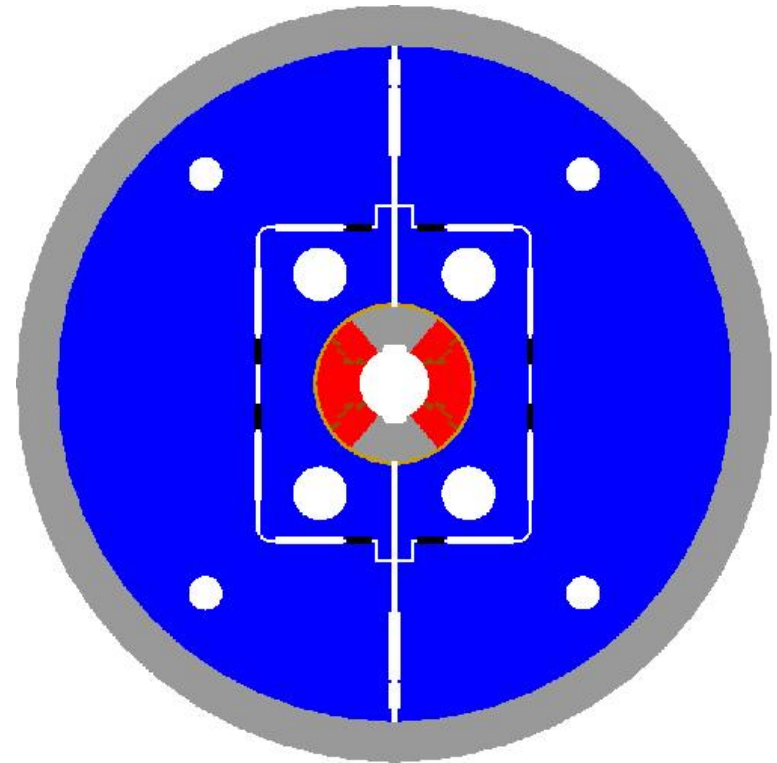
Shell

- Thickness
 - It sets the cool-down force
 - 80-100 MPa of stress
 - more or less $(\alpha_{Al} - \alpha_{iron}) \cdot E_{al}$
 - Probably, an “healthy” condition is with shell providing 50-70% of the total force
- Diameter
 - Mainly given by what’s inside



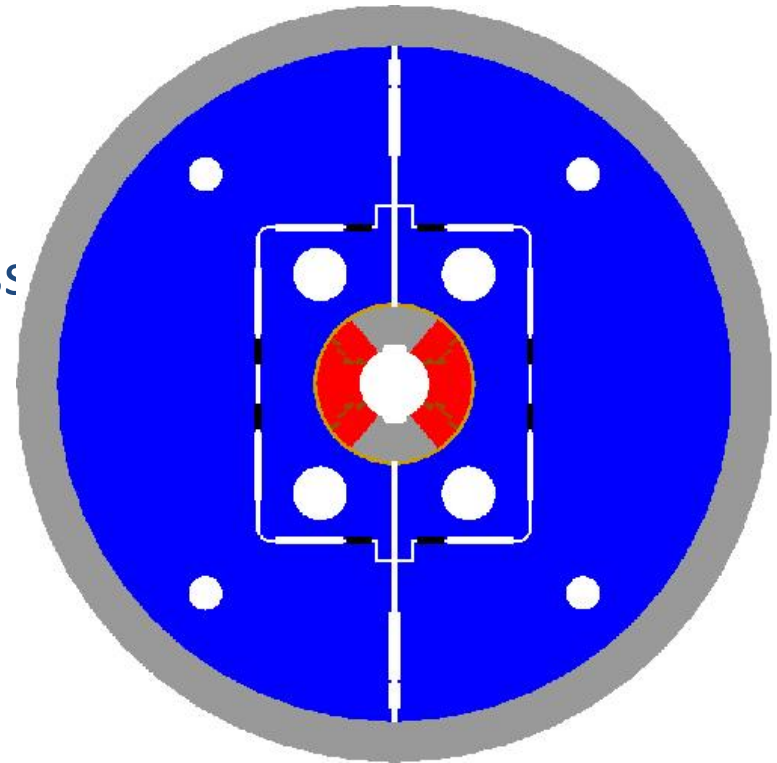
Yoke

- General size
 - At cold one of the most critical target is $\sigma_1 \leq \sim 200$ MPa
 - Keep an eye also to the room temperature peak stress < 180 MPa



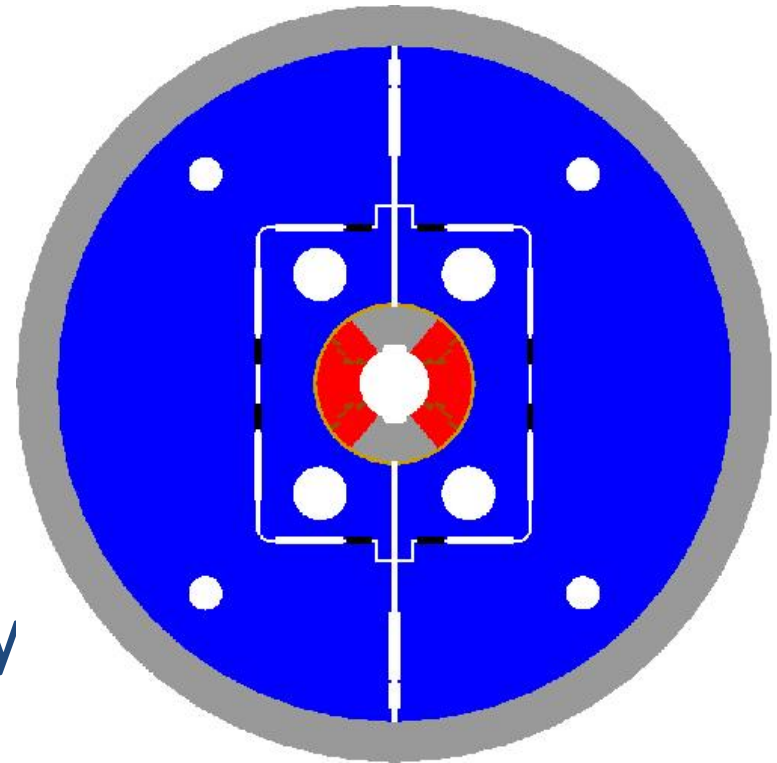
Pad

- General size
 - Some bending during bladder operation
 - Sometime made of stainless steel to increase limits
 - With keys, normally no issue
- Shape
 - Maximize bladder size
 - May include axial rods



Bladder

- Max pressure, assume 50 Mpa for the “short sample condition”
 - In reality 70 MPa
- Assume over pressure to produce clearance for key insertion: ~ 0.100 mm



Bladder MQXFS1

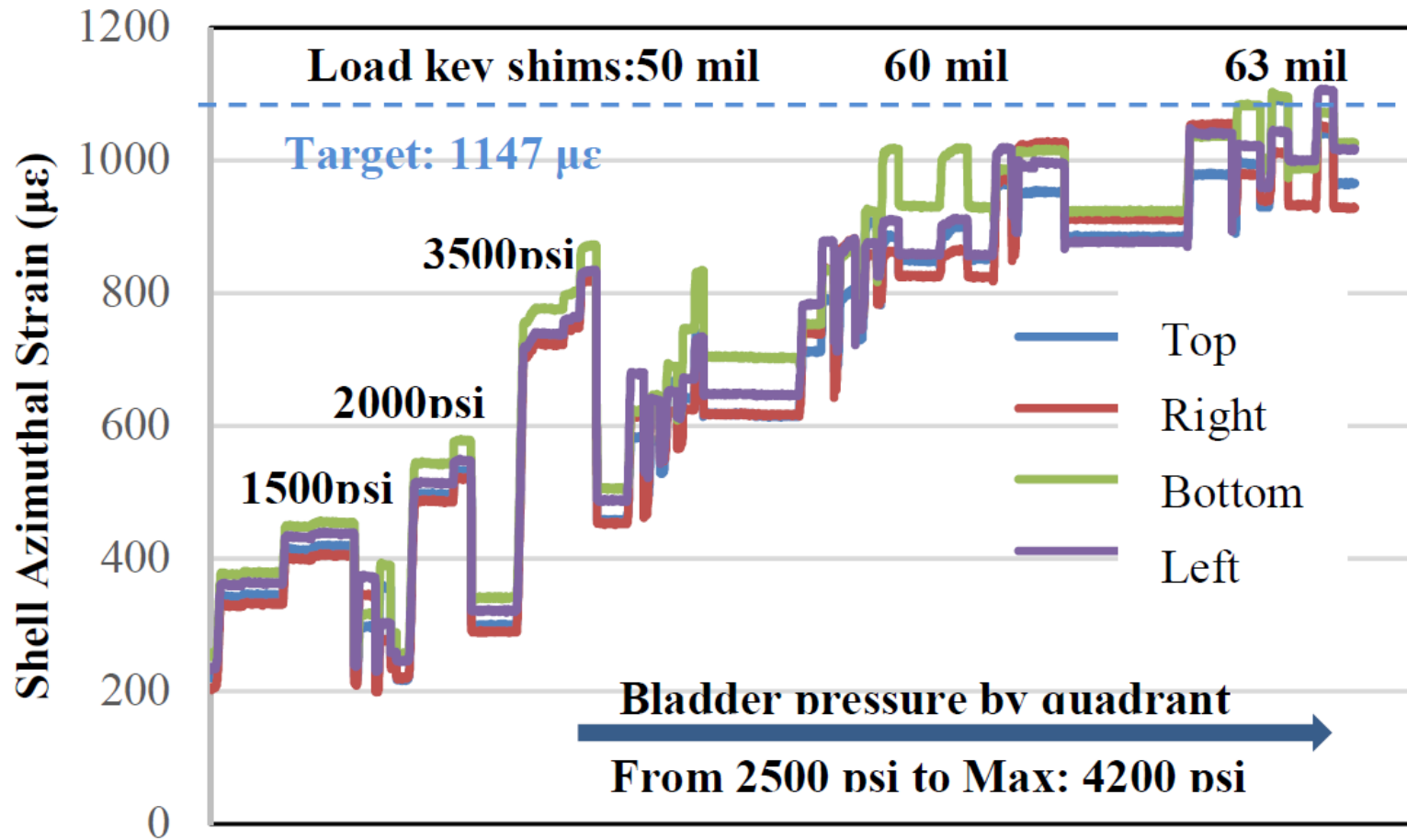
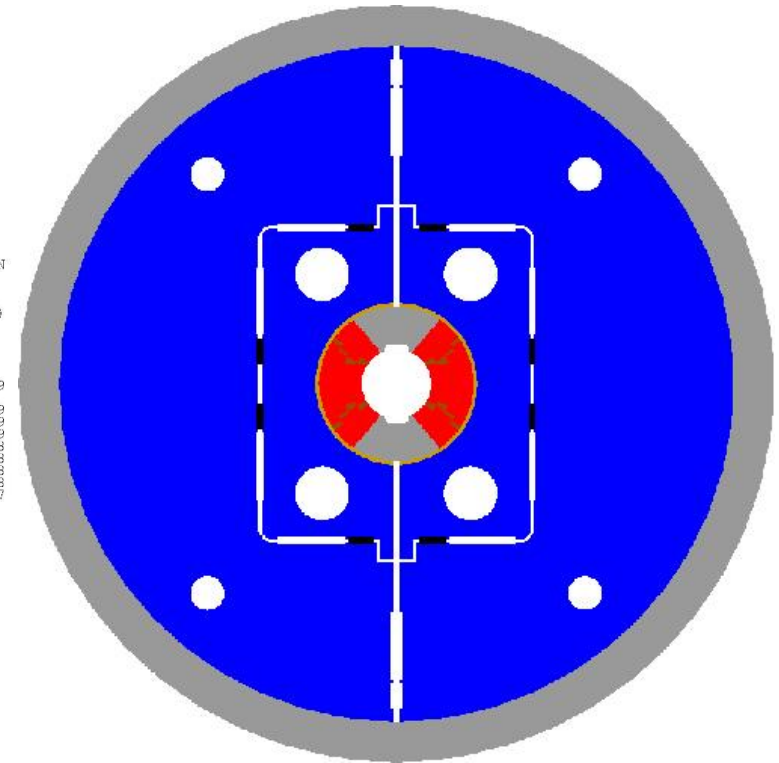
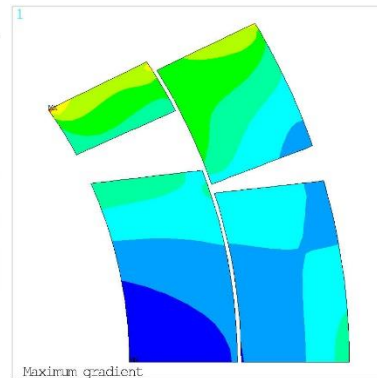
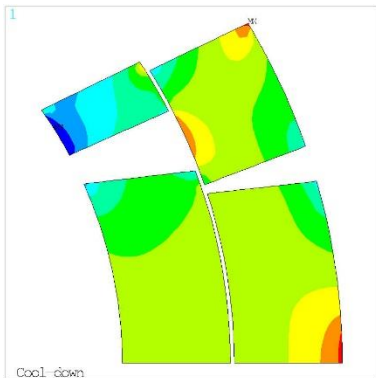


Fig. 9. Strain data of the mid-planes of the shell in the azimuthal pre-loading

Key

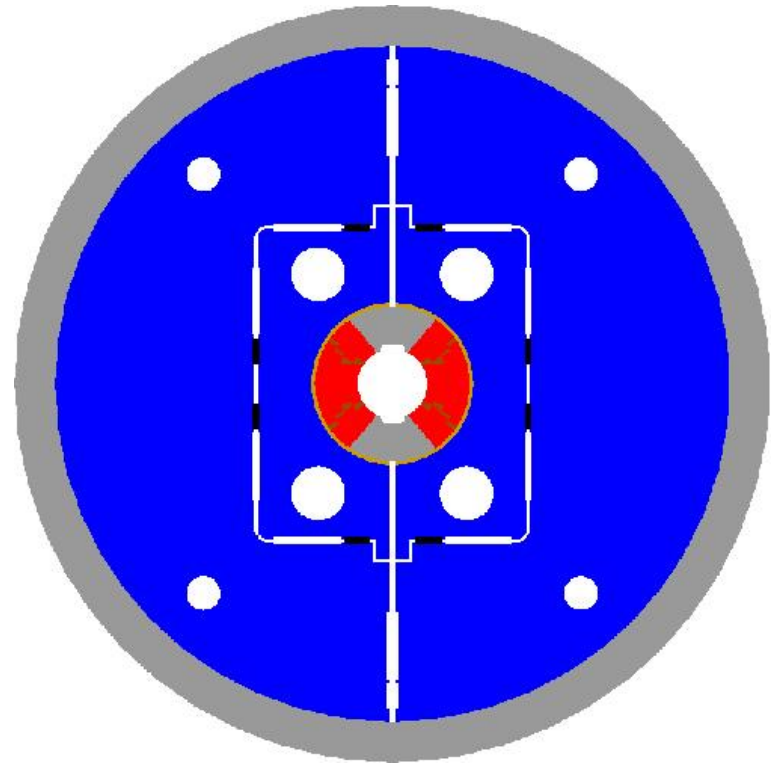
- Horizontal
 - Optimized to minimize coil stress at cold and with e.m. forces



- Interference/shim of ~ 0.5 mm: easy fine tuning of room temperature stress

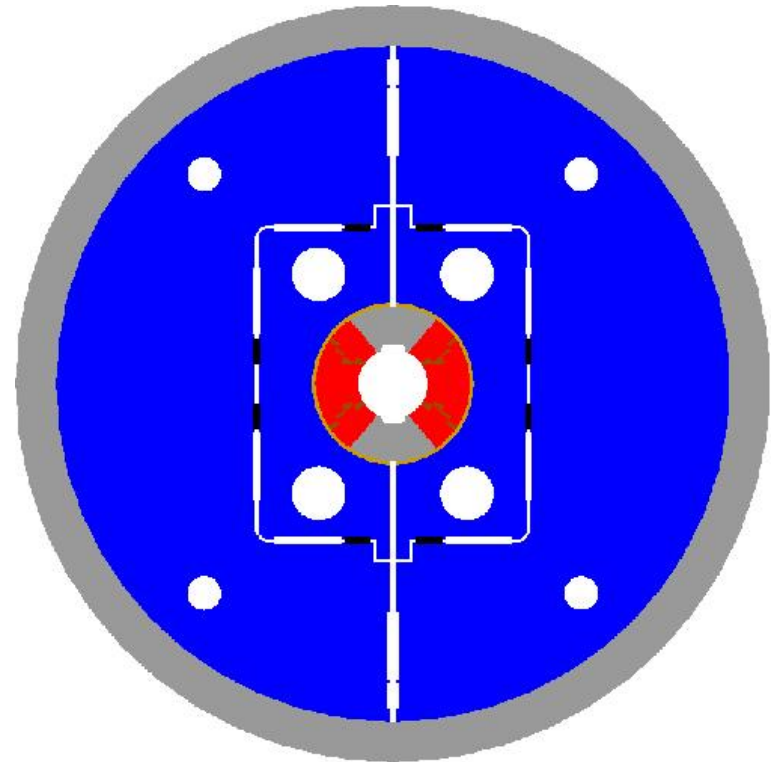
Key

- Vertical
 - Just tight at warm
 - In any case it is not easily controllable
 - At cold, usually not much force intercepted
 - Vertical pre-load provided by bending of the yoke



Coil

- A cut-out in the pole may help a lot to reduce peak stress at cold
 - But no strain gauges
- Hard to have uniform contact pressure on the pole with e.m. forces



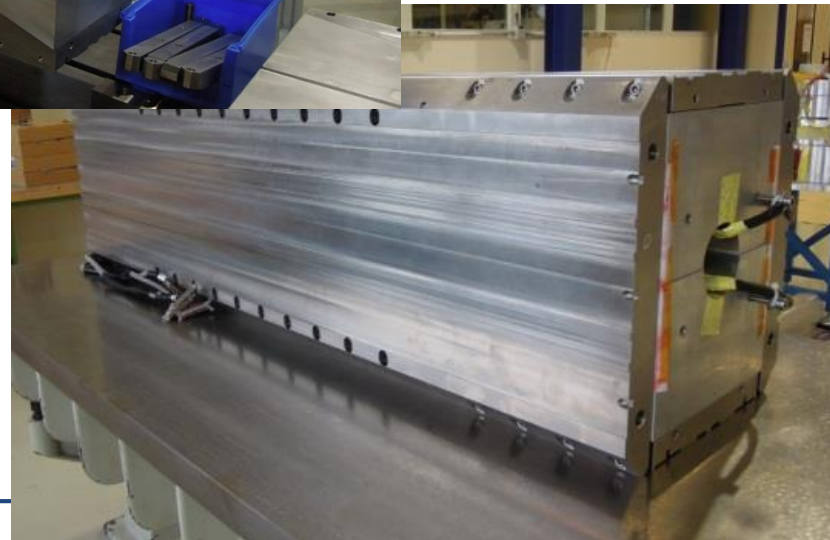
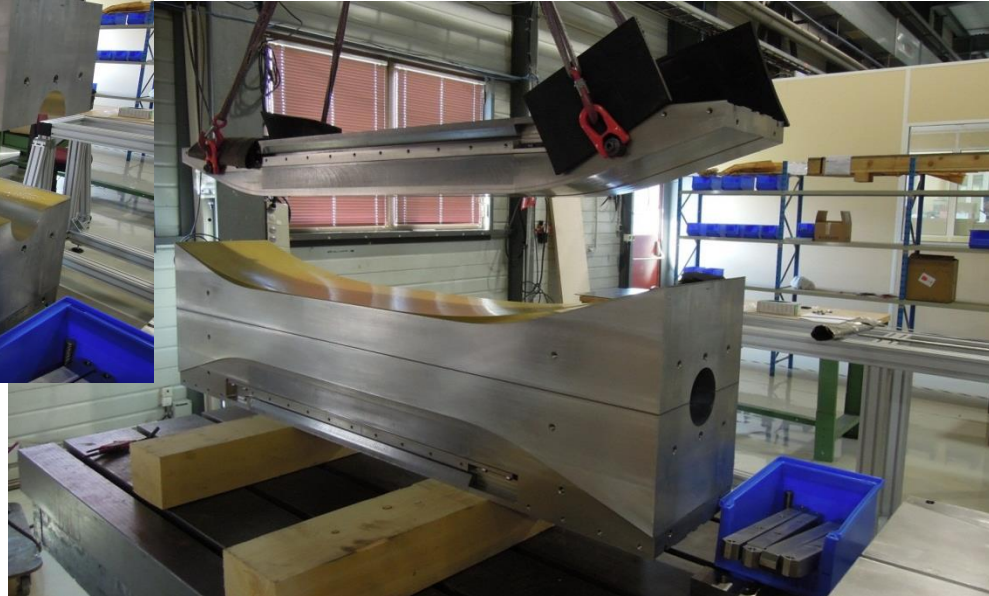
Outline

- Overview
- General concept
- Loading steps
- Design criteria
- **Assembly steps**
- Axial loading
- Additional topics
 - Alignment
 - Aluminum shell segmentation
 - Lhe containment

assembly

Assembly of the coil-pack with

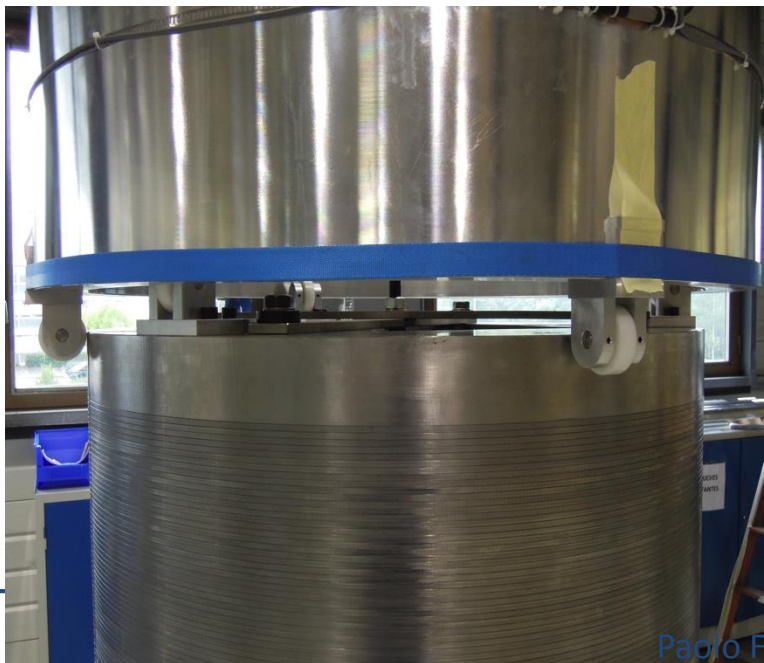
drummers



assembly

Sliding the shell around the yoke-

halves...



Paolo Ferracin

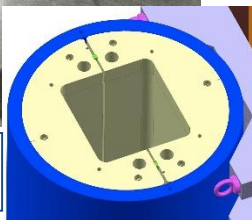
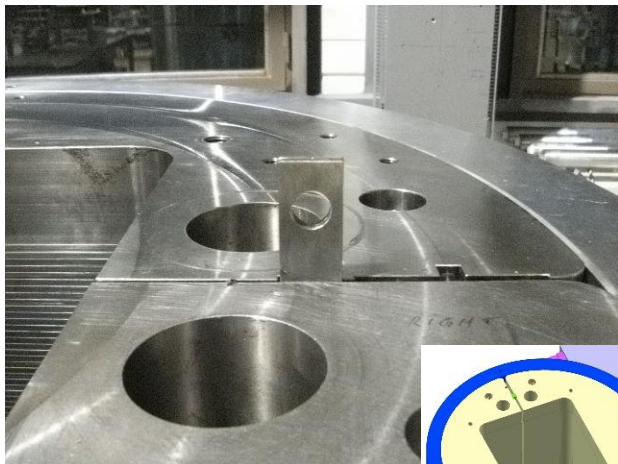
Jorge Enrique MUÑOZ GARCIA

20/01/2016

29

assembly

Handling the shell & yoke...



Gap-keys
insertion



assembly

Sliding the coil-pack in...

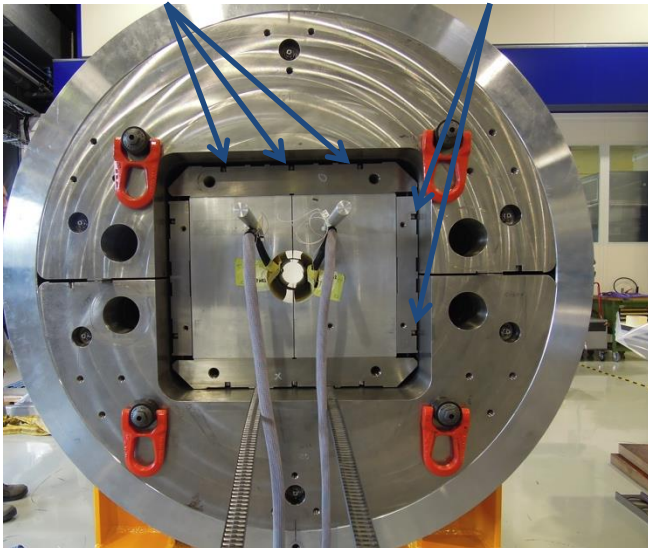


loading

Bladder operation...

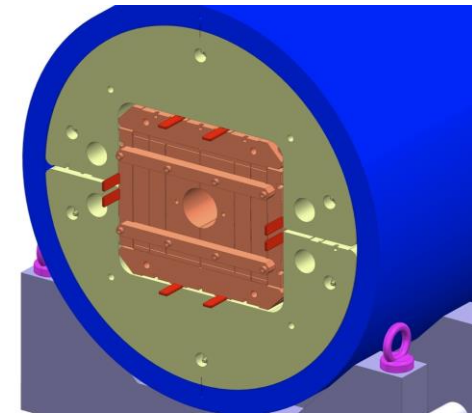
Horizontal bladders

Vertical bladders



Horizontal bladders

Vertical bladders



Paolo Ferracin

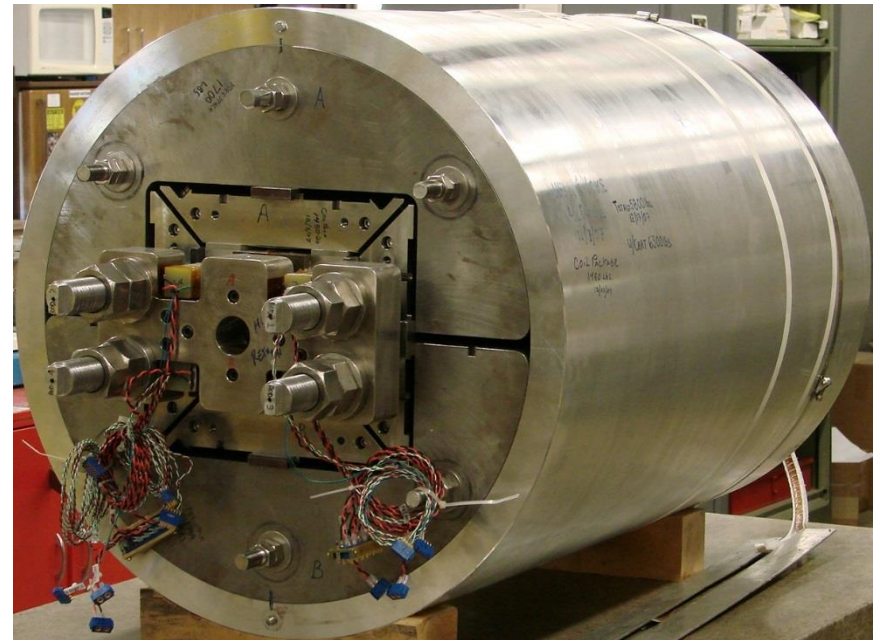
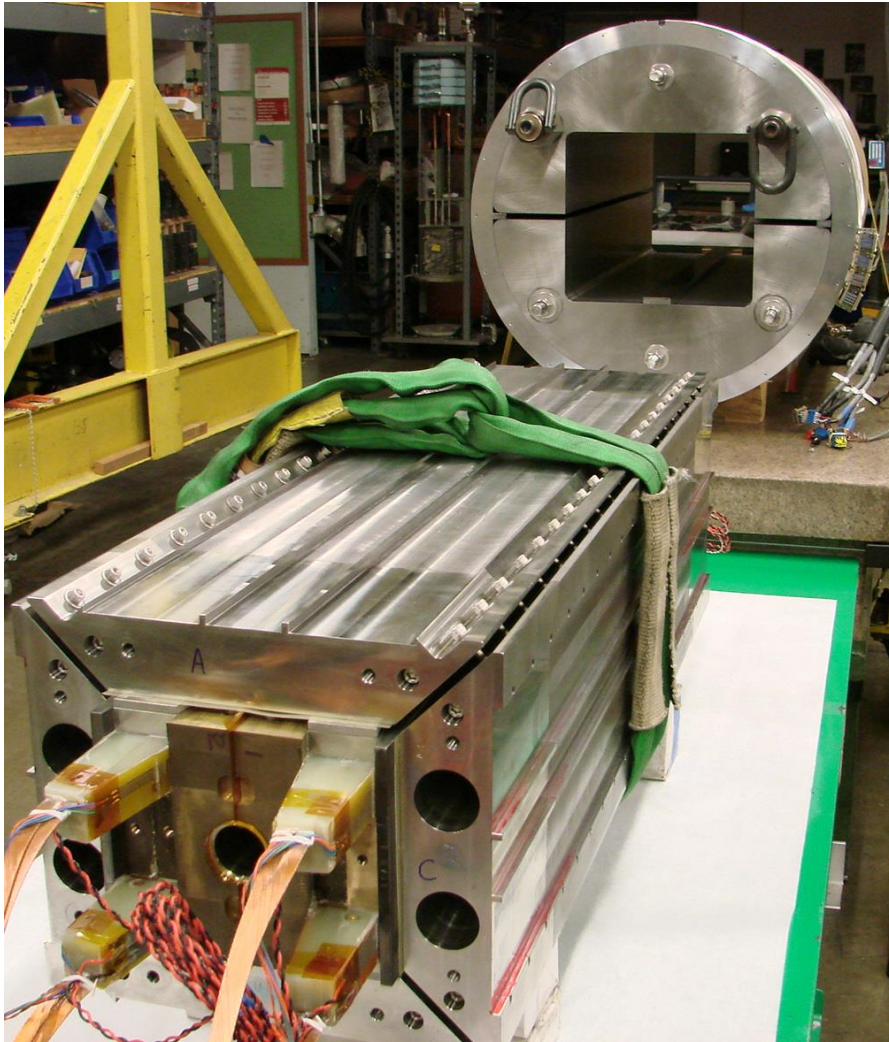
Jorge Enrique MUÑOZ GARCIA

20/01/2016



32

Assembly steps



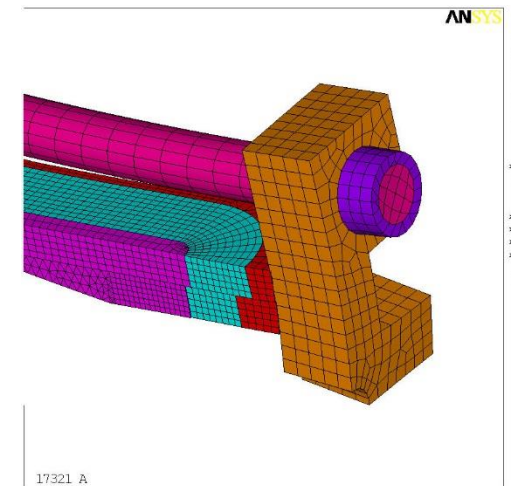
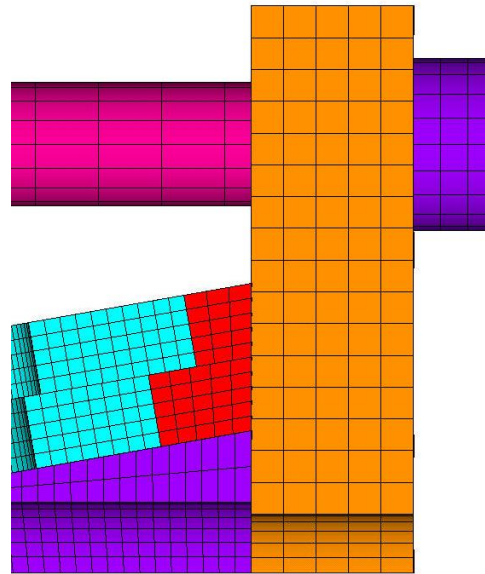
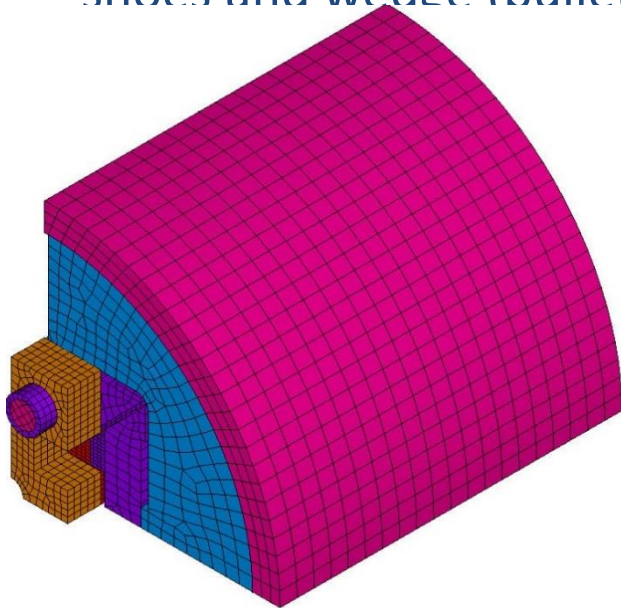
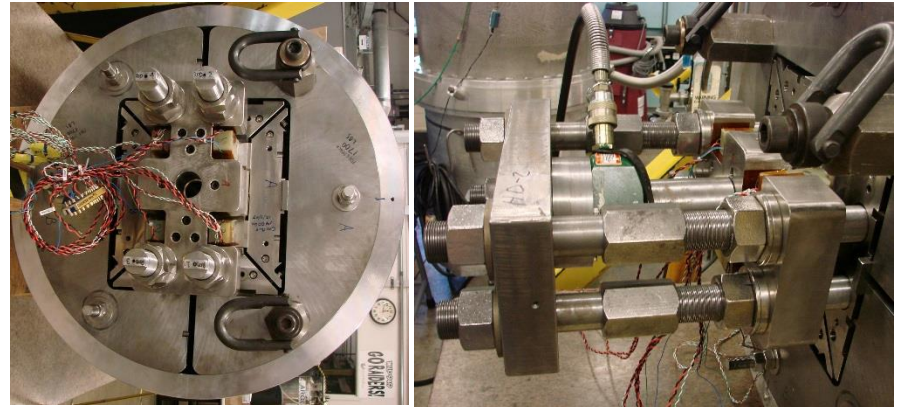
Outline

- Overview
- General concept
- Loading steps
- Design criteria
- Assembly steps
- **Axial loading**
- Additional topics
 - Alignment
 - Aluminum shell segmentation
 - Lhe containment

Mechanical analysis

End region

- Axial force at 15 T: 780 kN
- Full axial support at 4.5 K
 - No coil – pole separation in the ends
- Axial force shared between end-shoes and wedge (bullets)



loading

Rod pre-tension...



Rotating the assembled structure...



Structure fully assembled

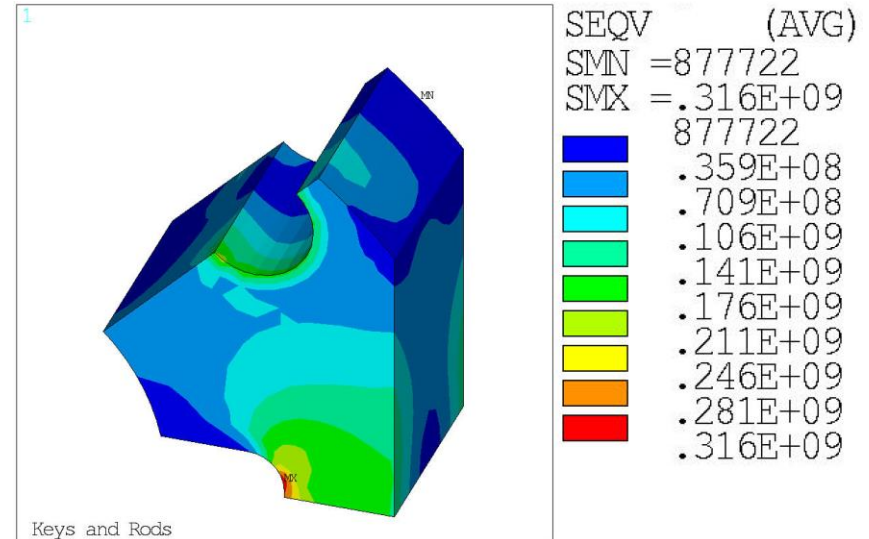
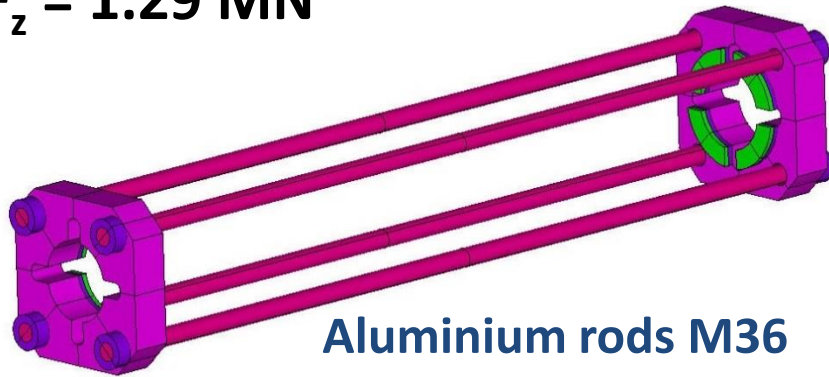


Structure ready for test

Axial preload system

Axial magnetic force at 140 T/m

$$F_z = 1.29 \text{ MN}$$

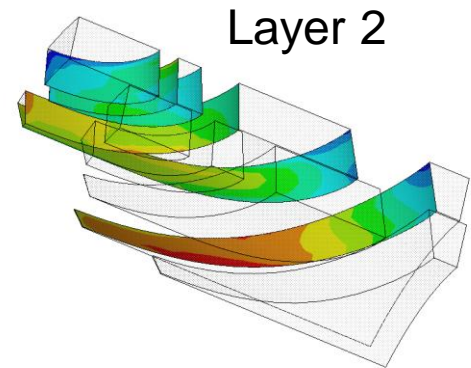
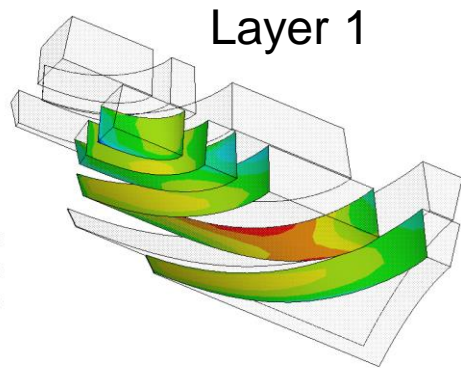
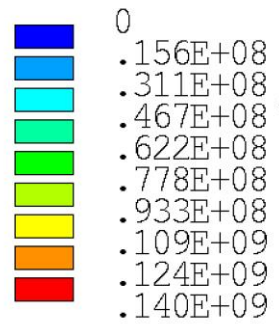
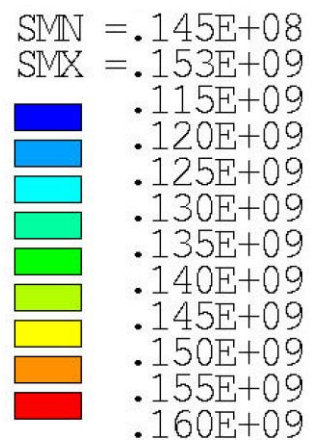
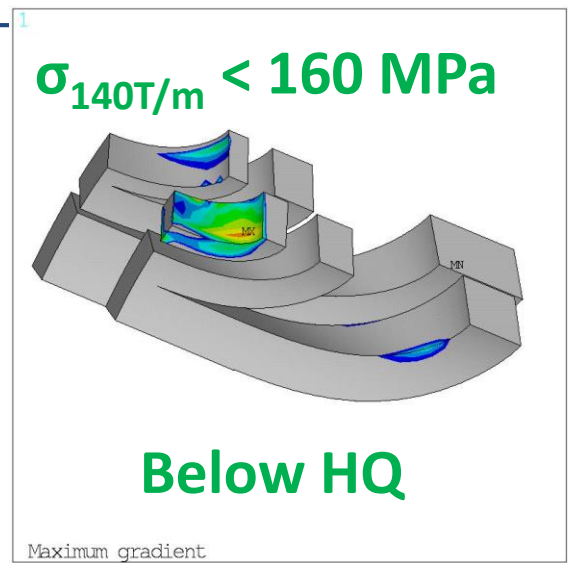
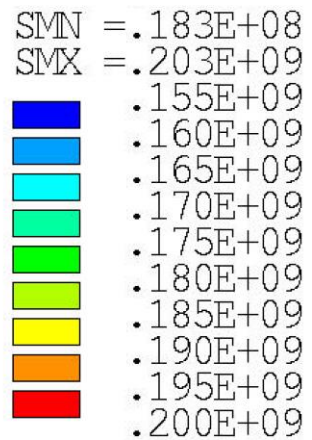
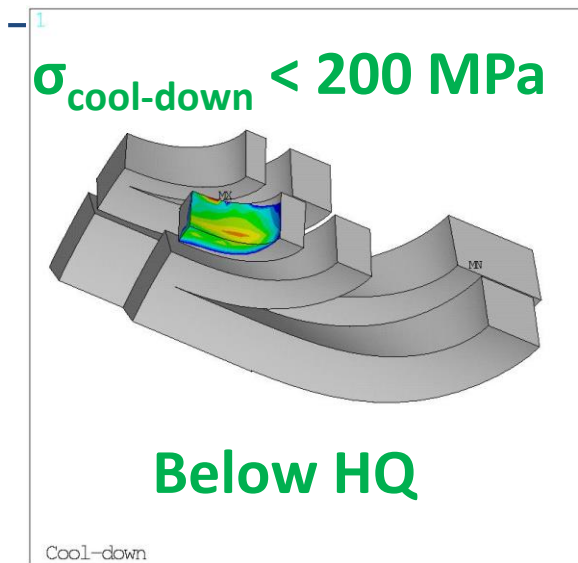


	Rods F_z [MN]	Rods σ_z [MPa]	Plate σ_{eqv} [MPa]
Warm	0.76	185	316
Cold	1.23	304	541
Forces 140 T/m	1.25	307	545

End-plate (lead-end)

- Nitronic 50 HS, 75mm thick
 - minimum YS: 515 MPa (in RT)
 - minimum UTS: 795 MPa (in RT)
- **Negligible plate deflection due to magnetic forces (few microns)**
- **Displaced by 50 μ m during powering (stretching of the rods)**

Stress and preload in the coil return-end



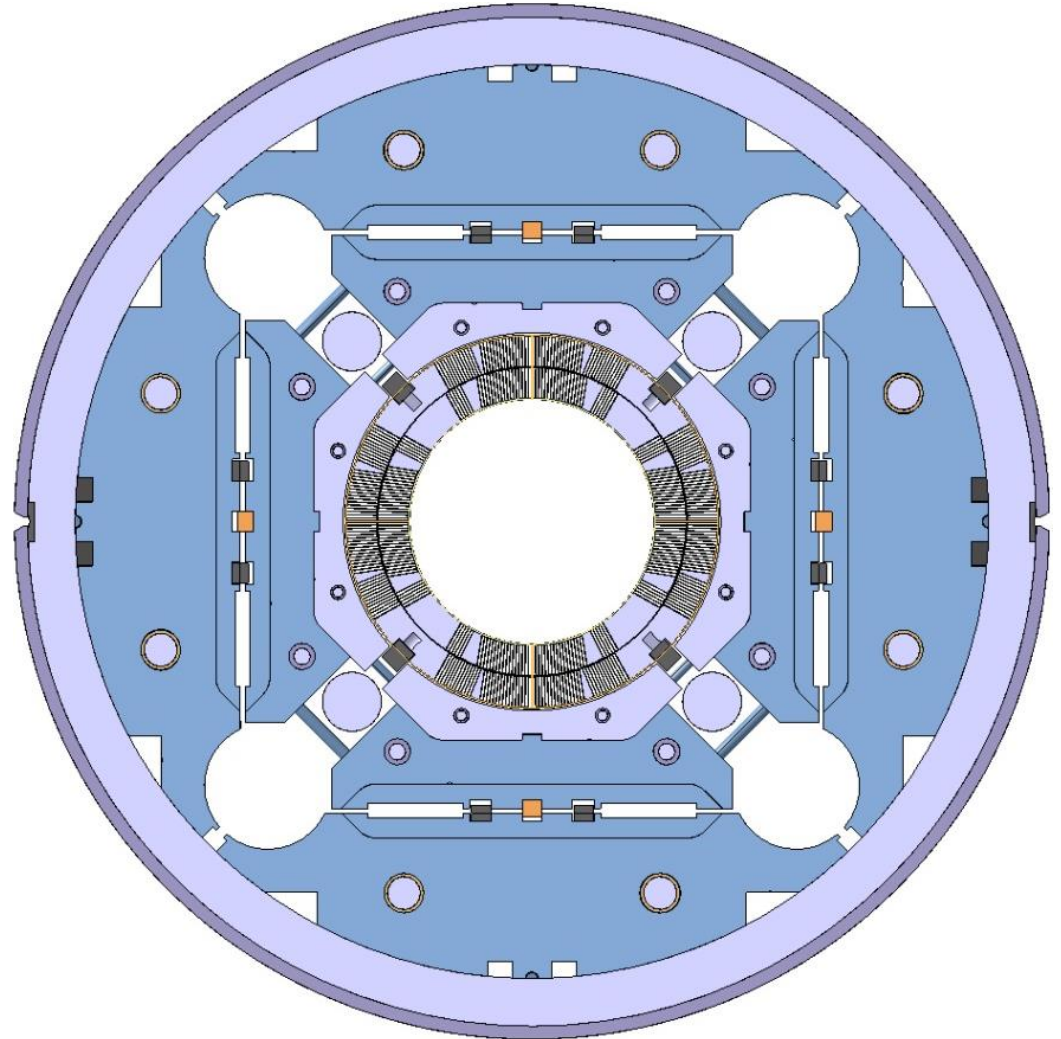
Contact pressure against poles and spacers

Outline

- Overview
- General concept
- Loading steps
- Design criteria
- Assembly steps
- Axial loading
- **Additional topics**
 - Alignment
 - Aluminum shell segmentation
 - Lhe containment

MQXF

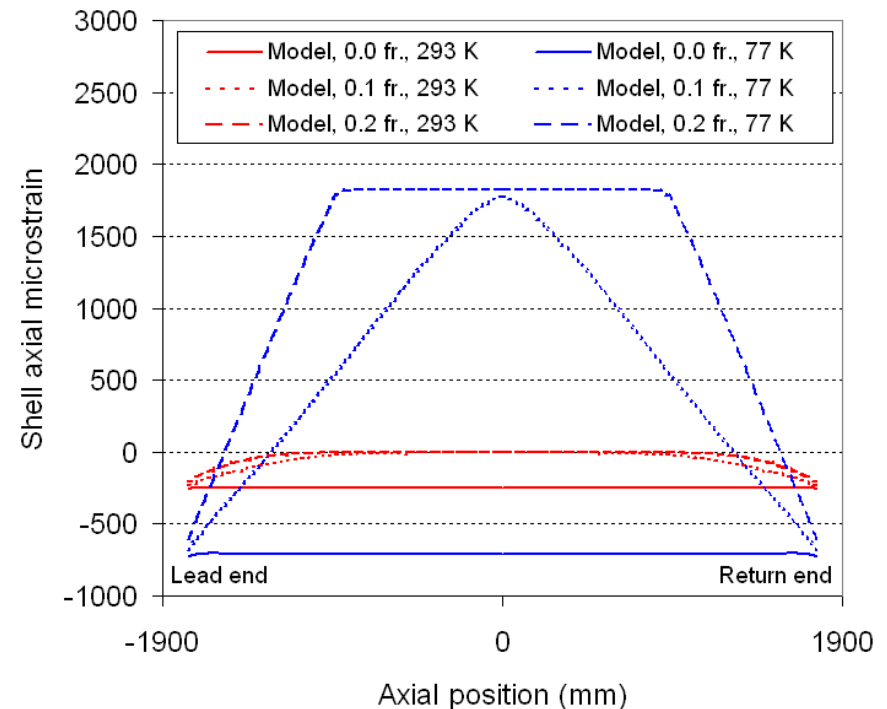
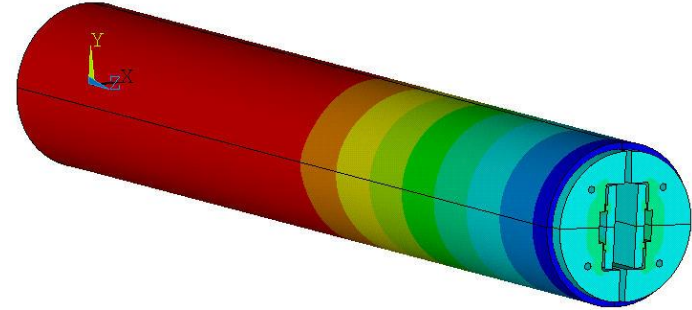
- Aluminum collars
 - No pre-load
 - Bolted on pole keys
 - Minimal interception of shell forces



Effect of friction in end region

Model results

- In a frictionless model the shell slides axially with respect to the yoke
 - Poisson effect
 - $\varepsilon_z = \nu\varepsilon_\theta$
 - Higher thermal contraction
- Friction between shell and yoke limits shell sliding
- The shell axial strain varies along the length depending on friction factor
- Similar behavior is expected on the dummy coils

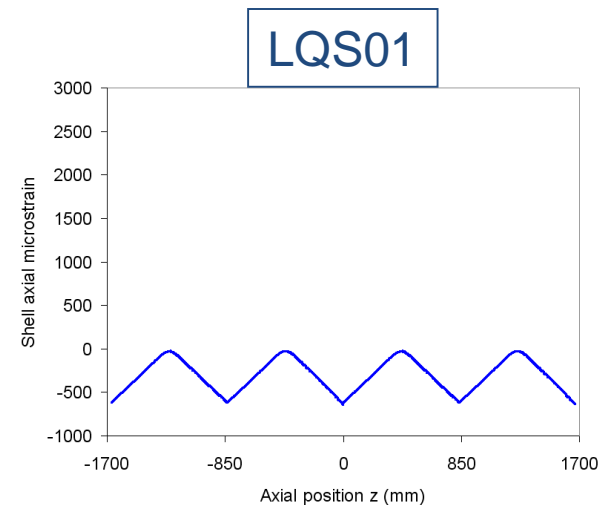
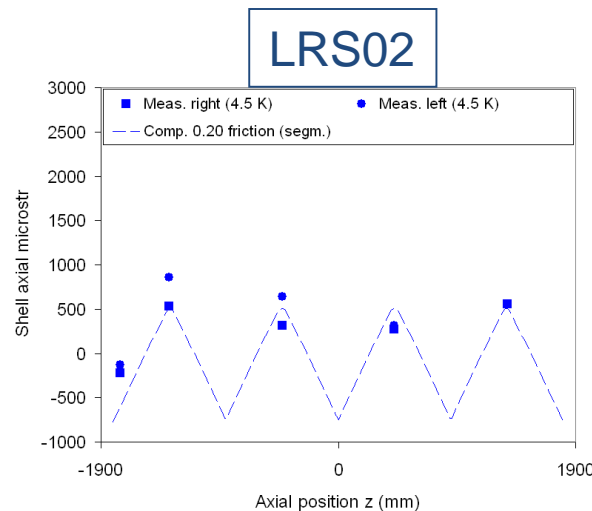
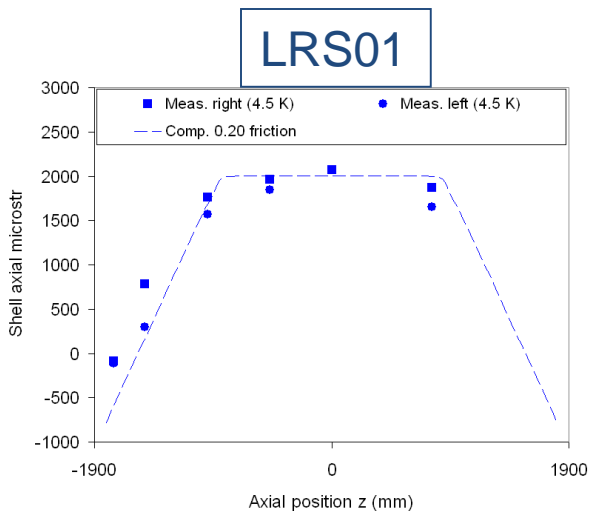


3D mechanical analysis

Axial strain in the aluminum shell

- During cool-down, shell shrinks more than yoke
 - Friction limits the shell contraction
- High measured axial strain in LRS01
 - Effect on azimuthal stress
- LRS02 and LQS01 with segmented shell
 - Reduction of axial strain

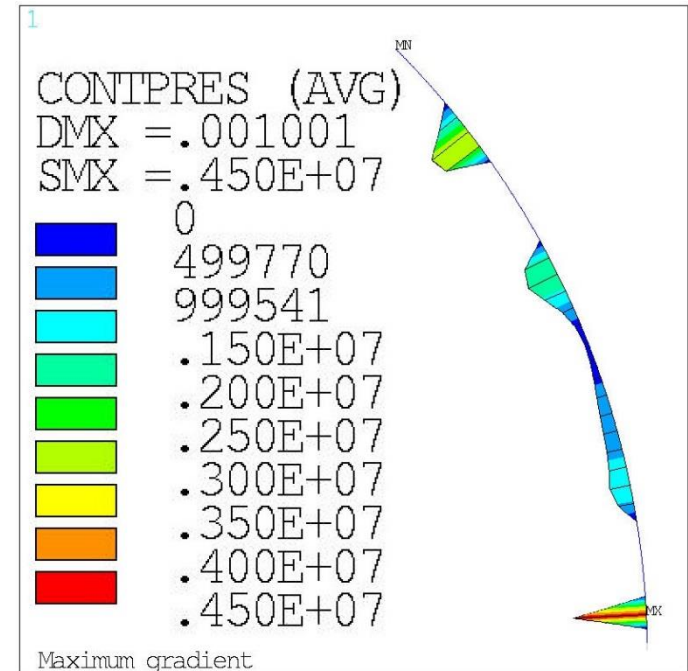
$$\sigma_{\theta} = \frac{E}{(1-\nu^2)} (\varepsilon_{\theta} + \nu \varepsilon_z)$$



Liquid helium vessel

- OD of the structure shrinks by ~2mm
- LHe vessel requires tensioning to maintain contact and alignment (weld shrinkage)
- Vessel of 8mm thickness modelled
- Weld shrinkage simulated with contact elements features

	F_{weld} kN	σ_{weld} MPa	σ_{vessel} MPa
Warm	760	95	120
Cold	128	16	51
Forces	224	28	71

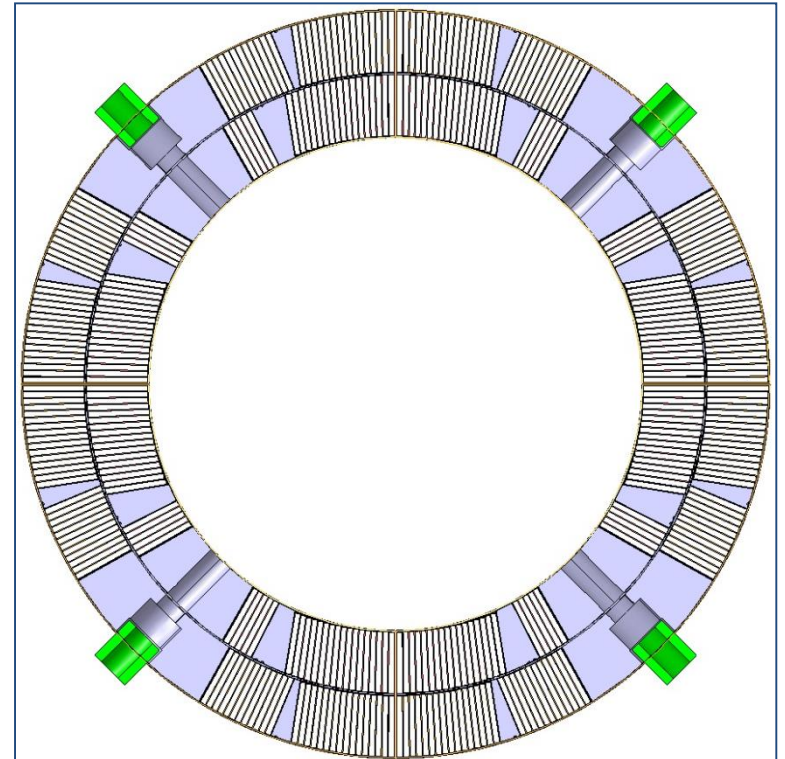
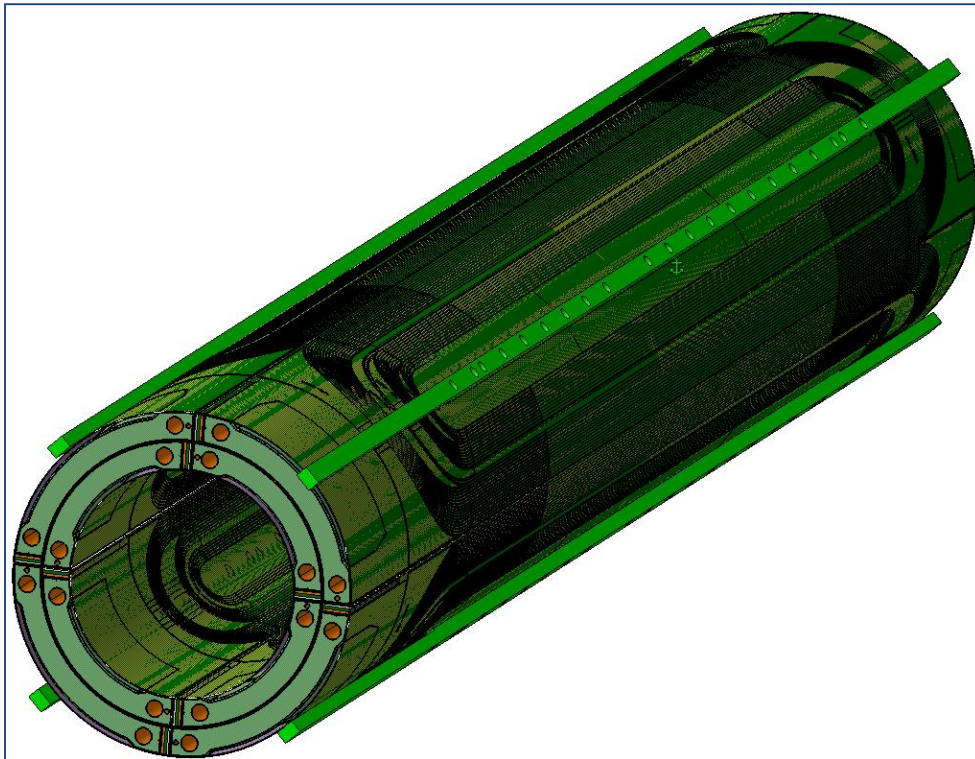


- **Contact between the shell and the vessel maintained (locally) after cool-down**
- **Vessel linked to the yoke through the backing-strip (tack-welded) and welding blocks between the shell segments (bolted to the yoke)**

Appendix

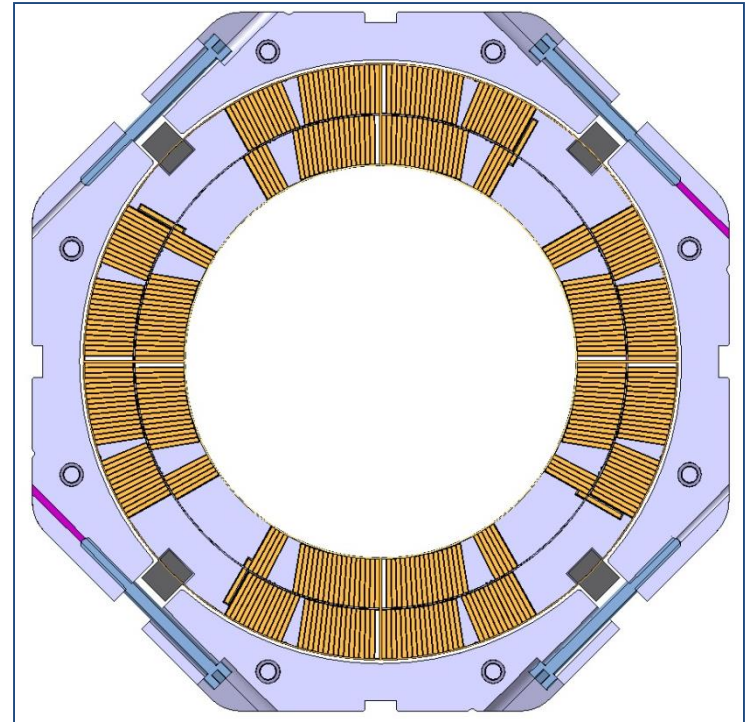
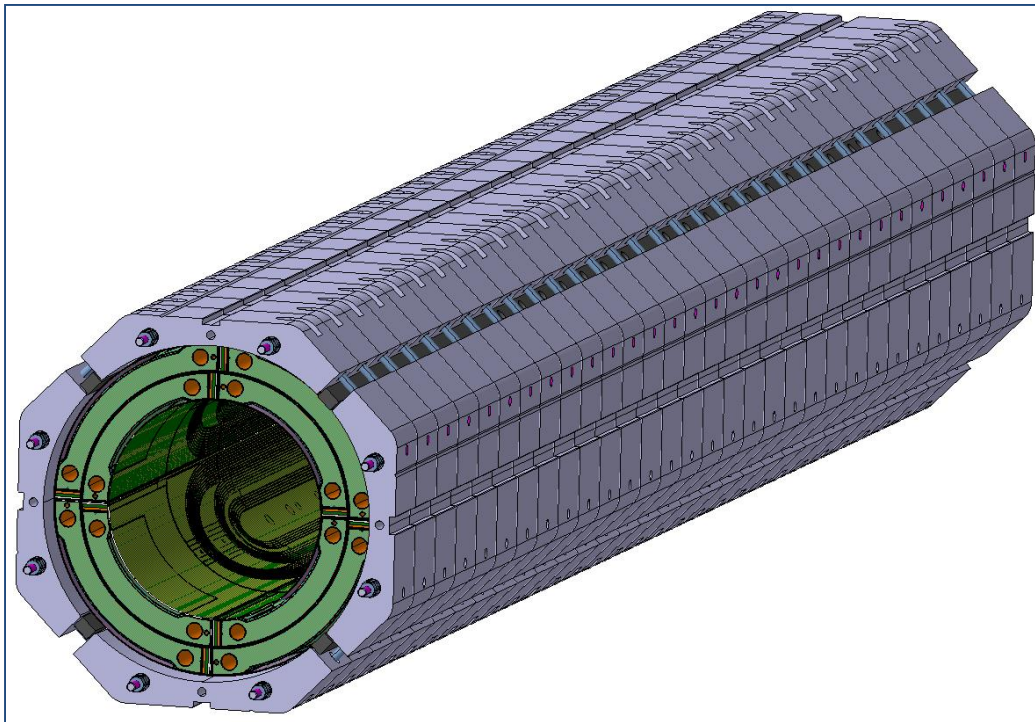
Coil and G10 pole key

- Ti alloy pole impregnated with the coil



Aluminum bolted collars

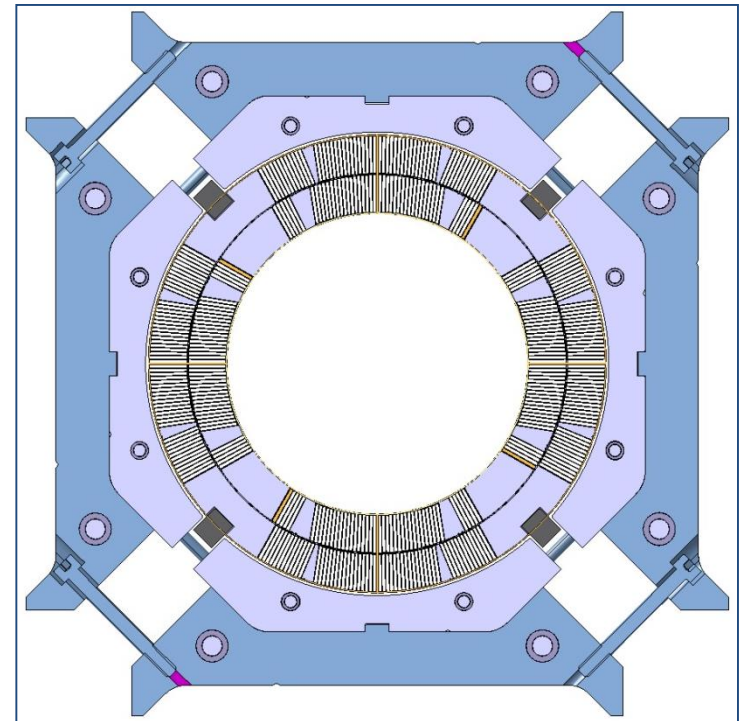
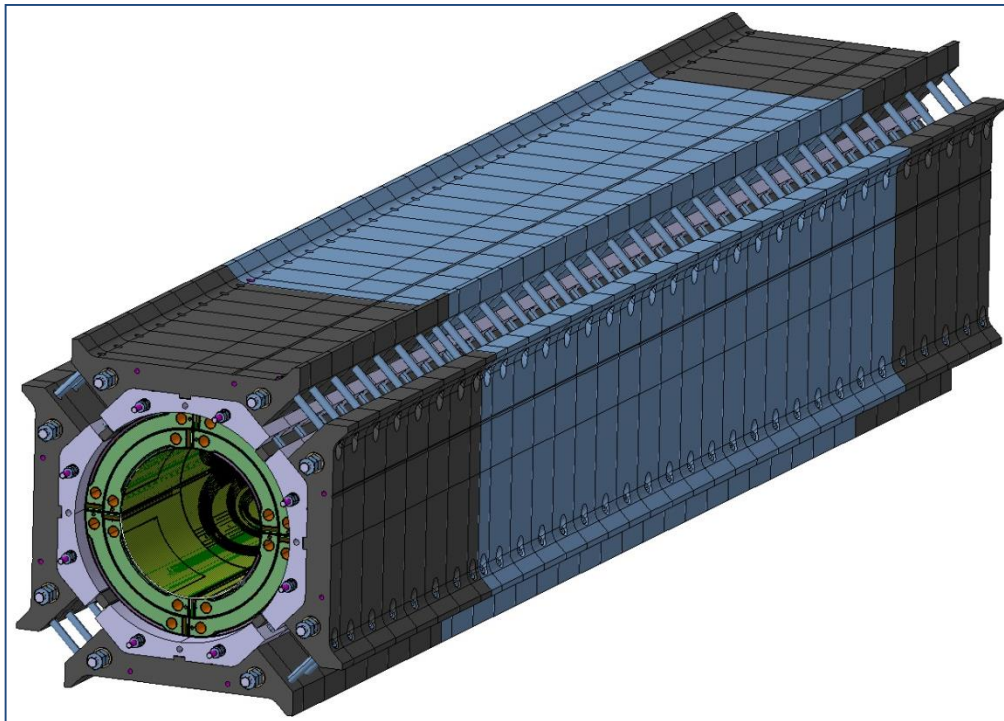
- 50 mm thick laminations
- Radial contact with coil and azimuthal contact with pole key (for alignment)
- No coil pre-load function
- Kapton shim used it to adjust radial contact between coil and collar



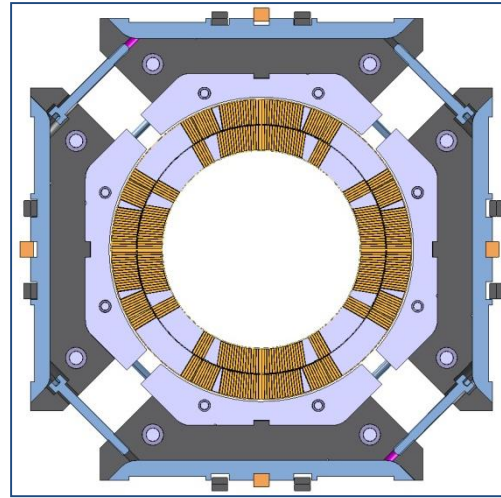
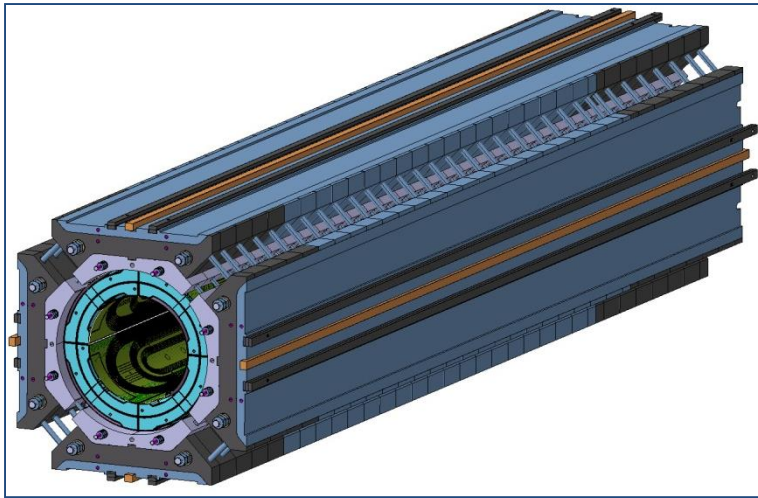
Iron and stainless steel bolted pads

Coil-pack sub-assembly

- 50 or 8 mm thick laminations
- Alignment with respect to collars
- Stainless steel laminations in the ends
- No coil pre-load function

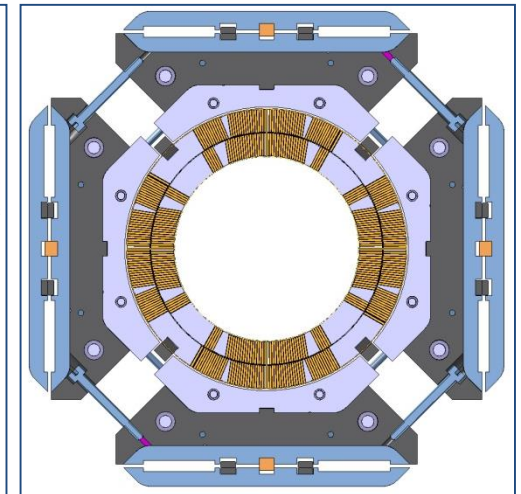
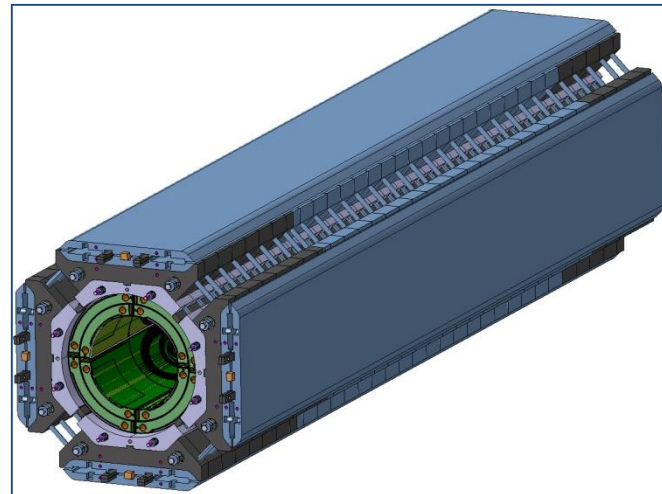


Iron masters and alignment-loading keys

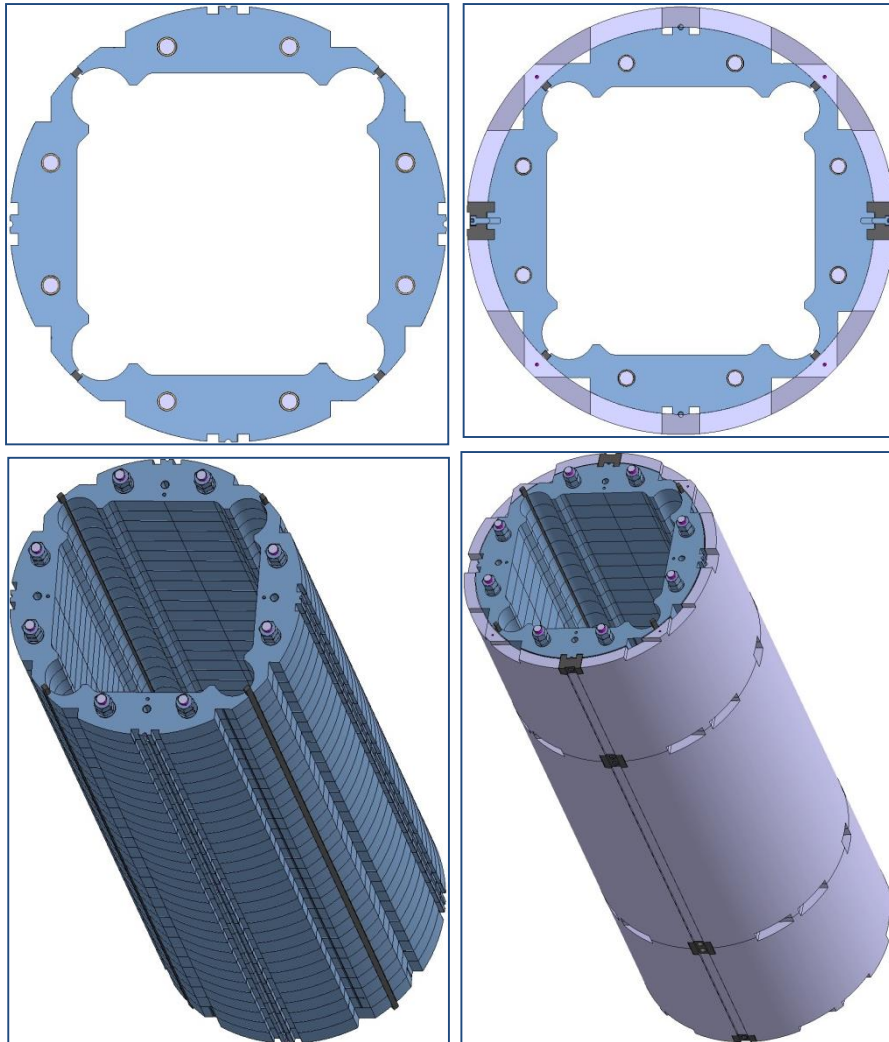


- Slots for
 - Bladders
 - Loading keys
 - Alignment keys
- Flat surface

- Nested into features in the load pads (and yokes)

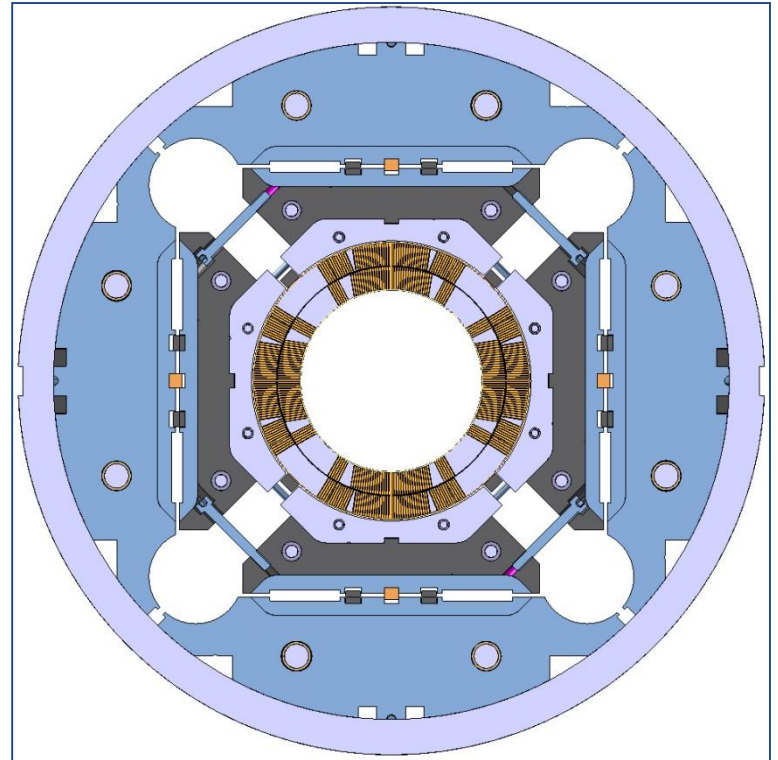
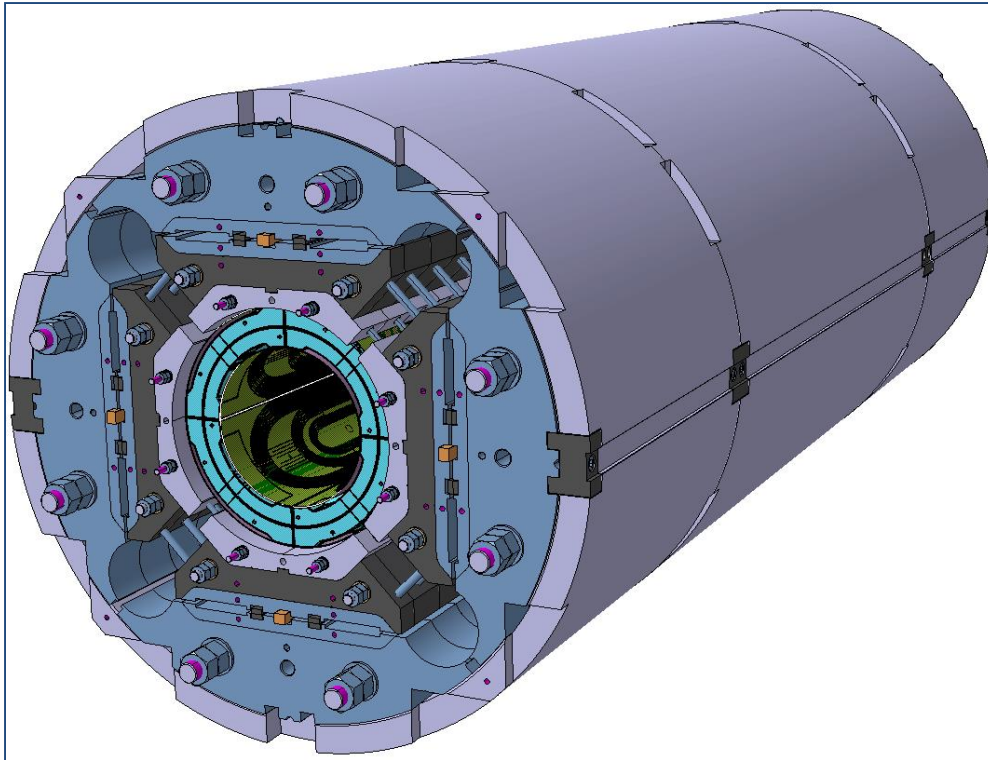


Yoke-shell sub-assembly

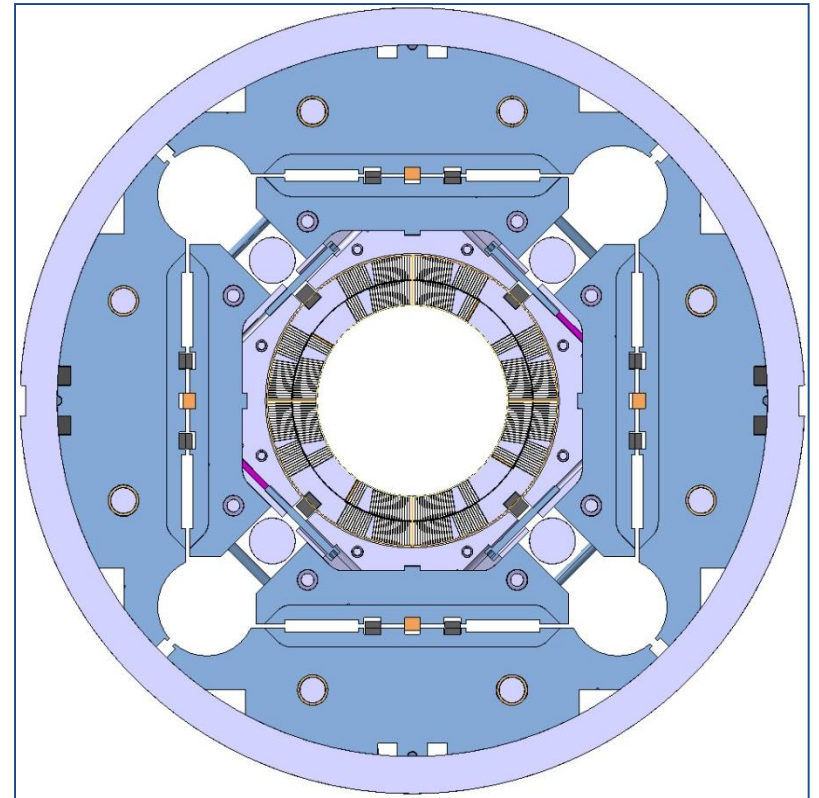
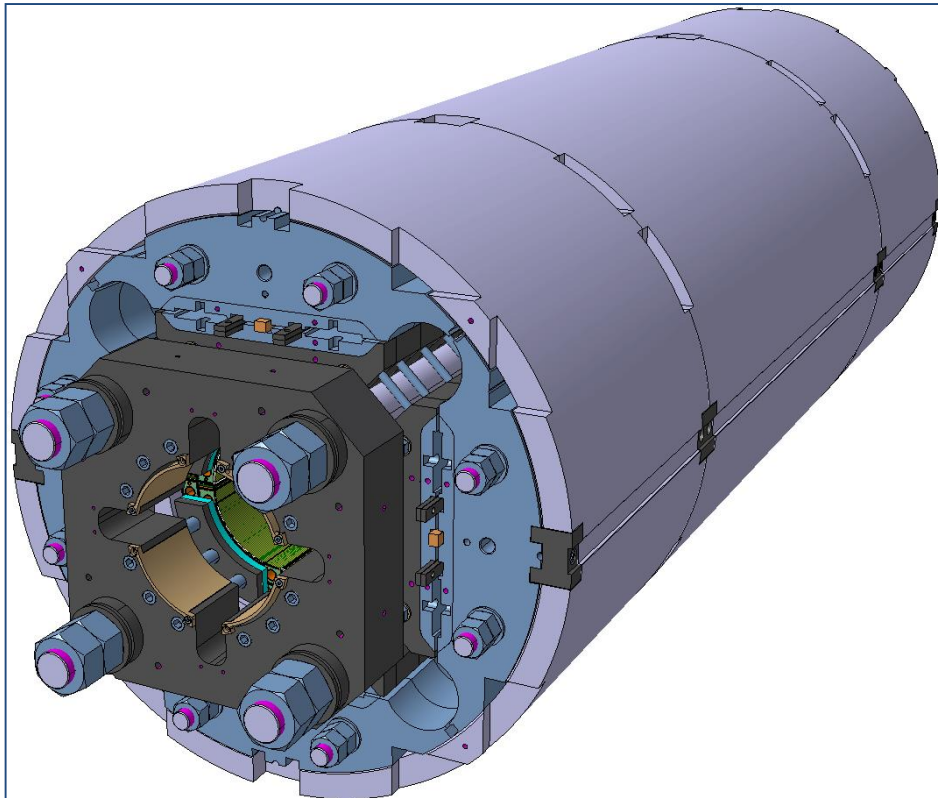


- 4 stacks of lamination assembled with ties rods
- Shell pre-load with temporary keys
- Tack-welding blocks bolted to the yoke
- Segmented shell with cut-outs for cold-mass assembly

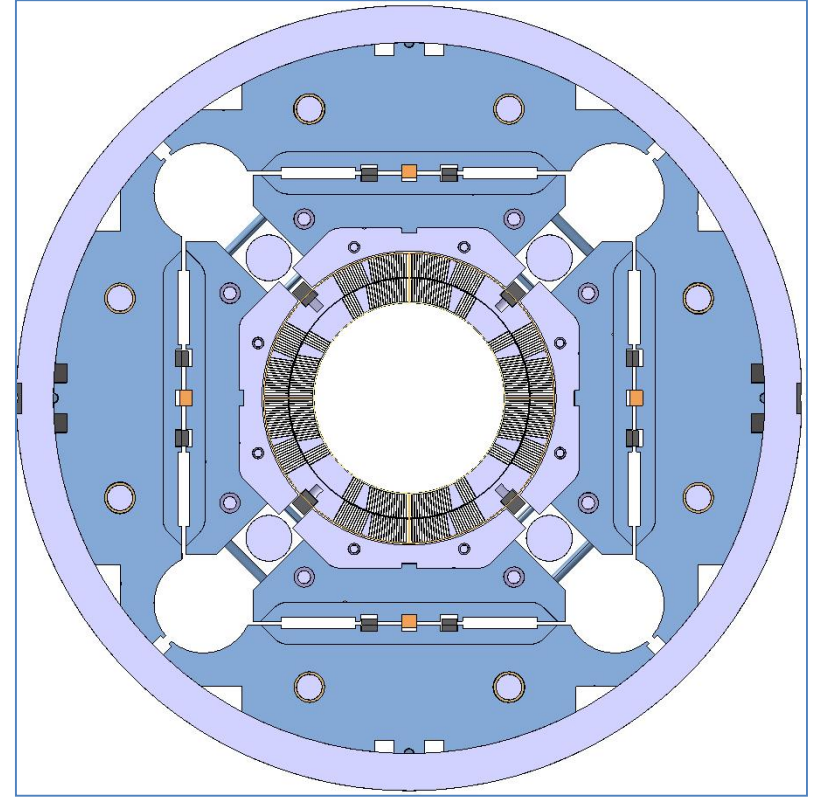
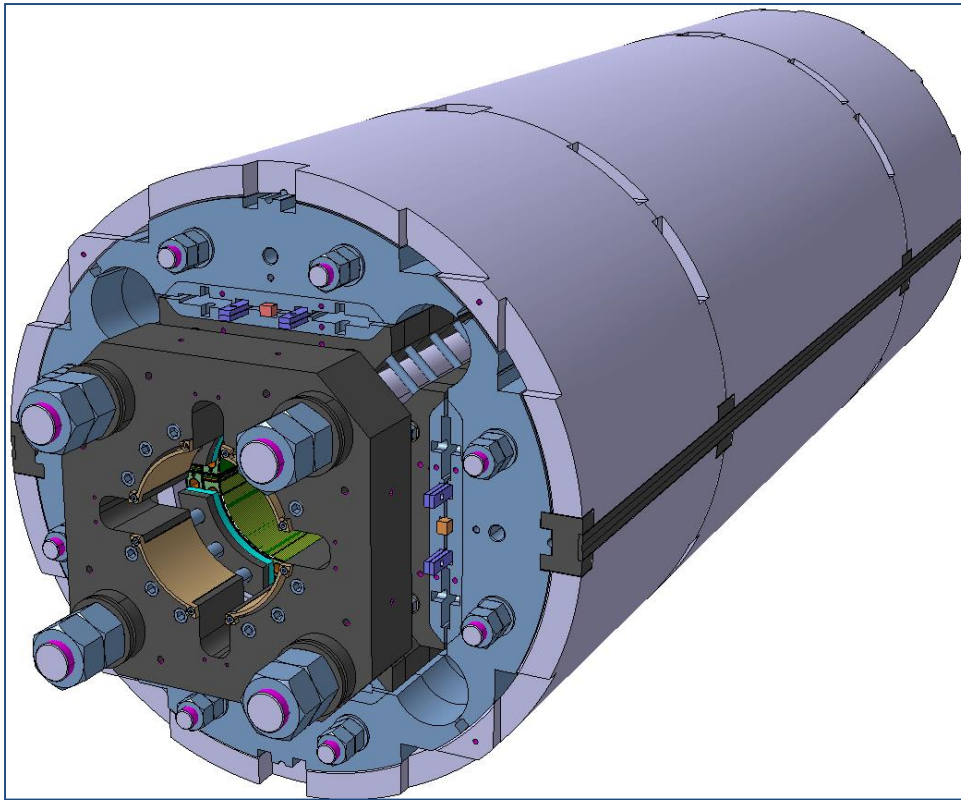
Coil-pack sub-assembly in shell-yoke-sub-assembly and pre-loading



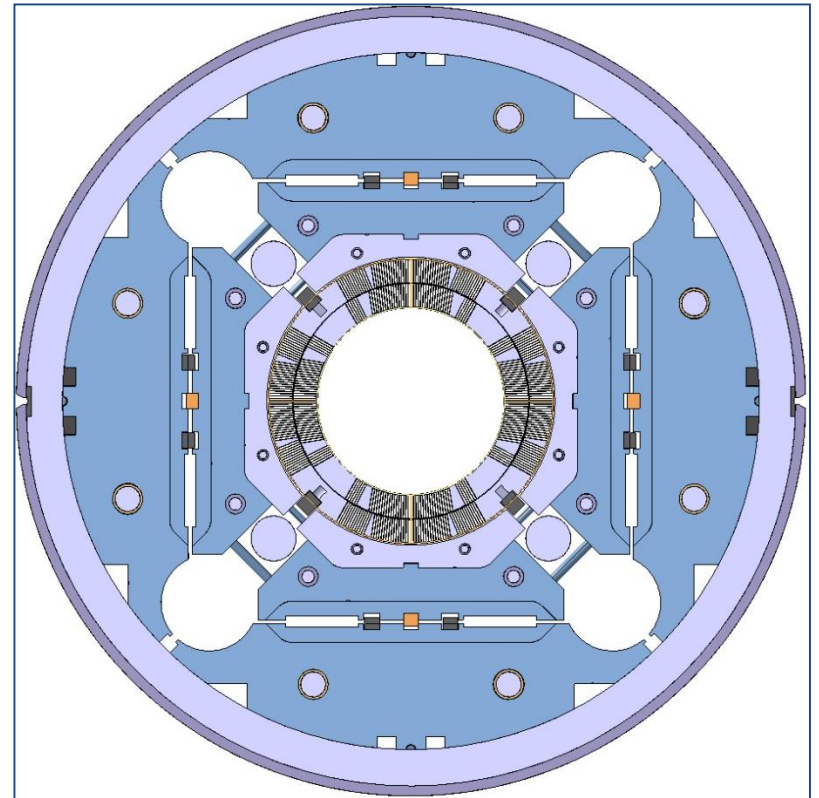
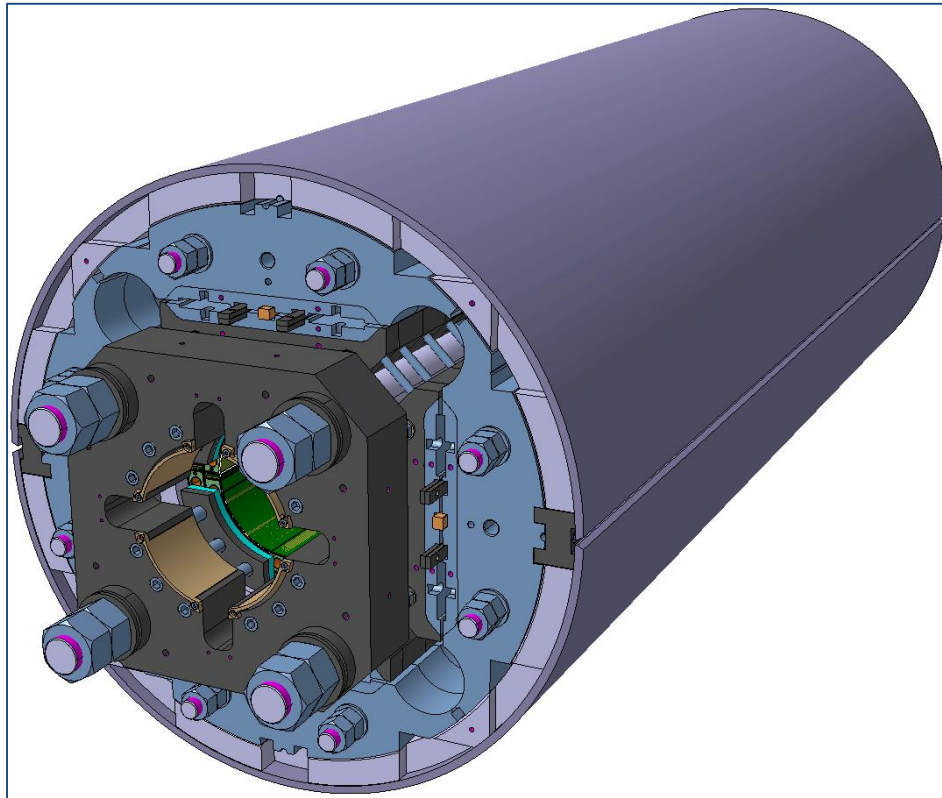
Aluminium axial rod insertion and assembly of end-plate



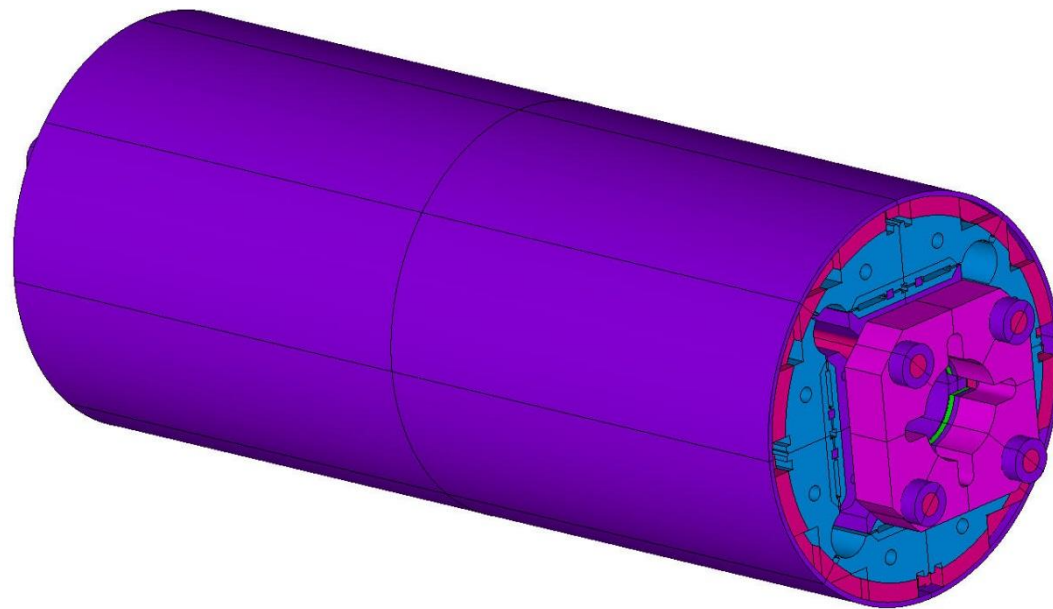
Backing-strip



Welded LHe vessel (stainless steel shell)



3D ANSYS model



3D ANSYS Model



3D finite element model

Lorentz forces

- ANSYS

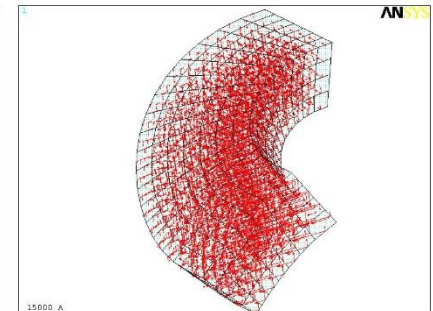
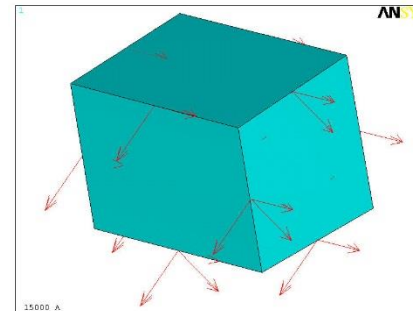
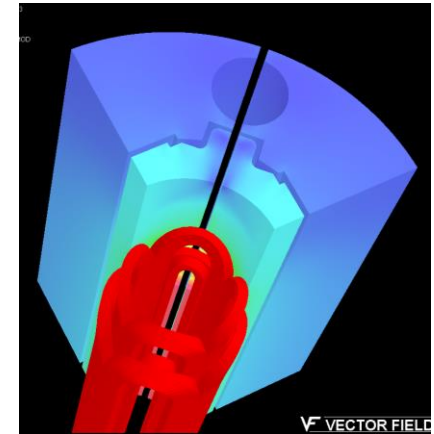
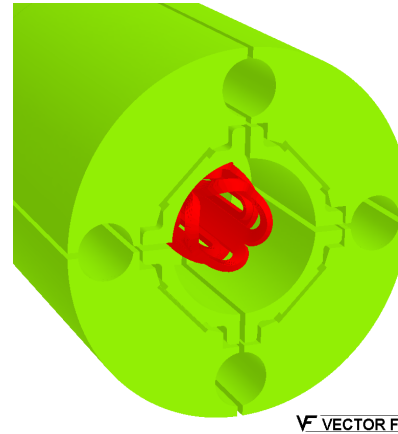
- (x, y, z) coordinates of each coil element center

- OPERA

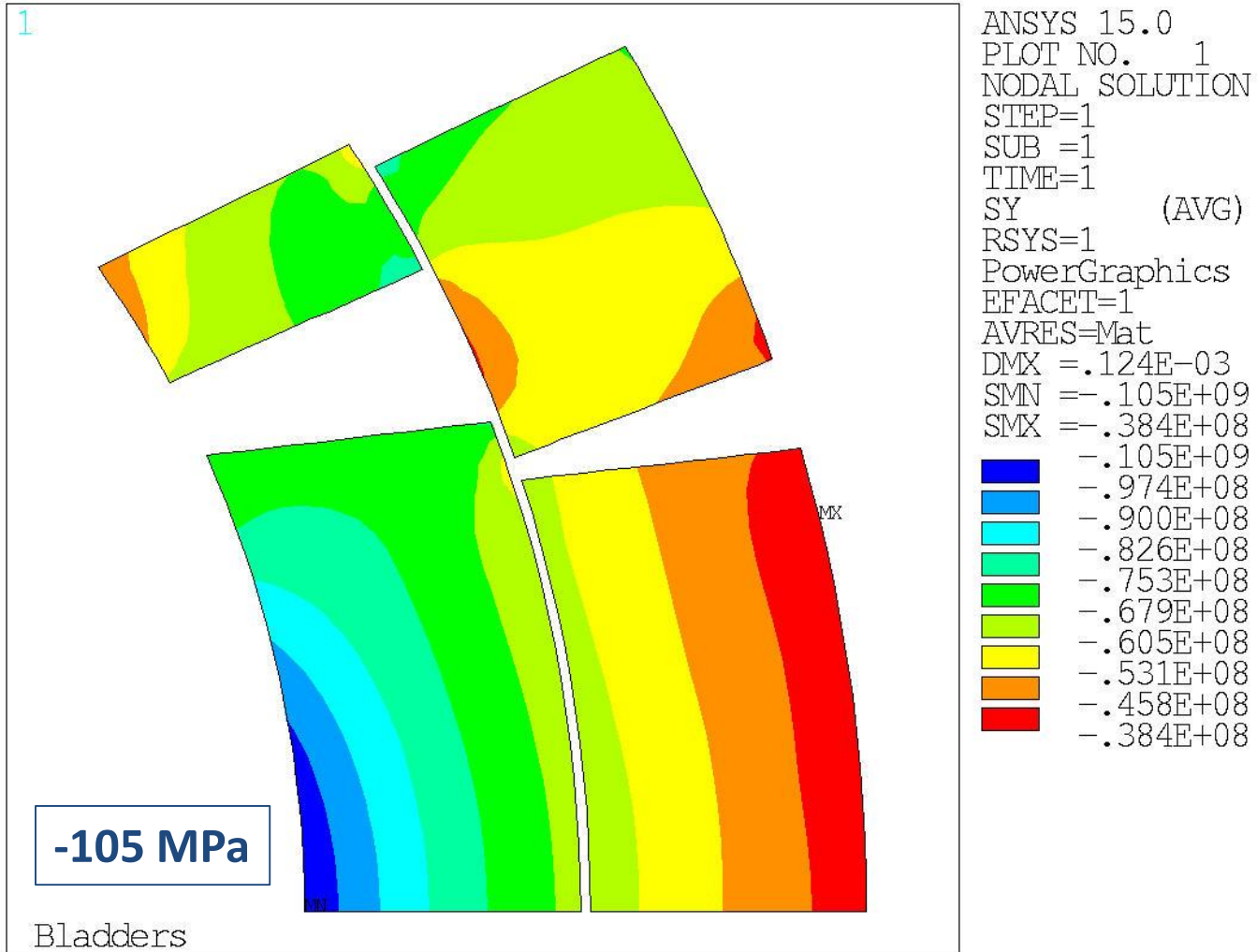
- Computation of $J \times B$ (N/mm^3) at each (x, y, z) coordinate

- ANSYS

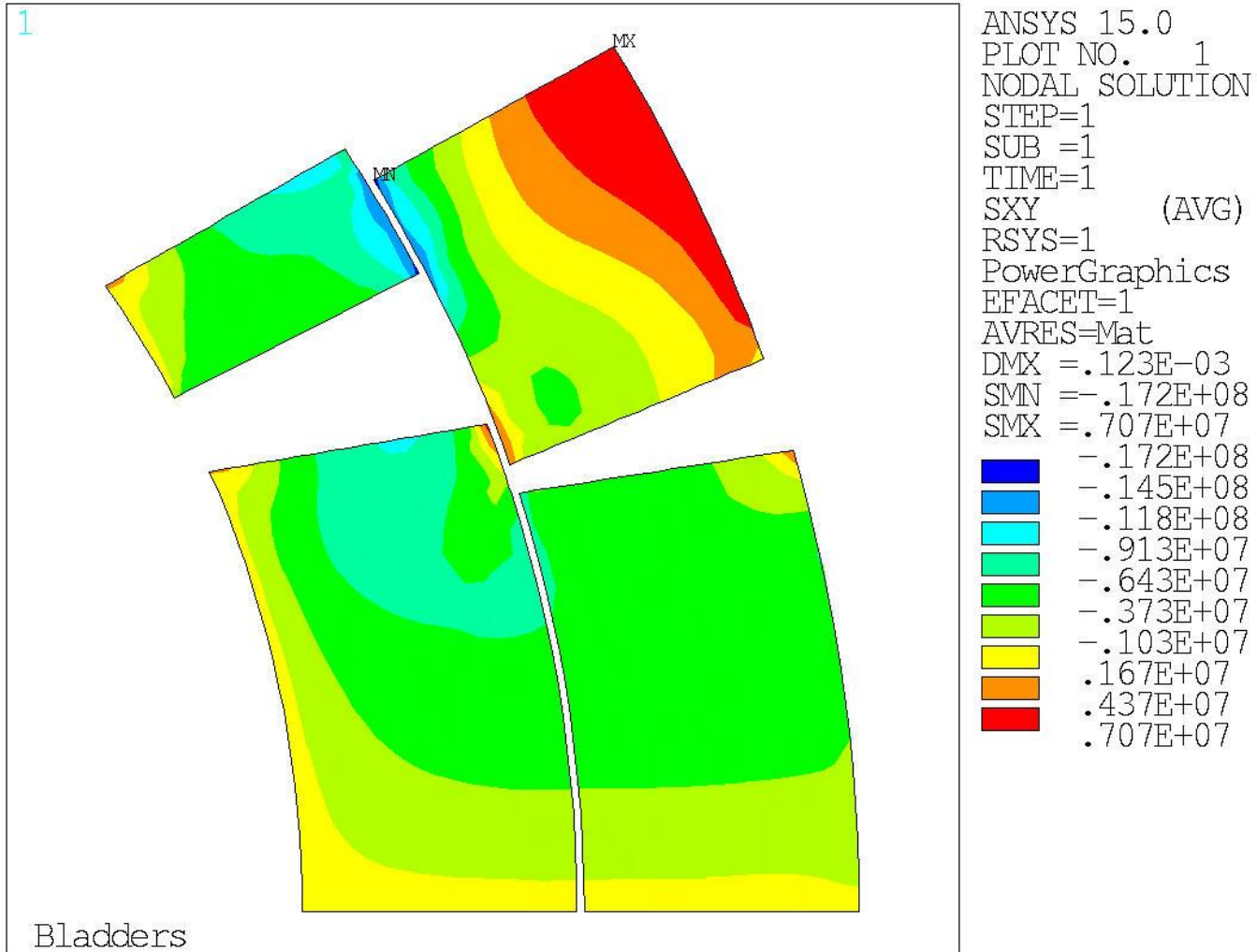
- Computation of $J \times B \cdot V_{el}$ (N)
- Final force applied to each coil node



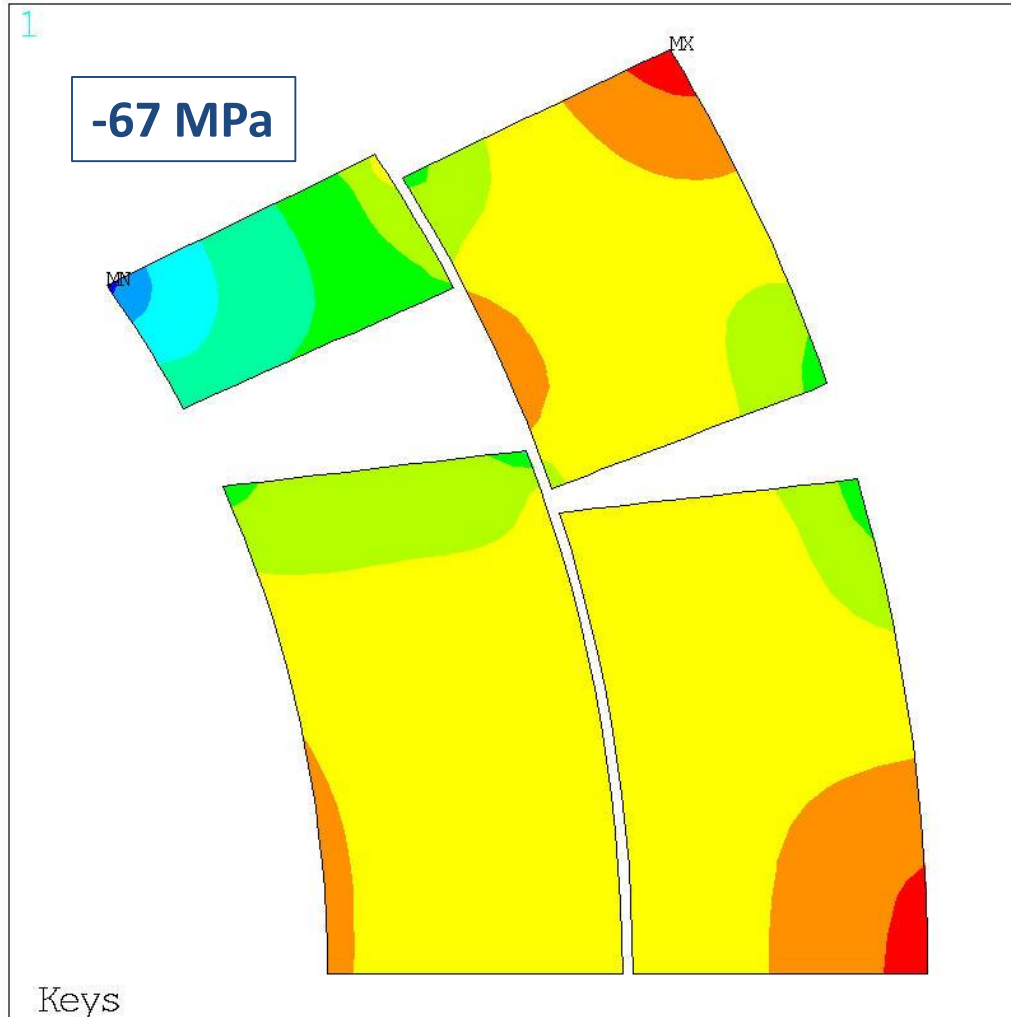
Bladders: 45 MPa (700 μm gap)



Bladders: 45 MPa (700 μm gap)



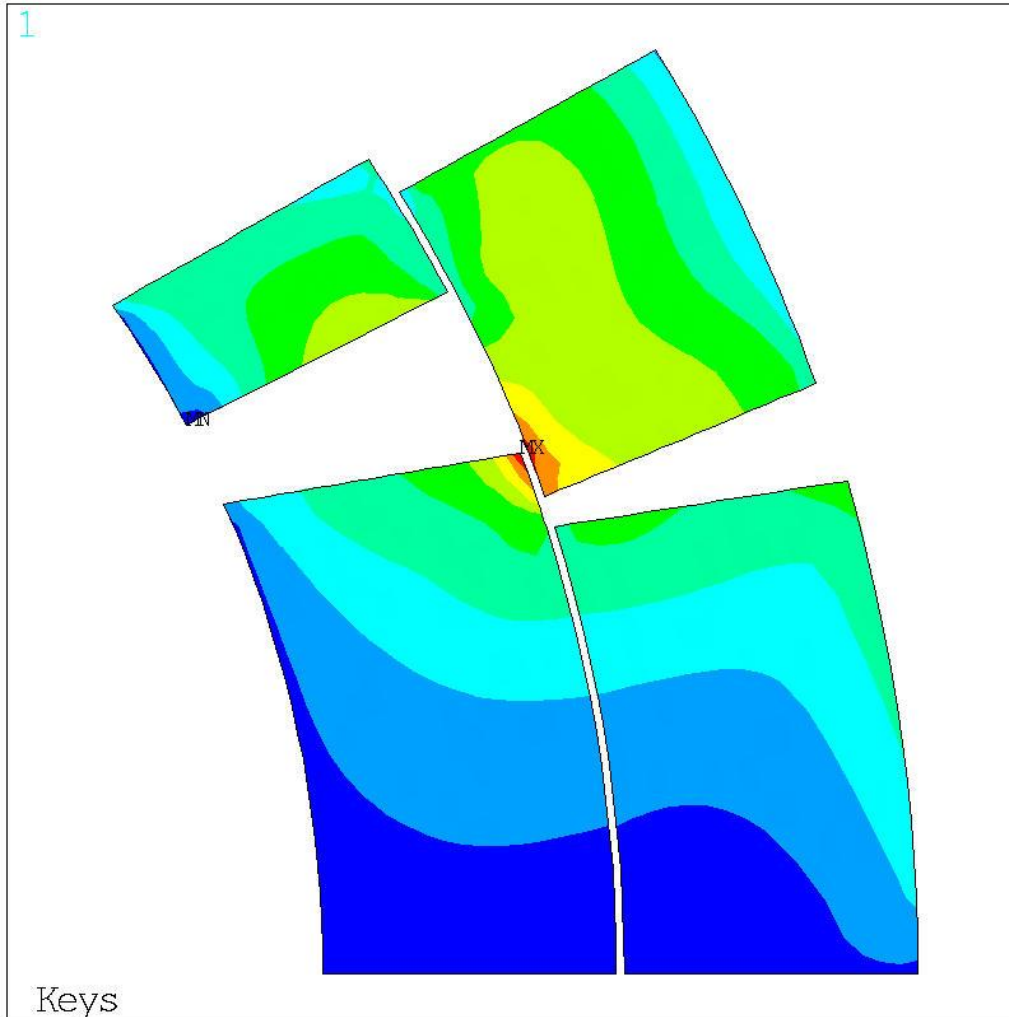
Key: 550 μm



```
ANSYS 15.0  
PLOT NO. 1  
NODAL SOLUTION  
STEP=2  
SUB =1  
TIME=2  
SY (AVG)  
RSYS=1  
PowerGraphics  
EFACET=1  
AVRES=Mat  
DMX =.624E-04  
SMN =-.667E+08  
SMX =-.181E+08
```

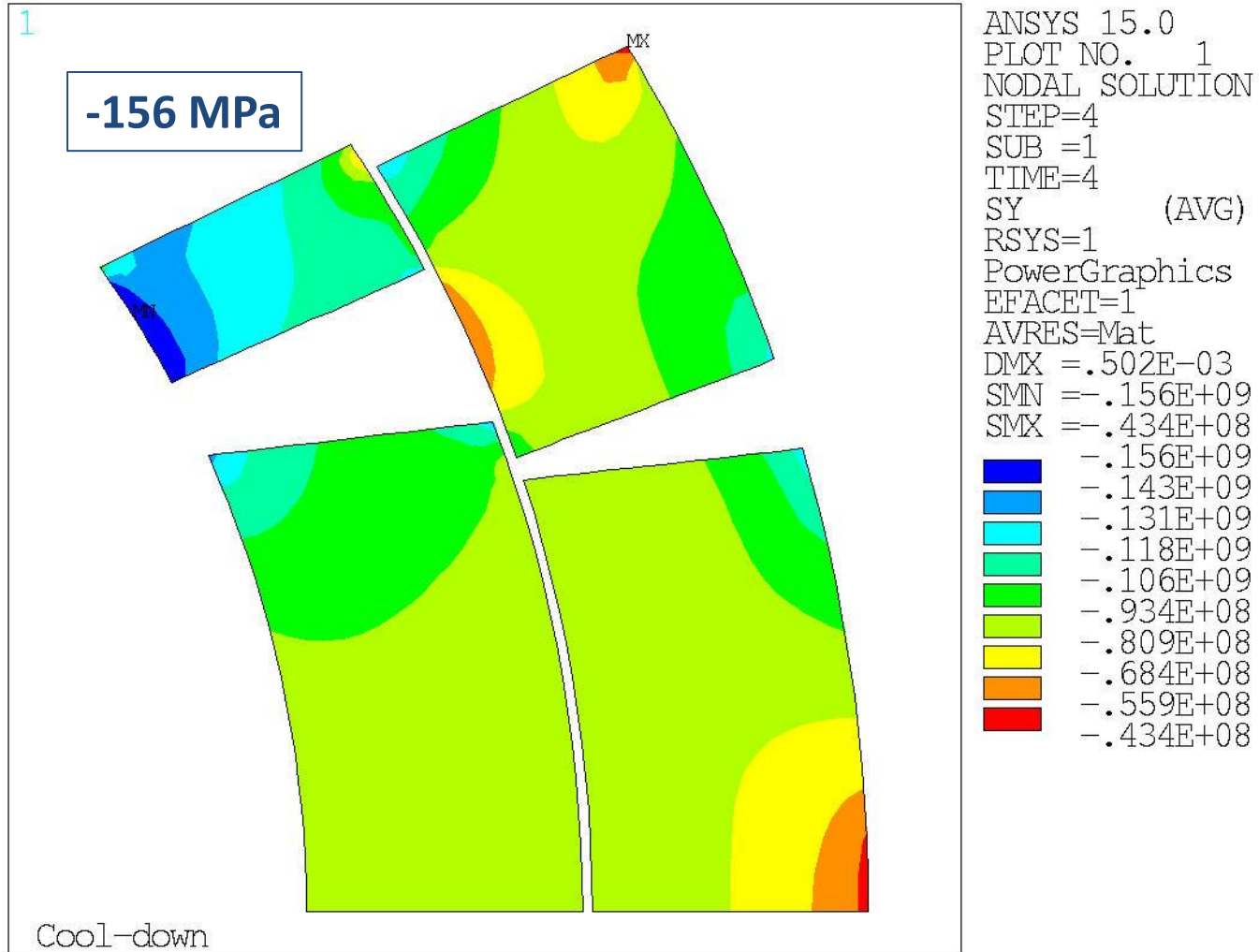
■	-.667E+08
■	-.613E+08
■	-.559E+08
■	-.505E+08
■	-.451E+08
■	-.397E+08
■	-.343E+08
■	-.289E+08
■	-.235E+08
■	-.181E+08

Key: 550 μm

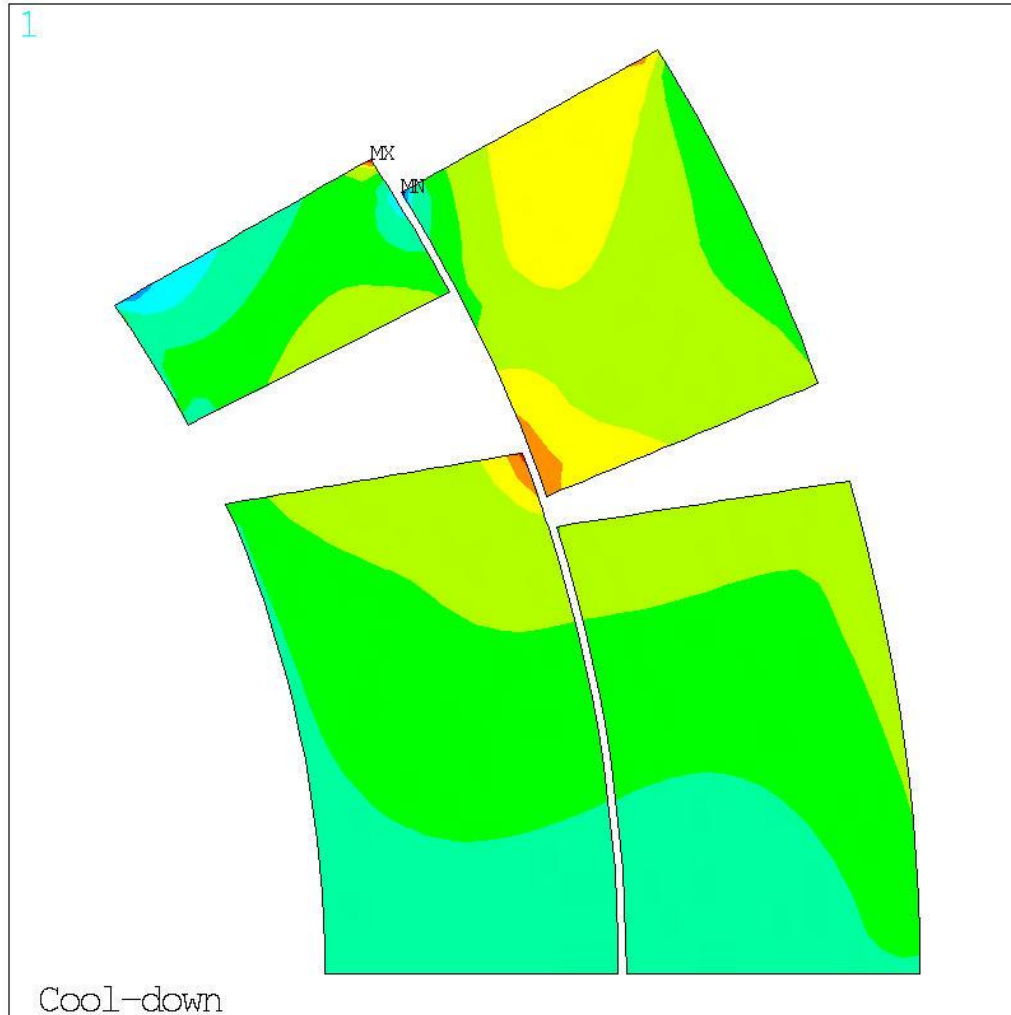


```
ANSYS 15.0  
PLOT NO. 1  
NODAL SOLUTION  
STEP=2  
SUB =1  
TIME=2  
SXY (AVG)  
RSYS=1  
PowerGraphics  
EFACET=1  
AVRES=Mat  
DMX =.620E-04  
SMN =-.179E+07  
SMX =.169E+08  
-.179E+07  
283538  
.236E+07  
.443E+07  
.650E+07  
.857E+07  
.106E+08  
.127E+08  
.148E+08  
.169E+08
```

Cool-down to 1.9 K

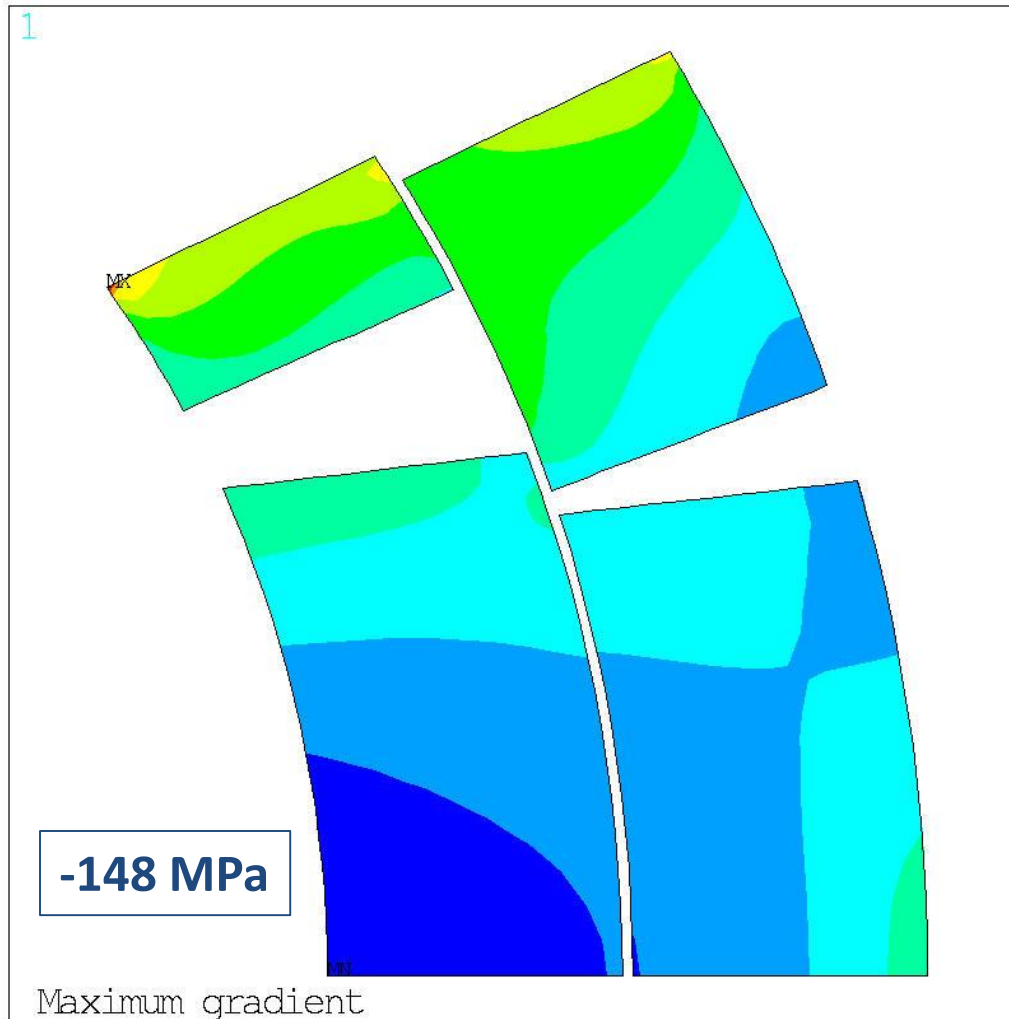


Cool-down to 1.9 K



```
ANSYS 15.0  
PLOT NO. 1  
NODAL SOLUTION  
STEP=4  
SUB =1  
TIME=4  
SXY (AVG)  
RSYS=1  
PowerGraphics  
EFACET=1  
AVRES=Mat  
DMX =.501E-03  
SMN =-.409E+08  
SMX =.533E+08  
-.409E+08  
-.304E+08  
-.199E+08  
-.946E+07  
.100E+07  
.115E+08  
.219E+08  
.324E+08  
.429E+08  
.533E+08
```

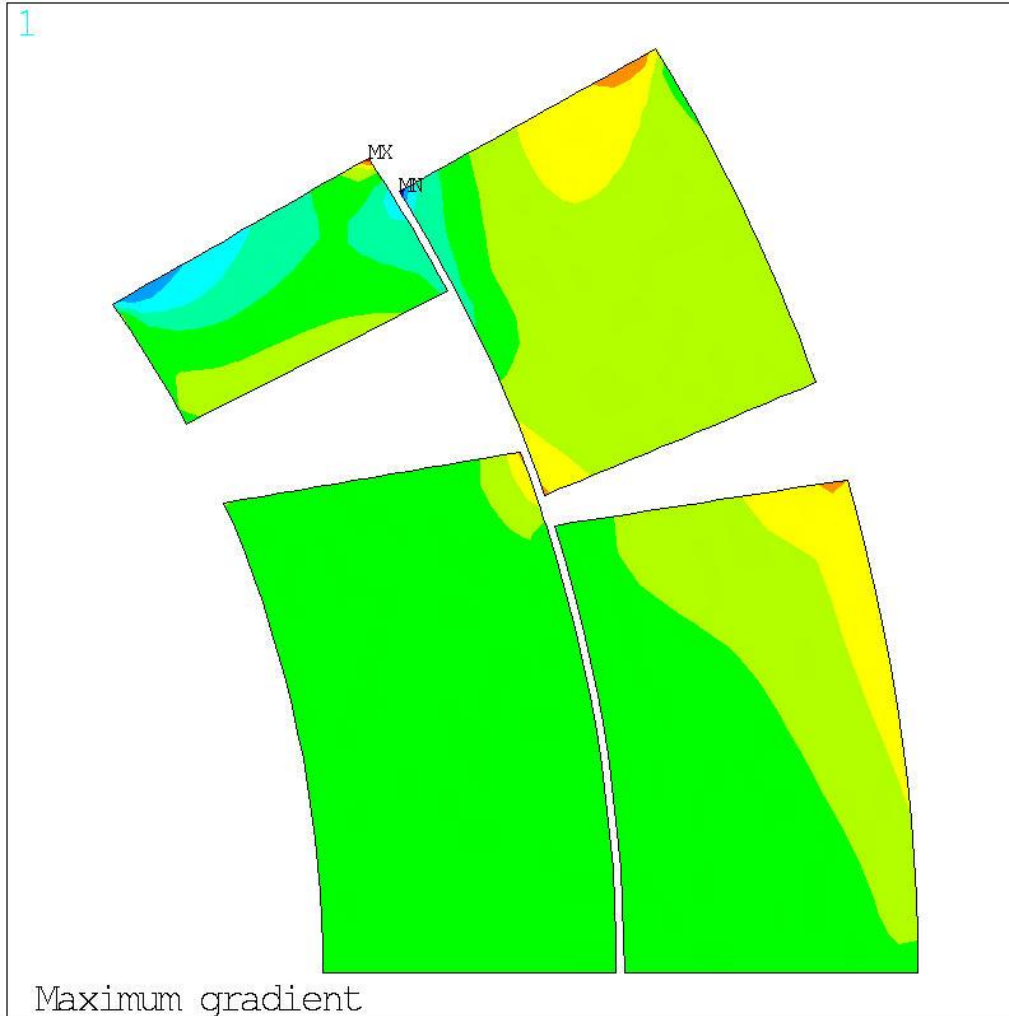
132.6 T/m



```
ANSYS 15.0  
PLOT NO. 1  
NODAL SOLUTION  
STEP=5  
SUB =1  
TIME=5  
SY (AVG)  
RSYS=1  
PowerGraphics  
EFACET=1  
AVRES=Mat  
DMX =.471E-03  
SMN =-.148E+09  
SMX =.406E+08
```

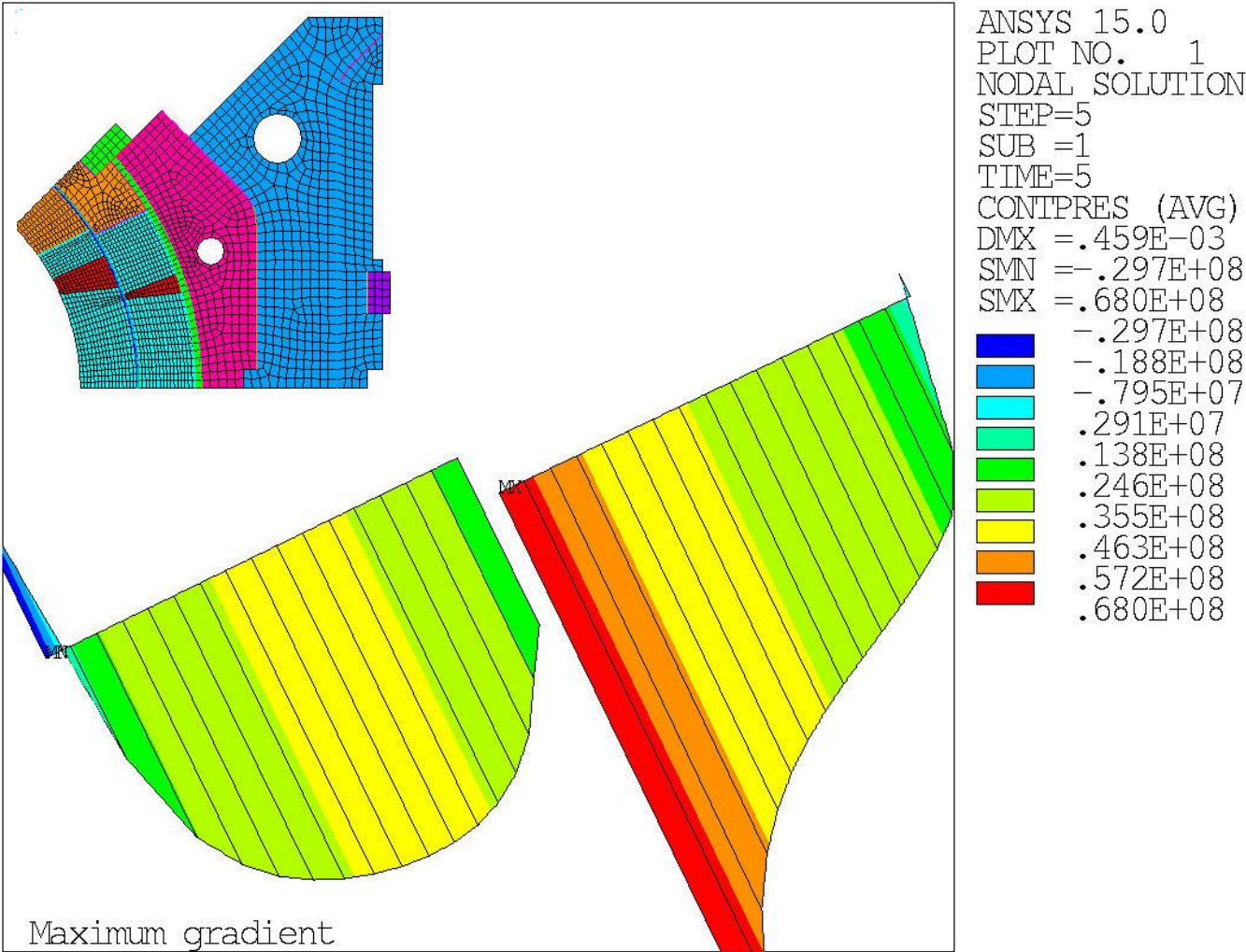
■	-.148E+09
■	-.127E+09
■	-.106E+09
■	-.850E+08
■	-.641E+08
■	-.431E+08
■	-.222E+08
■	-.125E+07
■	.197E+08
■	.406E+08

132.6 T/m



```
ANSYS 15.0  
PLOT NO. 1  
NODAL SOLUTION  
STEP=5  
SUB =1  
TIME=5  
SXY (AVG)  
RSYS=1  
PowerGraphics  
EFACET=1  
AVRES=Mat  
DMX =.470E-03  
SMN =-.485E+08  
SMX =.411E+08  
-.485E+08  
-.385E+08  
-.286E+08  
-.186E+08  
-.867E+07  
.128E+07  
.112E+08  
.212E+08  
.311E+08  
.411E+08
```

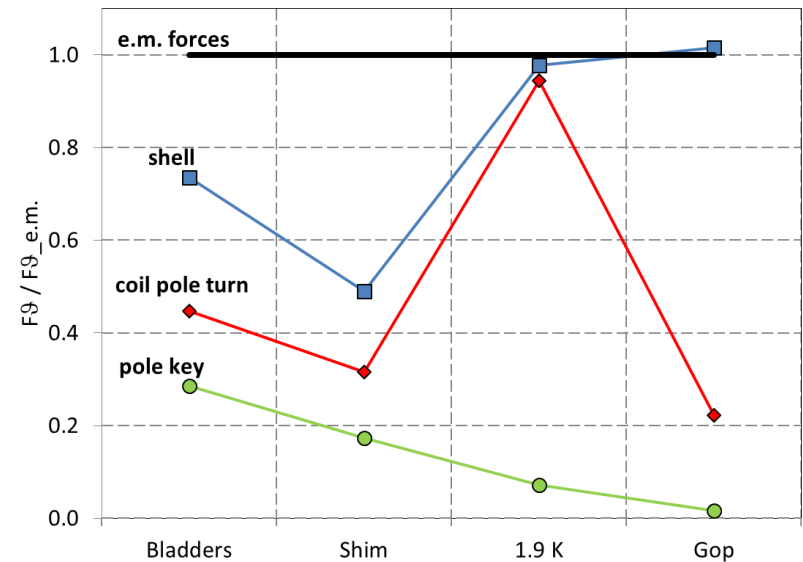
132.6 T/m Pole contact



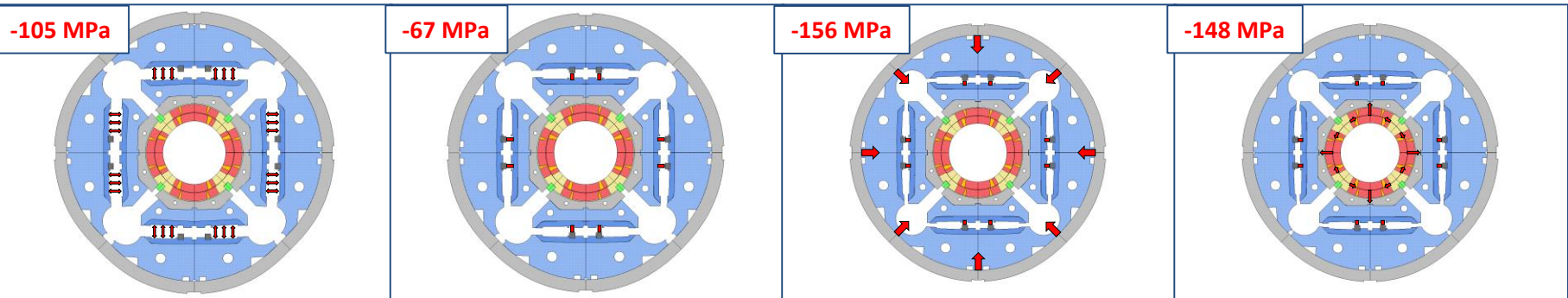
Mechanical analysis

1. ~30% of shell force intercepted by collars
2. Spring back
3. Full pre-load at 1.9 K
4. Coil still compressed at G_{op}
 - Alignment maintained

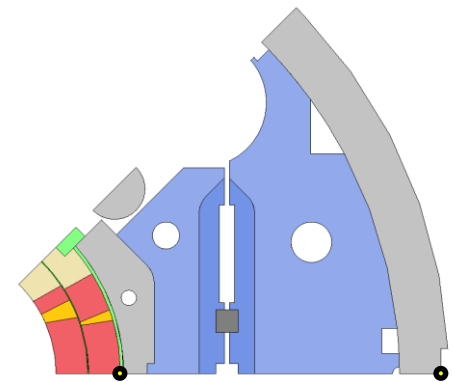
AZIMUTHAL FORCE



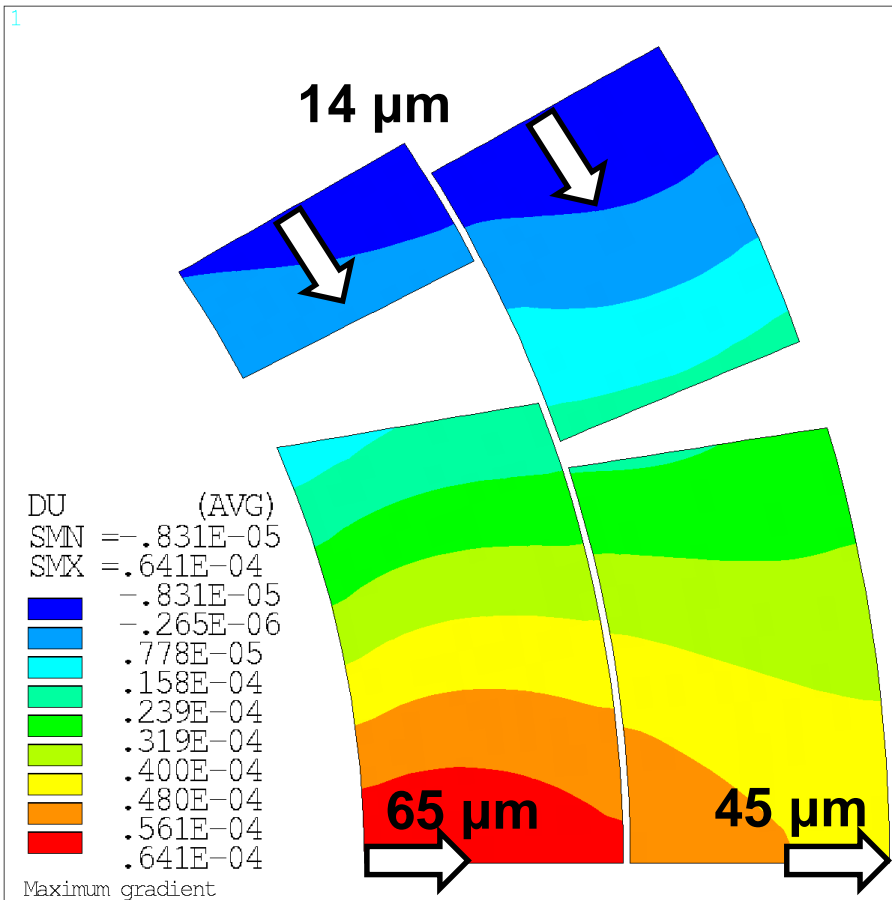
Coil peak azimuth. stress



Structure rigidity



$$R_{\text{out } 140\text{T/m}} = R_{\text{out}} - 457 \pm 7 \mu\text{m}$$



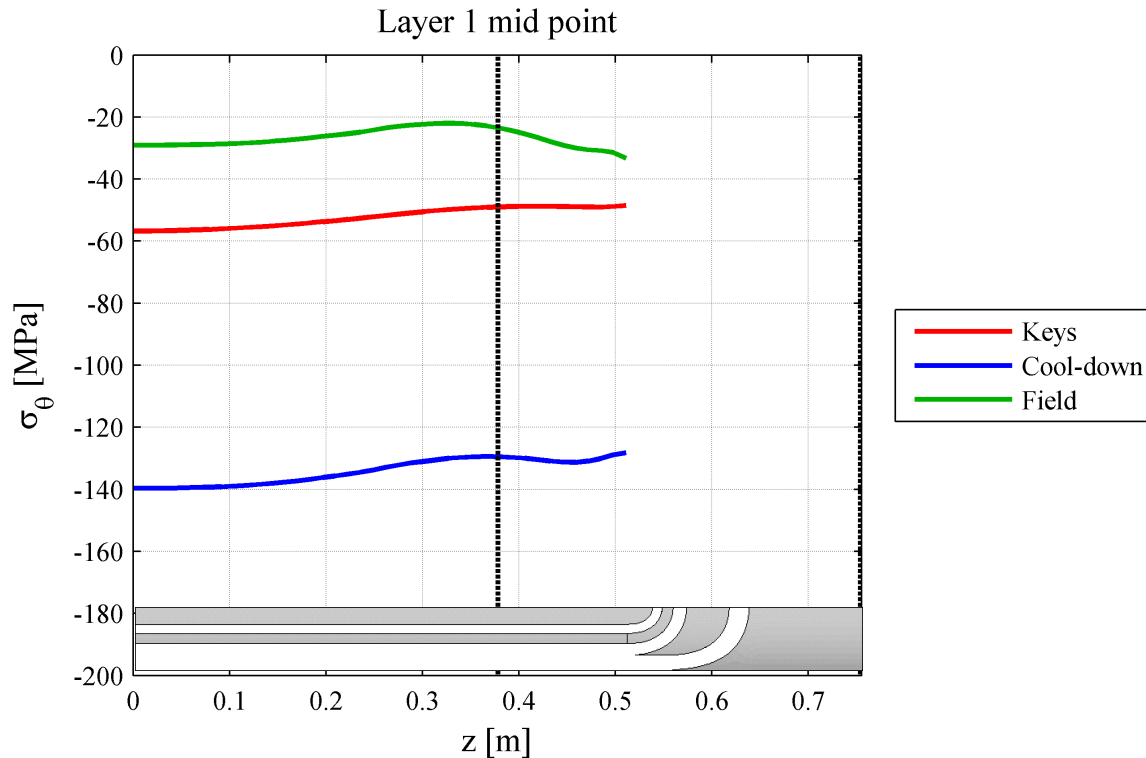
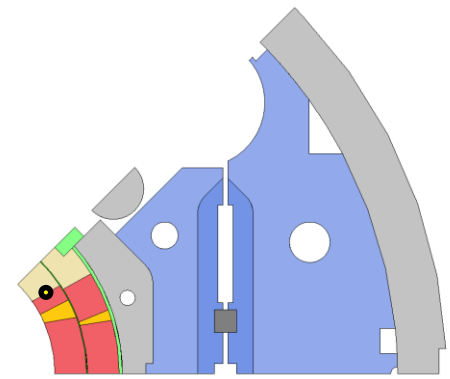
	Coil OD ΔU_r [μm]	SHELL OD ΔU_r [μm]
Warm	-80	+420
Cold	-430	-960
Forces (140T/m)	+45	+30

Effect on the coil displacement on the field quality

- Room temperature assembly and cool-down
 - B2: +1.23 T/m
 - b6: + 0.95 unit
- Magnetic forces at 140 T/m
 - B2: -0.07 T/m
 - b6: -0.02 unit

NEGLIGIBLE

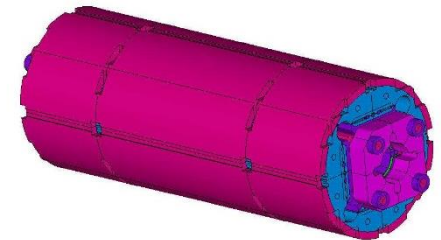
Stress variation (MQXF5)



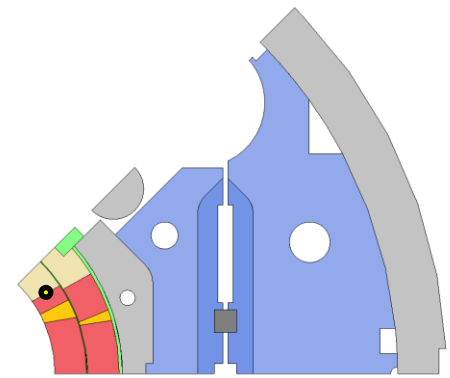
- Preload guaranteed at 140 T/m
- Stress variation under central segment **+/- 5 MPa** (affected by ends)
- Half-shells at the extremities decrease the stress variation

• Optimised layout

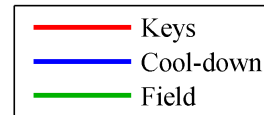
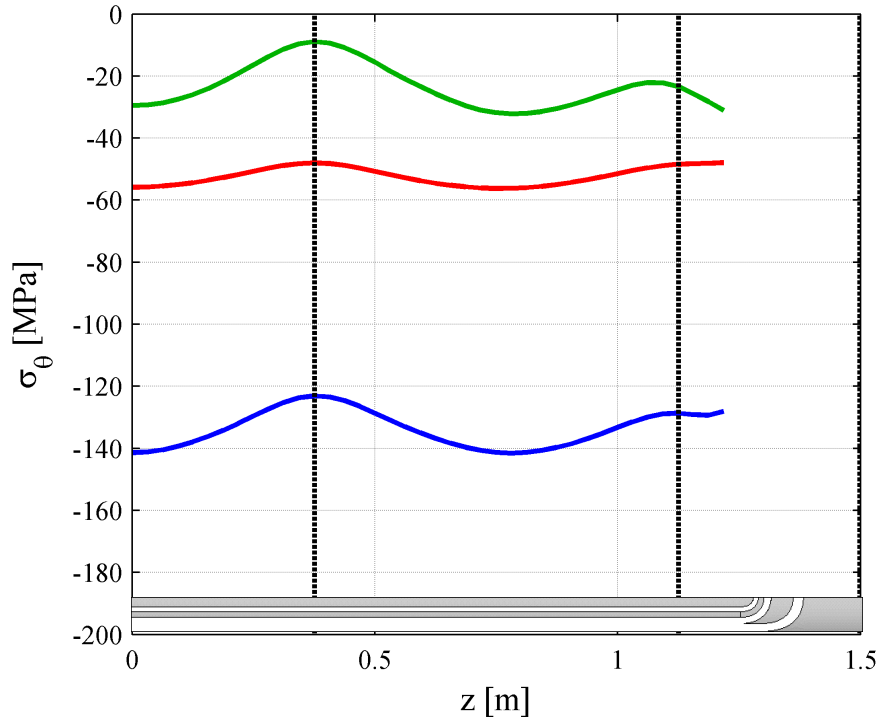
- 1 normal shell (0.755m long)
- 2 half-shells at extremities (0.377m)



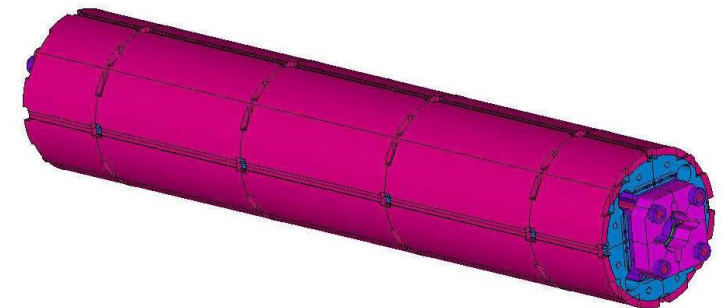
Stress variation (3m)



Layer 1 mid point



- Stress variation under central segments **+/- 10 MPa**
- Half-shells at the extremities decrease the stress variation (affect adjoining long segments)

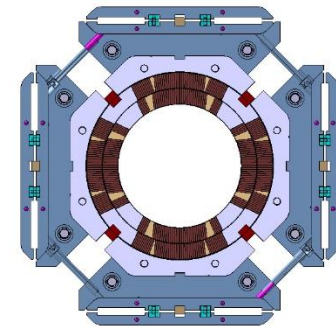
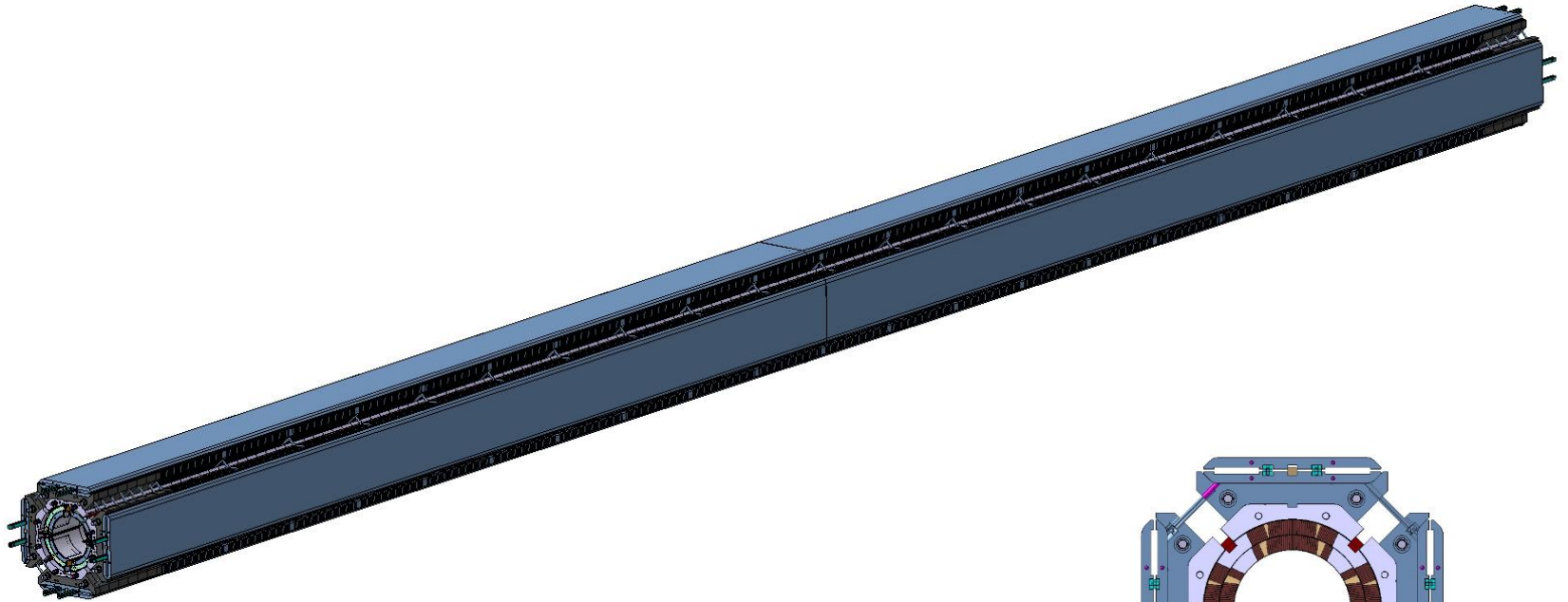


• Optimised layout

- 3 normal shell (0.755m long)
- 2 half-shells at extremities (0.377m)

Magnet design

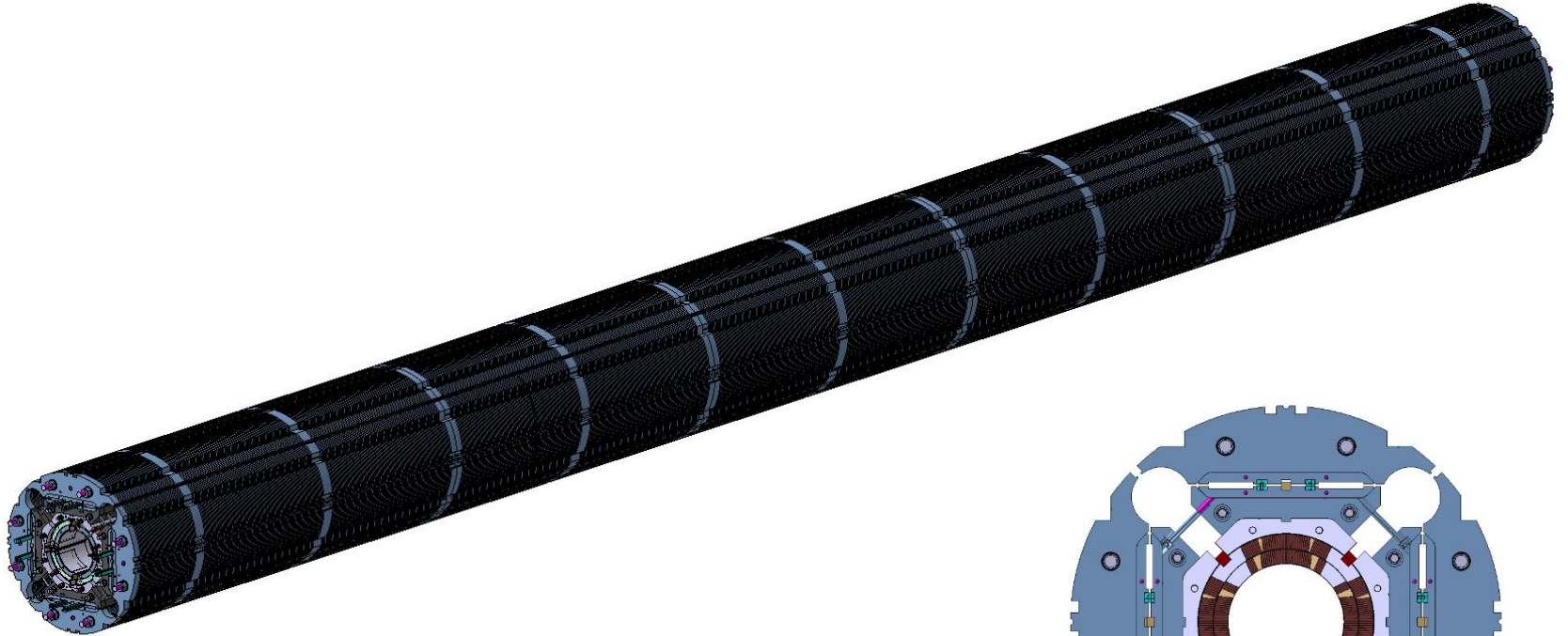
MQXFB



- **Second iron master**
 - Coil-pack sub-assembly

Magnet design

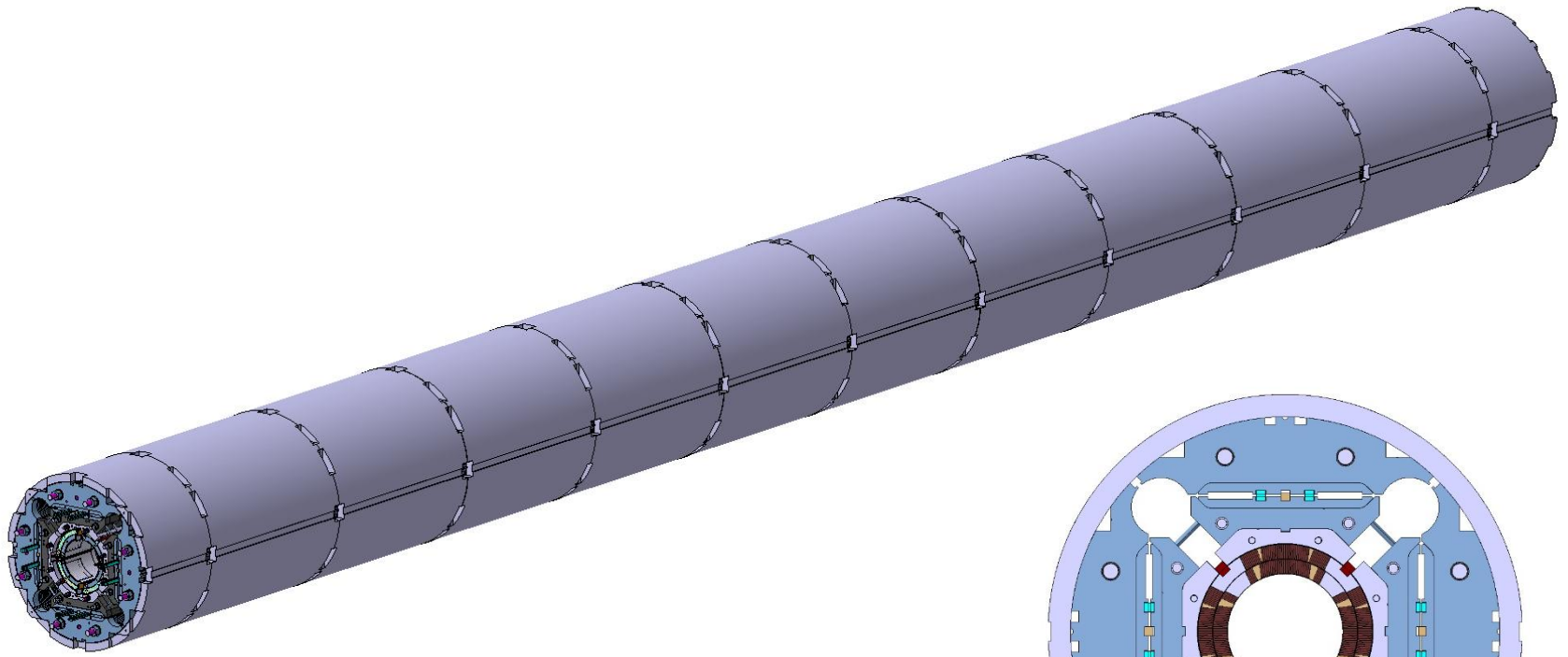
MQXFB



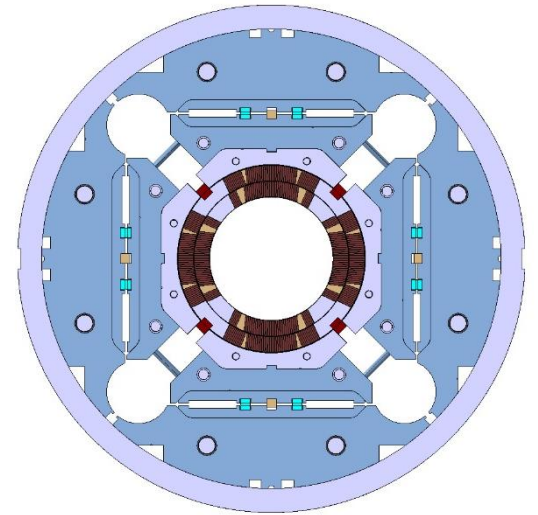
- Iron yoke laminations

Magnet design

MQXFB

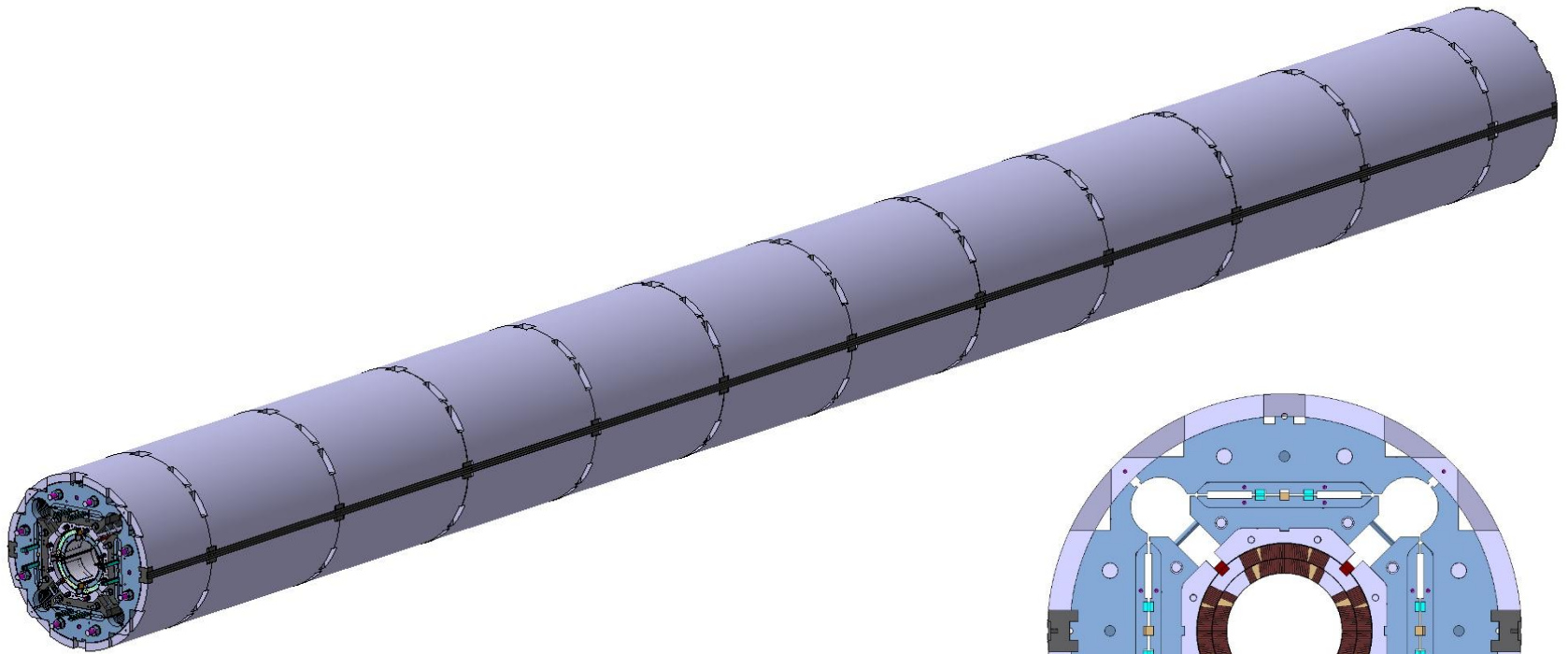


- Segmented aluminium shell



Magnet design

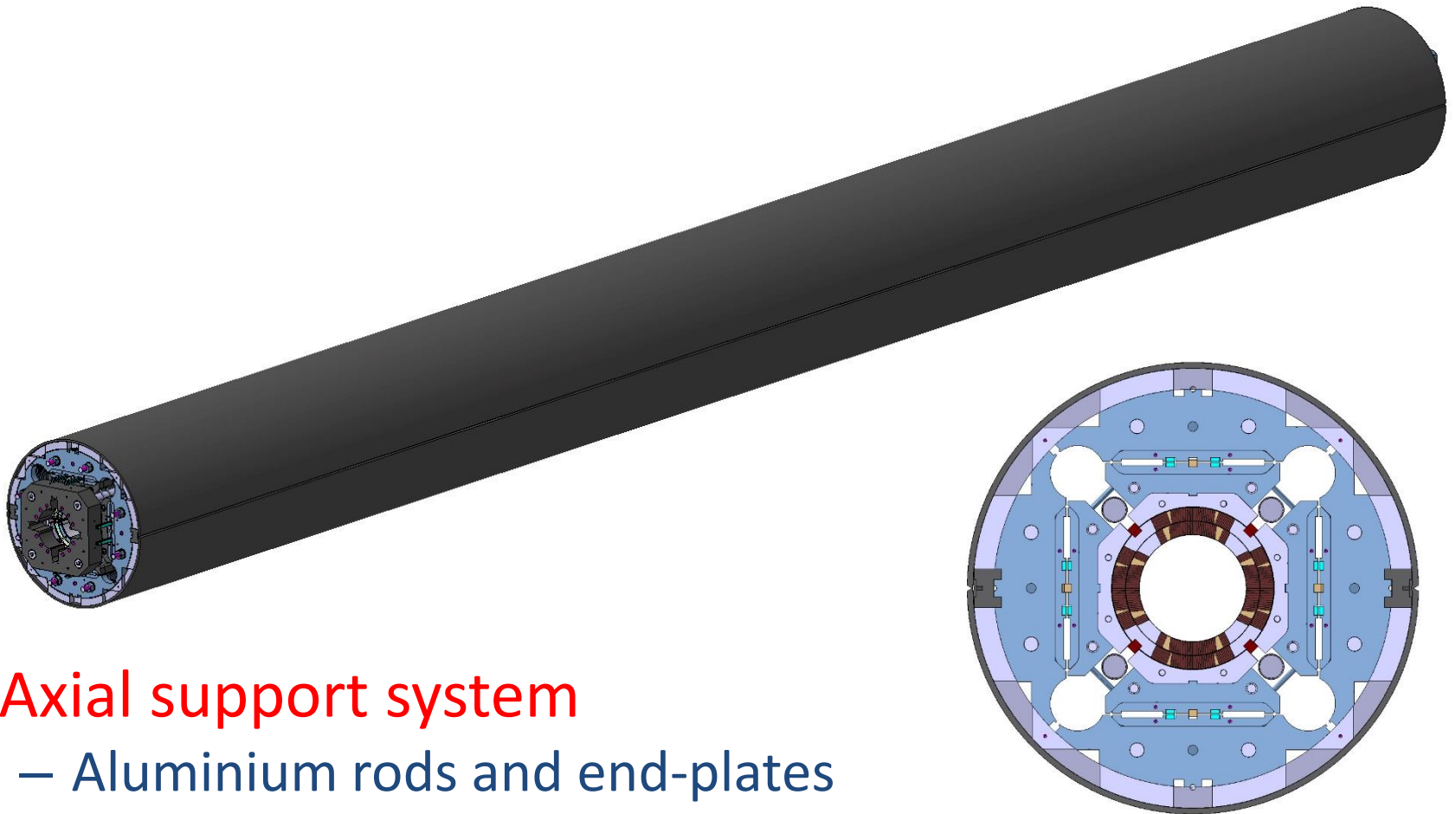
MQXFB



- **Backing strip**
 - For the vessel welding

Magnet design

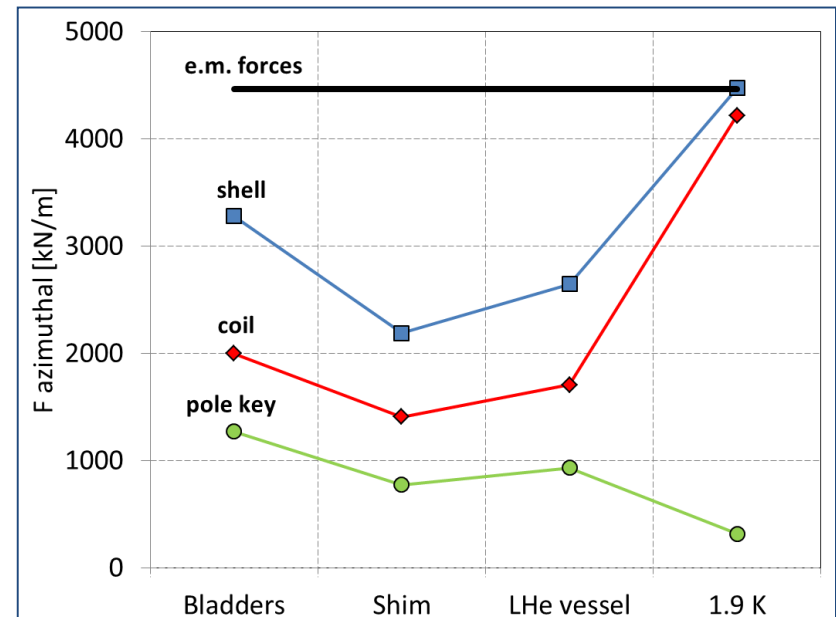
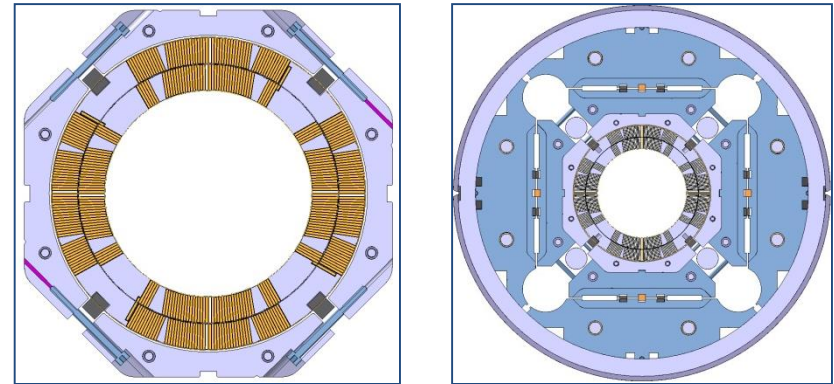
MQXFB



- **Axial support system**
 - Aluminium rods and end-plates

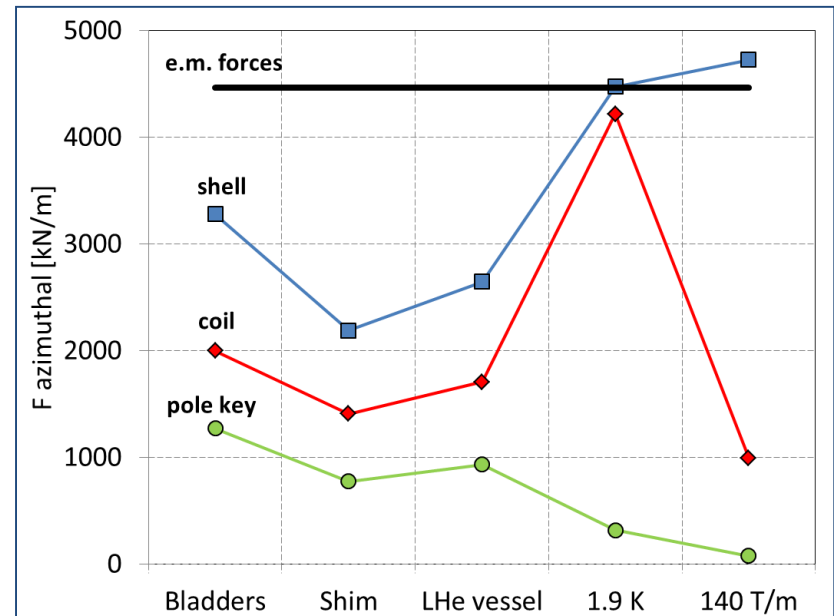
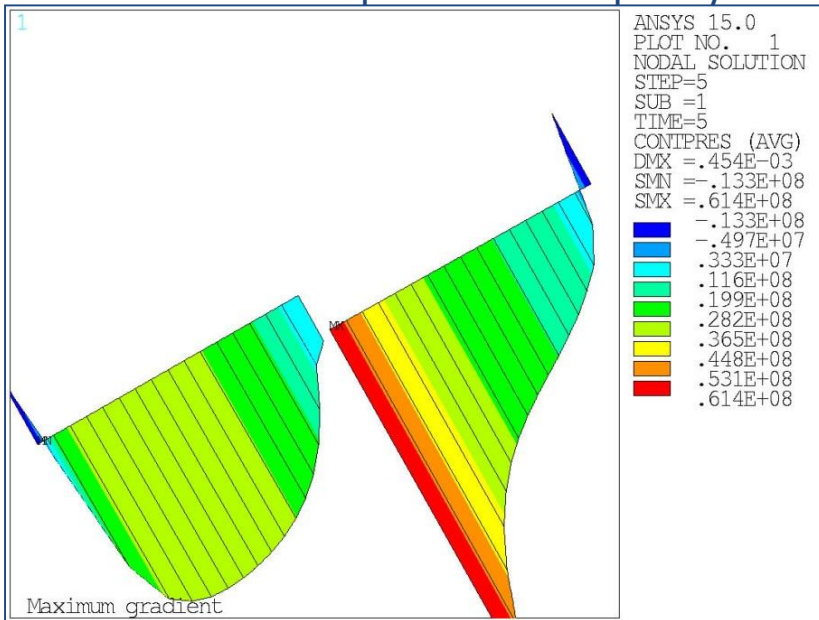
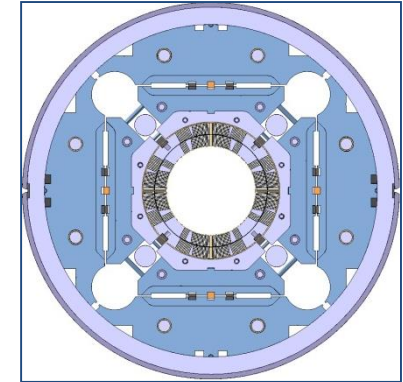
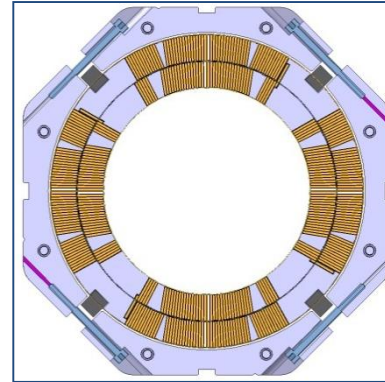
Pre-loading sequence

- Target:
 - Coil pre-load = e.m. force
- Room temperature
 - **45 MPa bladder pressure**
 - Overshoot to insert shim
 - **~30%** of force on collars
 - Marginal impact of vessel
 - Coil peak stress **<100 MPa**
- 1.9 K
 - 0.4 mm coil radial displ.
 - Minimum force on collars
 - Vessel still in contact
 - Coil peak stress **~175 MPa**

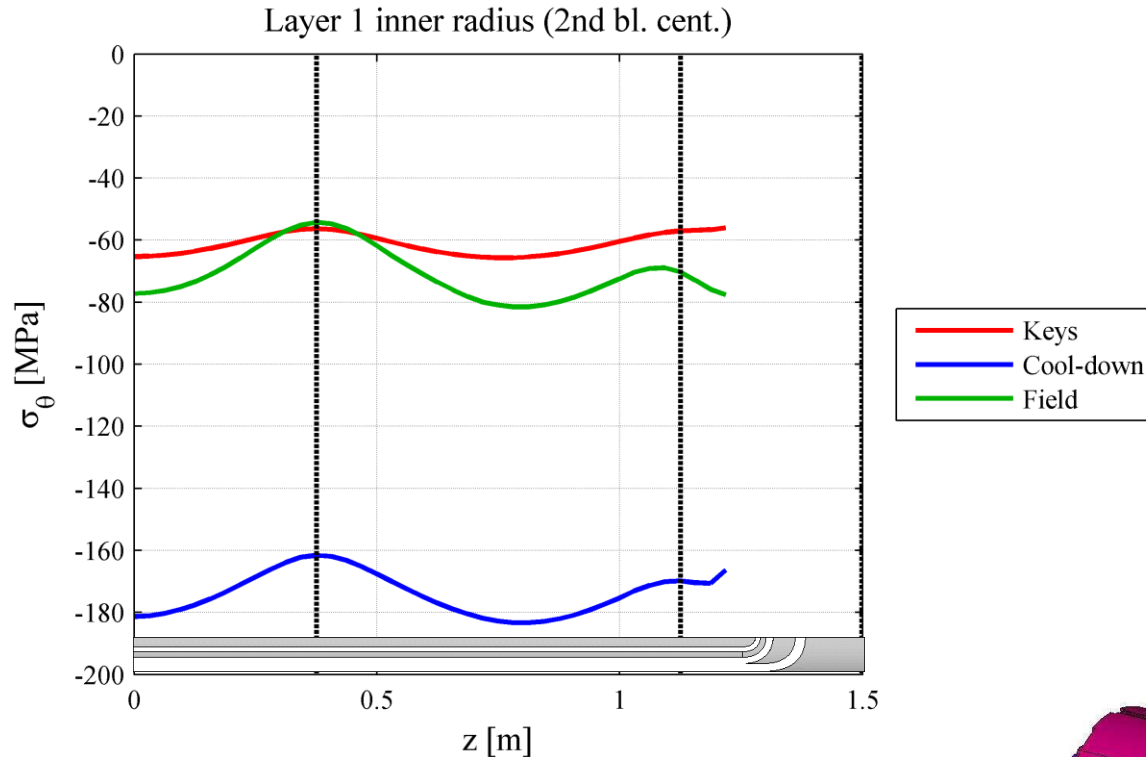
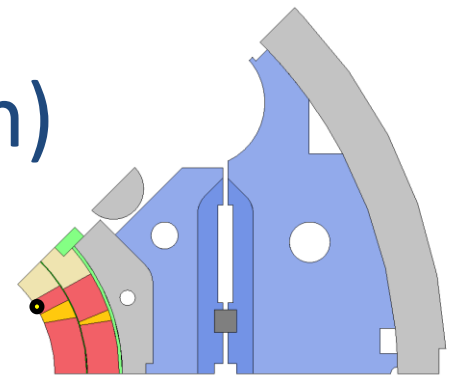


Excitation to 140 T/m

- Coil under pressure
 - Capability to pre-load to 155 T/m
- Coil peak stress **~140 MPa**
- Structure rigidity
 - ~0.045 mm on the mid-plane
 - No impact on field quality



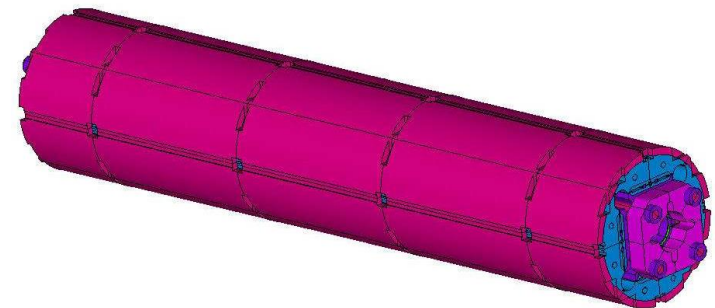
Peak cool-down stress (3m)



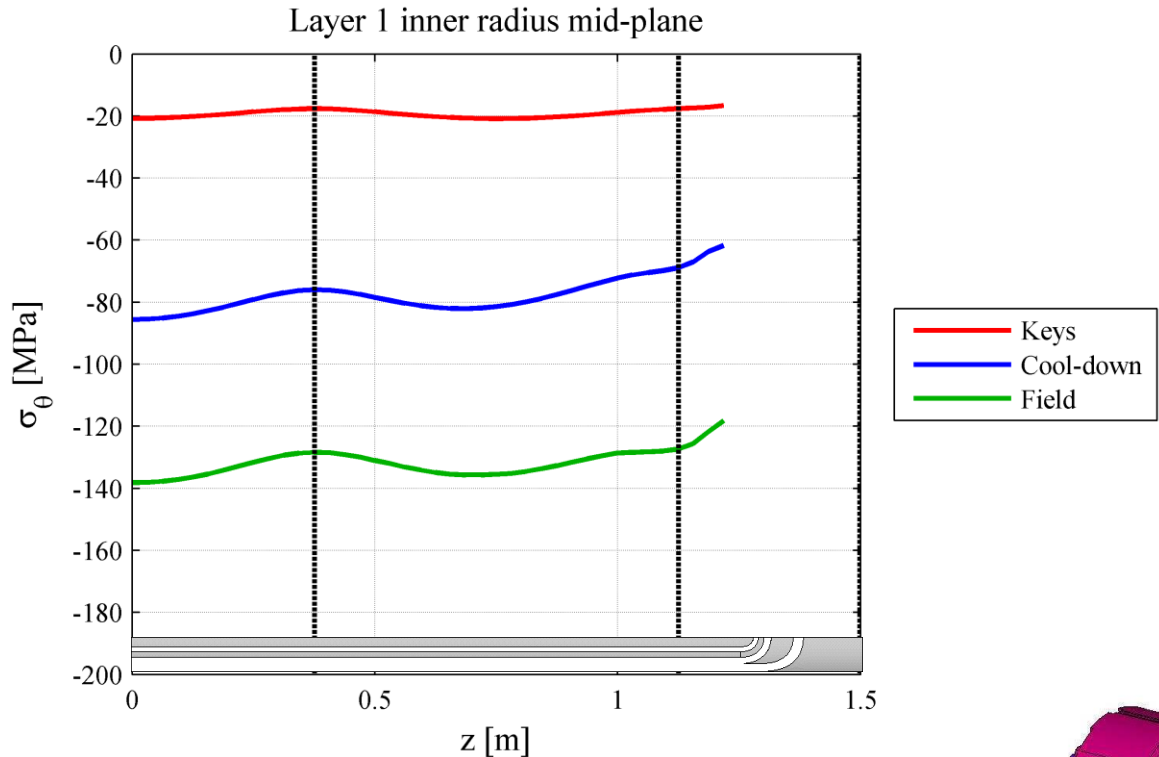
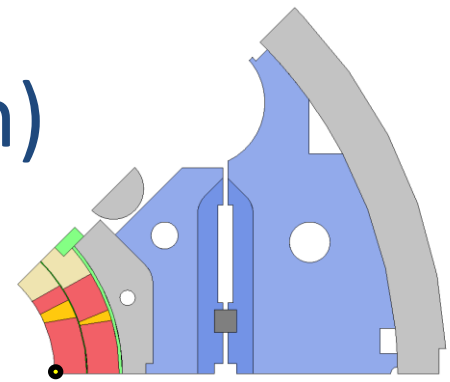
- Peak stress after cool-down **below 182 MPa** (below TQ/HQ)

- **Optimised layout**

- 3 normal shell (0.755m long)
- 2 half-shells at extremities (0.377m)



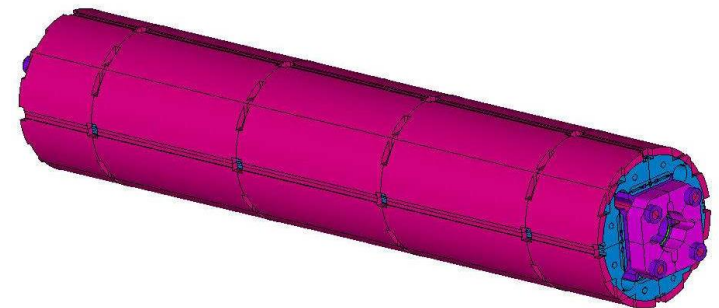
Peak mid-plane stress (3m)



- Peak stress with magnetic forces at 140 T/m **below 138 MPa** (below TQ/HQ)

- **Optimised layout**

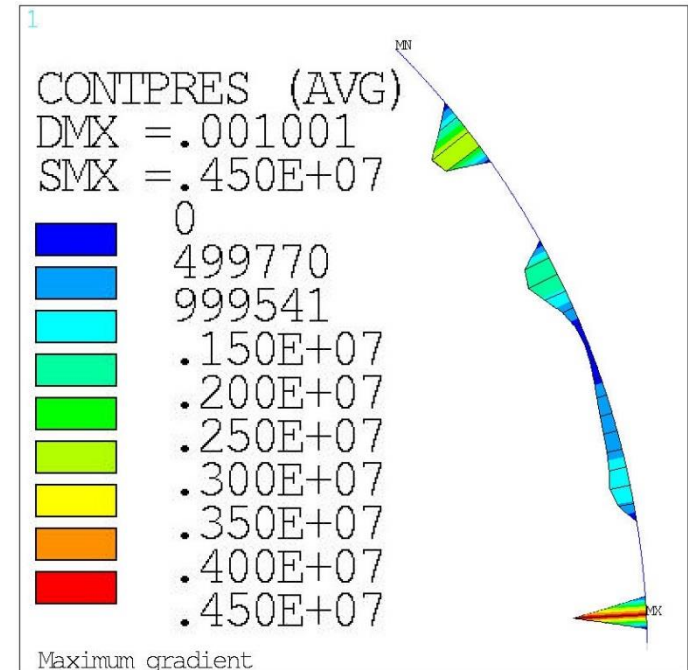
- 3 normal shell (0.755m long)
- 2 half-shells at extremities (0.377m)



Liquid helium vessel

- OD of the structure shrinks by ~2mm
- LHe vessel requires tensioning to maintain contact and alignment (weld shrinkage)
- Vessel of 8mm thickness modelled
- Weld shrinkage simulated with contact elements features

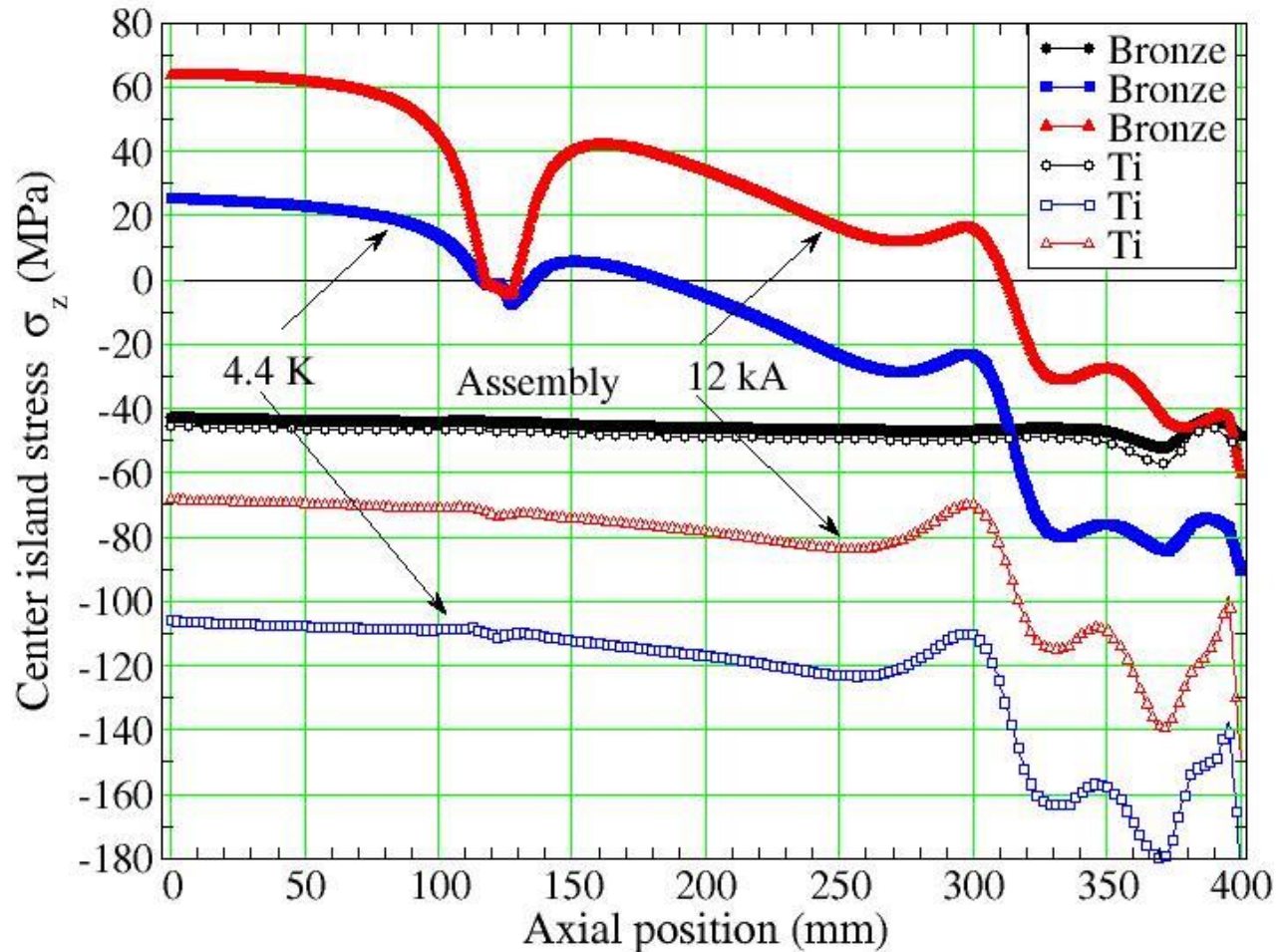
	F_{weld} kN	σ_{weld} MPa	σ_{vessel} MPa
Warm	760	95	120
Cold	128	16	51
Forces	224	28	71



- **Contact between the shell and the vessel maintained (locally) after cool-down**
- **Vessel linked to the yoke through the backing-strip (tack-welded) and welding blocks between the shell segments (bolted to the yoke)**

Bronze vs Titanium - island

Axial scan of axial stress along the mid-island ir



MQXF ANSYS model materials

Material	E [GPa]		pr	$(L_{4.3K} - L_{293K}) / L_{293K}$
	293 K	4.3 K		
Coil	EX = 44 EY = 52 GXY = 21	EX = 44 EY = 52 GXY = 21	0.3	X = 3.36e-3 Y = 3.08e-3
Stainless stell	193	210	0.28	2.84e-3
Aluminum Bronze	110	120	0.3	3.12e-3
Iron	213	224	0.28	1.97e-3
Aluminum	70	79	0.34	4.2e-3
G10	30	30	0.3	7.06e-3
Titanium	130	130	0.3	1.74e-3
Nitronic 40	210	225	0.28	2.6e-3